PERFORMANCE CHARACTERISTICS OF A VERTICAL AXIS WIND TURBINE OPERATING IN DIFFERENT ENVIRONMENTAL CONDITIONS

Ghada Aboufares

Master of Science by Research

2015

University of Huddersfield

School of Computing and Engineering

DECLARATION

i. The author of this thesis (including any appendices and/or schedules to this thesis) owns any copyright in it (the "Copyright") and she has given The University of Huddersfield the right to use such copyright for any administrative, promotional, educational and/or teaching purposes.

ii. Copies of this thesis, either in full or in extracts, may be made only in accordance with the regulations of the University Library. Details of these regulations may be obtained from the Librarian. This page must form part of any such copies made.

iii. The ownership of any patents, designs, trademarks and any and all other intellectual property rights except for the Copyright (the "Intellectual Property Rights") and any reproductions of copyright works, for example graphs and tables ("Reproductions"), which may be described in this thesis, may not be owned by the author and may be owned by third parties. Such Intellectual Property Rights and Reproductions cannot and must not be made available for use without the prior written permission of the owner(s) of the relevant Intellectual Property Rights and/or Reproductions.

The University of Huddersfield

ACKNOWLEDGEMENTS

First and foremost, I would like to thank Allah. I offer my sincerest gratitude to my supervisors Dr. Taimoor Asim and Prof. Rakesh Mishra , who have supported me throughout my thesis with their patience and knowledge whilst allowing me to work in my own way . I attribute the level of my Master's degree to their encouragement and effort, and without them, this thesis would not have completed. One simply could not wish for better or friendlier supervisors.

The School of Computing and Engineering at the University of Huddersfield, has provided the support I needed to complete my thesis.

Finally, I thank my parents, especially my mother for supporting me throughout my studies at the University of Huddersfield

ABSTRACT

Renewable energy is an essential source for harnessing natural forces such as wind energy in an age which is very conscious of the environmental effects of burning fossil fuels, and where sustainability is an ethical norm. Therefore, the focus is currently on both the adequacy of long-term energy supply, as well as the environmental implications of particular sources. In that regard, the near certainty of costs being imposed on carbon dioxide emissions in developed countries has profoundly changed the economic outlook of clean energy sources.

Wind turbines have vastly been developed in recent decades due to technology becoming more advanced. Since there is a continuous exhaustion of fossil fuels, it is of high interest with government encouragement to utilise wind technology. Wind turbines are currently advancing into cross-flow vertical axis operation, whereby research has shown a significant increase in performance compared to existing technologies. This research is based on the Savonius type Vertical Axis Wind Turbines (VAWTs). The VAWT design considered in the present study comprises of 12 rotor blades and 12 stator blades, where the wind speed of 4m/s has been considered. This wind speed is the average annual wind speed in Huddersfield, UK.

Erosion is a serious issue in Vertical Axis Wind Turbines that causes roughness on the blades via airborne dirt, debris and insects. Erosion has been shown to degrade the performance characteristics of a VAWT significantly. A number of different strategies have been employed to analyse erosion in VAWTs, and with the advent of powerful and advanced computational methods, it has become possible to investigate erosion at microscopic levels. Hence, this study is based on the predictions from numerical simulations performed using a Computational Fluid Dynamics based solver.

The first aspect of this study comprises of detailed numerical investigations on the performance evaluation of VAWTs operating in clean environments. Although many numerical studies are available in this particular area, however, most of these studies use rather simplified modelling techniques. The results presented in this study are based on transient modelling approaches, where instantaneous pressure and velocity fields have been computed and analysed. Furthermore, instantaneous torque output of the VAWT has been recorded in order to develop a generic semi-empirical prediction tool that accounts for the variations in the geometric configurations of the VAWT.

The second aspect of this study is related to the erosion in VAWTs. This is of particular importance to VAWT designers who wish to install VAWTs in dusty environments, such as desserts, where wind velocities are significantly higher than in urban areas. Various dusty environmental conditions have been numerically created, comprising of different sand particle sizes and mass flow rates. Their effects on the performance degradation has been critically analysed in this study. Furthermore, erosion rates on rotor blades of the VAWT have been recorded. The results obtained have then been used in order to develop a novel semi-empirical

prediction model for the torque generation from the VAWT that takes into account various sand particles' parameters.

CONTENTS

LIST OF FIGURES

LIST OF TABLES

NOMENCLATURE

A	Frontal area of the VAWT (m^2)
C_d	Drag coefficient (-)
C_T	Torque coefficient (-)
d	Diameter (m)
F_D	Drag Force (N)
g	Acceleration due to gravity (m^2/sec)
$\dot{m}$	Mass flow rate (kg/sec)
P	Local static gauge pressure (Pa)
R	Radius of the rotor (m)
Re	Reynolds number (-)
T	Torque output (Nm)
t	Time (sec)
V	Linear velocity (m/sec)

Greek Symbols

ρ	Density (kg/m^3)
μ	Dynamic Viscosity (kg/m.sec)
θ	Angular position (º)
λ	Tip Speed Ratio (-)
ω	Angular Velocity (rad/sec)

SUBSCRIPTS

∞	Freestream
p	Particles
w	Water

CHAPTER 1
INTRODUCTION

For the past few years, attention has been significantly drawn towards the requirements for finding a cost effective and clean energy source. This is primarily due to the continuous reduction in fossil fuels. Wind is an energy source that fits into these criteria and is harnessed via wind turbines. There are two types of wind turbines, namely being Horizontal Axis Wind Turbine (HAWT) and Vertical Axis Wind Turbine (VAWT), where VAWTs are the focus of the present study. This chapter introduces the research topic, providing an overview of wind energy as a renewable source to power, further discussing the advantages of VAWTs in comparison to HAWTs.

1.1 Wind Energy as Renewable Energy Source

Wind energy is a clean and renewable energy source that has developed a variety of technological applications and industrial uses in recent years. Researchers regard wind energy as the first and foremost source of renewable energy that is affordable, understood as being capable of generating electricity for business, industrial and residential uses at rates that are comparable with conventional energy sources, with or without subsidies. Since 2007, Germany has been the leading producer of wind-based power, followed by Spain and India. In 2008, the United States advanced to the top rank of global wind energy producers, but China surpassed the United States in this area in 2010. While surpassing the United States in terms of production of wind energy, China simultaneously outpaced India, which had led the Asian region until 2007. Tabassum-Abbasi et al. [1] noted that China is currently generating three times more energy from wind sources than India. With plans to begin production of another 200GW, China is expected to remain the world leader in wind energy production in the near future. With the need for sustainable energy increasing annually as a direct consequence of ongoing depletion of fossil fuels and the resulting energy crisis, wind energy has taken on as being of prime significance. Unlike fossil fuels, wind energy is both renewable and not a contributor to any kind of environmental ill effects. Therefore, it can be identified as both a clean and a renewable energy source.

Figure 1.1 depicts production of global demand for electricity. It is anticipated, according to Tabassum-Abbasi et al. [1] that electricity demand will nearly double from 2010 to 2050. In order to meet 20% of this demand from wind energy alone, its production must grow by a factor of 50 times. Increasing energy production based on wind energy would not only reduce reliance on fossil fuels, but it would also assist countries or regions in reducing greenhouse gases. Keegan et al. [2] noticed that since 2000, the total capacity of installed wind power in the European Union (EU) has been 12.9GW and by 2012, this figure has grown to 106GW. It is anticipated that by 2020, under development by the European Wind Energy Association (EWEA), growth in wind energy will reach 230GW with 40GW obtained from offshore installations.

As Salem et al. [3] have pointed out, the public sector organisations have become interested in expanding the generation of wind energy via turbine operation for heating and cooling purposes. There are a number of variables driving this move, such as costs involved. The generation of energy based on wind is less costly in the long-term than the extraction of fossil fuels, processing and refining. It has also been observed that wind energy is an almost infinite energy source. While it is true that the amount of wind energy available at any geographic location at any given time can be variable, and equally true that some locations are more likely to be capable of providing consistent or relatively consistent sources of wind energy than others, wind energy is a renewable energy source. More significant still is the fact that wind energy production and its use does not come with greenhouse gas emissions.

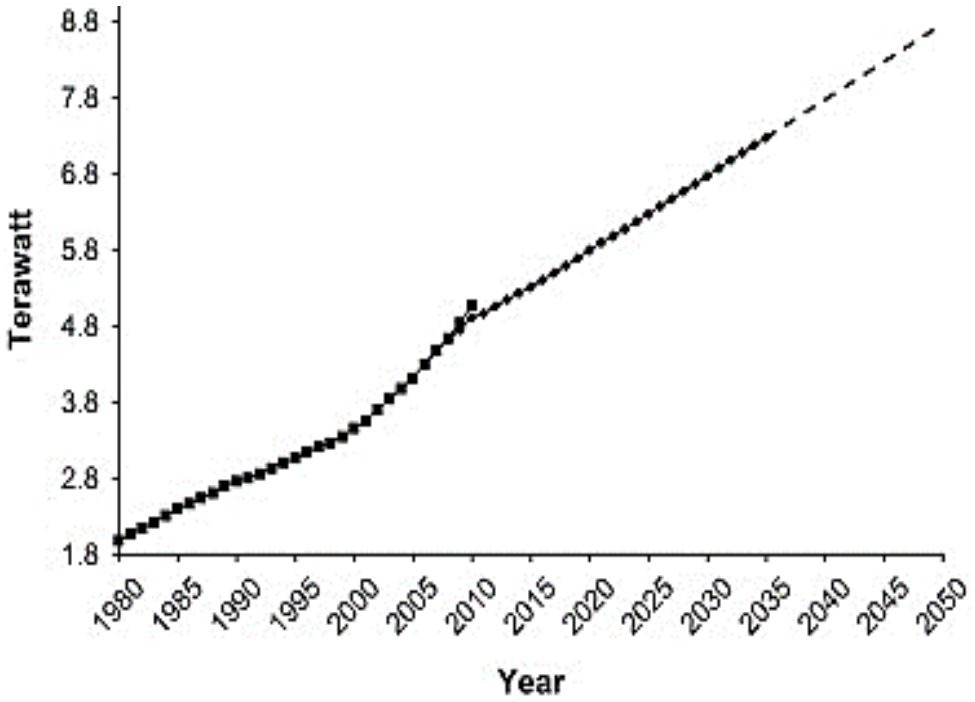

Figure 1.1 Global Electricity Demand [1]

The increased emphasis on wind energy is associated inevitably to concerns regarding reliance on fossil fuels as a major source of energy. Many voices have been raised in support of the idea that overreliance on fossil fuels is the root cause of climatic fluctuations, and a direct cause for many different forms of environmental degradation (Freedenthal [4]). The argument advances the idea that whilst the use of fossil fuels has undeniably facilitated industrial development and many different forms of production, humanity is at a juncture where it must decide whether or not it will continue to rely on these energy resources, accept the risks attendant upon continued use of such resources, or become more focused on alternative energy sources that are less likely to have a negative impact upon the environment. Chow et al. [5] pointed out that energy is quite simply a necessity for technological and economic development, while also noting that the energy choices made by countries such as the United States and other industrialised nations have significant ramifications for the rest of the world. These ramifications are economic, environmental, and political as well as military. Energy resources and specifically fossil fuels or mineral resources have long formed the basis of energy consumption in both the developed and the developing world.

Chow et al.[5] further noted that the world's supply of proved, economically recoverable fossil fuel reserves, which include almost one trillion metric tons of coal, one trillion barrels of petroleum, and 150 trillion cubic meters of natural gas are actually quite extensive. Moreover, mineral resources equally important to energy generation are substantial with, for example, over three million metric tons of uranium reserves. Essentially, the arguments presented by Chow et al.[5] are 1) it appears on balance that the world is not running out of mineral fuels, 2) fossil fuel reserves are concentrated in a small number of countries, 3) total global energy consumption depends heavily upon petroleum, natural gas, coal, hydroelectric power, nuclear power, and a

small amount of non-hydro renewable energy, and 4) there are striking disparities in annual energy consumption per capital when industrialised and non-industrialised countries are compared. Nevertheless, wind energy is a viable addition to these resources.

Chow et al. [5] found that enormous advances have been made in terms of controlling the acknowledged ill effects of fossil fuel exploration, recovery, and use. It has also been pointed out that traditional alternatives to fossil energy such as hydroelectricity and nuclear power are also accompanied by environmental and social costs, which are not the case with respect to wind energy. No primary energy source and its associated technology are seen by these analysts as completely free of environmental and other drawbacks. Chow et al. [5] concludes that it is impossible not to recognise the very real benefits of fossil fuels and equally impossible not to recognise that transformation of energy use to alternative fuels will be accompanied by significant economic, technological and political challenges.

Researchers at Kennesaw State University [6] pointed out that coal has been a source of energy for almost as long as man has inhabited this planet, and is a ready supply of energy that is nevertheless possessed of certain disadvantages. Coal continues to be the energy of choice for many applications in the United States because it is in abundant supply, is produced very cheaply, and is affordable for many different uses. Coal currently accounts for a little over 50% of the electricity that is generated in the United States and China. The problem with coal is that the exploration and recovery are costly, and if not carefully monitored, can leave very significant negative effects on the environment. In particular, strip mines damage the environment but it is the burning of coal and the release of carbon dioxide (a greenhouse gas that damages the ozone layer) that is most controversial.

Nevertheless, the Kennesaw State University researchers do note that efforts have been aggressively undertaken to achieve clean coal use. Clean coal refers not only to the process by means of which coal is extracted from the earth, but also to the ways in which it is burned by using staged combustion chambers which reduce the amount of nitrogen released into the environment. However, to truly achieve a zero negative impact, more research needs to be carried out in order to ensure that this cheap, readily available energy resource offers more benefits than deficits.

Natural gas is yet another fossil fuel, which an organization called Natural Gas [7] sees as an important source of energy, which is capable of reducing pollution and maintaining a clean and healthy environment. In addition to being a domestically abundant and secure source of energy in many locales, natural gas offers some substantial benefits over other fossil fuel energy sources.

Natural Gas identifies natural gas as the cleanest of all fossil fuels. Natural gas does produce emissions containing carbon dioxide, carbon monoxide, nitrogen oxides, sulphur dioxide, and particulates. It does so at levels, which are significantly lower than either oil or coal. It is considered as the cleanest of the fossil fuels. The use of natural gas does not contribute significantly to smog formation because it emits low levels of nitrogen oxides and virtually no particulate matter. The natural gas industry has been extremely proactive, joining the United

States Environmental Protection Agency in an effort to reduce methane emissions, an effort that has resulted in a reduction in such emissions over the last 15 years. Overall, natural gas appears to be a fossil fuel that has fewer ill effects than other fossil fuels, but one must recognise that no fossil fuel is without any environmental impact.

Researchers at Kennesaw State University also provide information about oil, noting that the United States and other countries quite literally relies heavily on oil for any number of functions, in addition to running automobiles and other vehicles that use combustion engines. Oil is a cornerstone of the domestic economy and the United States imports over 50% of all the oil that is consumed in the country, which essentially means that oil is a primary consideration in international politics.

Domestic production of crude oil, despite the fact that the United States has many untapped but proven reserves of this fuel, has decreased since the 1960s and consumption has continued to increase. Critics of overreliance on crude oil in the form of gasoline or other products argue that the methods used to explore for oil, extract oil, process oil, and use oil, all contribute substantially to environmental degradation. From emissions during vehicle use to oil spills, the burning of oil in factories, gases released from refineries and the process of distillation, each of these activities clearly and definitively impact upon the environment.

At the same time, modern day oil companies are working not only to convince the public that they have become more environmentally conscious, but also to improve all aspects of their operations. Oil companies also point out that some aspects of their business actually help the environment. For example, oilrigs in the oceans provide a stable base near the surface of the water for coral and other creatures. This creates a community for other forms of wildlife such as game fish. Some fishermen are convinced that the best places for deep sea fishing are near oil rigs.

One must also recognise that oil is an economic driver on many different levels. Oil exploration, extraction, refining, and retailing are big businesses that provide many jobs in the global economy. Countries such as Great Britain are as dependent on oil and other fossil fuels as the United States, and for that matter, the vast majority of industrialised First World nations. Moreover, oil and products that are based upon oil are essential in maintaining an adequate standard of living.

Freedenthal [4] discusses the use of fossil fuels and found that there is no evidence indicating that the so-called green revolution is likely to succeed in replacing dependence upon fossil fuels. The author discusses that fossil fuels cause environmental damage and while this damage can be and has been minimized, it will prove to be impossible to eliminate all possible sources of environmental degradation that is associated to the uses of fossil fuels. The questions that must be asked are not whether or not fossil fuels cause environmental problems, but instead, what can be done that is not being done to minimise these problems. Questions arise as to what kind of fossil fuel, or which alternatives can be considered for such resources, i.e. wind power, that is most likely to produce the least amount of greenhouse gas emissions and pollution. Such questions can be viewed as representing a realist position on a controversial issue.

Industrialisation is a necessity for development and globally there are a few countries that are not in need of some type of an on-going industrial development.

The energy policy that should be promoted is one that will focus on reducing the environmental effects of fossil use, exploring viable alternative energy sources, and on the most efficient environmentally accepted sources of energy. In essence, Freedenthal suggests that those who call for nothing but green energy are not cognisant of the realities of the green revolution and its limitations. There are certainly cases to be made for hydropower, wind power, and solar power. At the same time, it is difficult to consider a world in which any of these energy sources alone would be sufficient to provide the energy to an enclave. Solar power may be useful in providing power to run a medium sized home however, it would not be suffice to power a 40-story tall office building requiring heat in the winter and cooling in the summer.

When the issue of the benefits of fossil fuel versus their environmental implications is considered, even the staunchest defenders of fossil fuels must acknowledge that these fuels are acquired and used with some serious environmental impacts. At the same time, those who call for eliminating all fossil fuels and focus on green energy sources fail to recognise that these sources also have some negative environmental effects and may not be adequate to meet the energy needs of the developed and developing countries. It is therefore important that policymakers, energy sector leaders, and members of the general public move away from the emotional rhetoric on this issue for achieving a more effective approach to energy.

As this discussion demonstrates, fossil fuels currently provide the bulk of the energy that is needed for production, for home and for commercial consumption. It is likely that the benefits of fossil fuels continue to outweigh their environmental implications but equally, it is likely that improvements in the sector would be beneficial. Nuclear energy, natural gas, wind, and clean coal are energy sources that should be emphasised as alternatives to over-reliance on fossil fuels.

1.2 Wind Turbines

A wind turbine is a mechanical artefact that converts the kinetic energy of the wind into useful forms, such as electrical energy. Eriksson et al. [8] note that the turbine conception is often named after the axis of rotation for the turbine. A Horizontal Axis Wind Turbine (HAWT) has a horizontal shaft, whereas a Vertical Axis Wind Turbine (VAWT) has a vertical shaft. Figure 1.2 depicts comparison between the two different wind turbine concepts.

Argonne National Institute (ANI) [9] defined the wind turbines like aircraft propeller blades, turning in the moving air and powering an electric generator that supplies electric current. Moreover, a wind turbine is the opposite of a fan. Instead of using electricity to make wind, wind turbines use wind to make electricity. The wind turns the blades, which spin a shaft, which connects to a generator and makes electricity. It has been further stated that modern wind turbines fall into two basic groups i.e. horizontal-axis variety, like the traditional farm windmills used for pumping water, and the vertical-axis design, like the eggbeater-style Darrieus model, named after its French inventor. Most large modern wind turbines are horizontal-axis turbines.

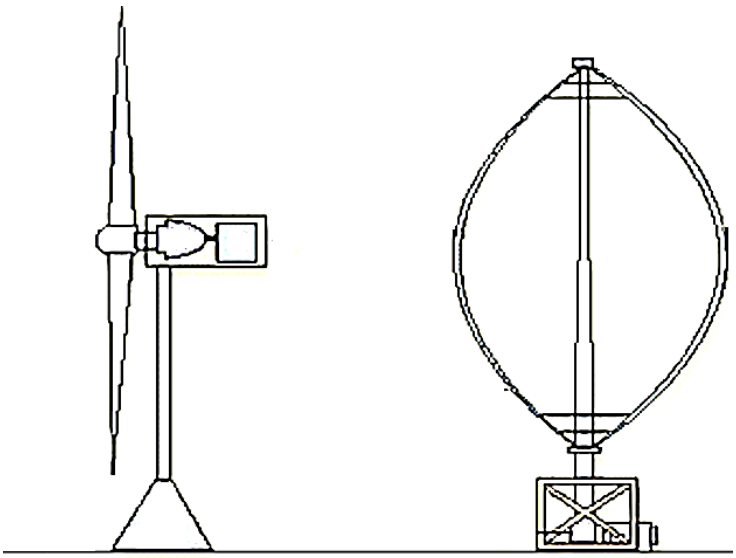

Figure 1.2 Comparison between the two different wind turbine concepts [8]

Wind turbines are available in a variety of sizes, and therefore power ratings. The largest machine has blades that span more than the length of a football field, stands 20 building stories high, and produces enough electricity to power 1,400 homes. A small home-sized wind machine has rotors between 8 and 25feet in diameter, and stands upwards for 30feet, and can supply the power needs of an all-electric home or small business. Utility-scale turbines range in size from 50 to 750kW. Single small turbines, below 50kW, are used for homes, telecommunications dishes and water pumping.

1.2.1 Horizontal Axis Wind Turbines (HAWTs)

Horizontal Axis Wind Turbine (HAWT) has its axis of rotation parallel to the ground, as depicted in figure 1.3. These wind turbines are designed to manufacturing standards and are mainly employed for large wind farms positioned both on and off-shore.

Argonne National Institute ANI [9] describes the components of a typical HAWT as follows:

- Blade or rotor which converts the energy in the wind to rotational shaft energy
- A drive train, usually including a gearbox and a generator
- A tower that supports the rotor and drive train
- Other equipment including controls, electrical cables, ground support equipment, and interconnection equipment

Recent HAWTs have faced difficulties centered upon their delivery. In many projects, systems are fixed with yawing instruments, which helps in directing the device to the direction of wind. Even though this control mechanism is well understood, however its reaction times under different wind conditions are quite varied. Furthermore, due to large component inertia, a considerable quantity of energy is used in pointing the rotor into the primary wind direction. This can result in inefficiencies.

Similar systems are employed in the micro wind field in which small scale HAWTs are fitted with a basic yawing device which consists of a sail like paddle. Using the power contained in the wind, this paddle is yawed such that it sits inline with the prevailing stream-wise flow component resulting in the rotor being subjected to the full force of the wind. Therefore, the most recent generation of micro-HAWTs are found inefficient, due to this system. Furthermore, it has been confirmed that while using this passive paddle system, further difficulties are experienced through highly turbulent conditions. This results in large power fluctuations giving rise to structural and electrical instabilities. Reducing this difference in energy can consequently prolong device life and decrease the requirement for regular conservation, as stated by Asim et al. [10]. Such difficulties have led to the development of Vertical Axis Wind Turbines (VAWTs) as a possible replacement to HAWTs.

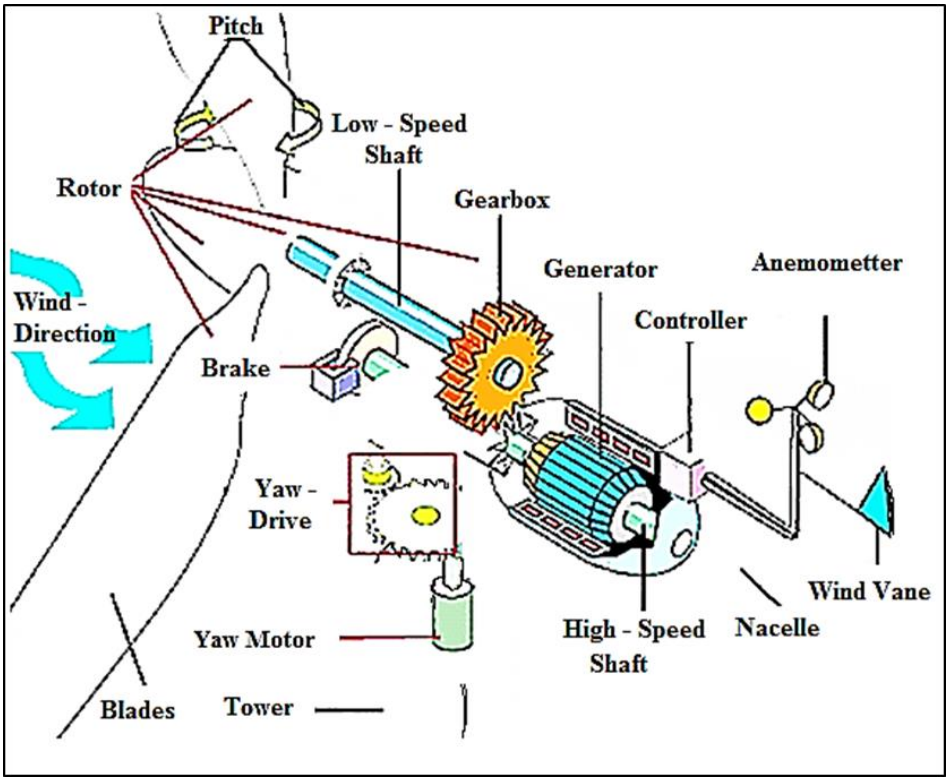

Figure 1.3 Wind turbine components [11]

1.2.2 Vertical Axis Wind Turbines (VAWTs)

Vertical Axis Wind Turbines have a long and well-documented history. Mittal [12] states that while the history of windmills can be traced back to approximately 500B.C. where they are described in a Hindu epic book titled Kautilya Arthasastra. At approximately 200B.C., Persia developed a simple vertical axis phenomenon that was used to grind grains. Its rotor was constructed from bundles of reeds tied to a frame that rotated in accordance with the thrust of prevalent winds. The design was modified over time with millstones situated under, rather than above the rotor, perhaps in response to recognition that wind speed increases with height, and a modified design would be more efficient and convenient.

A VAWT uses similar principals as a traditional horizontal axis turbine to extract energy from the wind using both a combination of aerodynamic lift and drag but has its axis of rotation normal to the ground. Vertical axis technologies have the advantage of being uni-directional in design and hence can accept and respond to changes in local wind direction [13-15]. This has resulted in many micro VAWTs outperforming equivalent horizontal axis technologies in environments where wind direction is constantly changing. Further, vertical axis technologies have major differences in structural dynamics, control systems and maintenance which make these machines less complex and cheaper to install. Although clear advantages of using this technology are documented below, they have not been investigated in sufficient detail and hence existing designs suffer from lower efficiencies when compared to more mainstream horizontal axis machines.

- Silent running
- Low start up speed
- Only one moving part, there is no gearbox
- Design allows a turbine to be mounted nearer to the ground. Also suitable for commercial roof mounting
- Giving easier access for maintenance / service
- Blends better into the environment
- Safe at high wind speeds
- Rotating diameter smaller than that of HAWT
- Safer to wildlife and birds

Sutherland et al. [16] commented that VAWTs are cross-flow turbines, since they revolve around an axis that has a vertical orientation w.r.t. the ground. The output shaft of the transmission in-turn drives a motor generator, converting the mechanical torque of the motor into electrical power.

1.3 Types of Vertical Axis Wind Turbines

There are primarily two types of VAWTs, namely Darrieus and Savonious types. Detailed discussion on both these designs are presented in the following sections.

1.3.1 Darrieus type Vertical Axis Wind Turbines

A Darrieus type Vertical Axis Wind Turbine is shown in figure 1.4. The Darrieus rotor exemplifies high speed and high efficiency. It is invented by France's Georges Jean Marie Darrieus in 1925, and reinvented in the late 1960s in Canada by the teams of Rangi, South, and Templin. The Darrieus VAWT is recognized as a high efficiency machine. Its heavy equipment, such as the gearbox and generator, are stationary and are located at ground level, fostering ease of maintenance.

Figure 1.4 The Darrieus vertical axis wind Turbine [17]

The Darrieus turbines operate using some degree of aerodynamic drag but primarily relies on aerodynamic lift for torque generation. Hameed et al. [18] noted that the long blades of the Darrieus Vertical Axis Wind Turbines, with high aspect ratios, are subjected to a large value of bending moments due to centrifugal forces that may result in the failure of the blades. Castelli et al. [19] states that modifications to the basic Darrieus VAWT can be made with reference to Tip Speed Ratio (TSR).

1.3.2 Savonius type Vertical Axis Wind Turbines

A Savonius Vertical Axis Wind Turbine is shown in figure 1.5. It was invented by the Finnish engineer Sigurdj Savonius in 1922. As described by D'Ambrosio et al. [20], it is a drag type VAWT meaning that it cannot rotate faster than the speed of wind. The maximum tip speed ratio is equal to one or less. This report will focus on the Savonius rotor due to its suitability for low speed environments.

The basic configuration of the Savonius drag rotor has two semi-circular blades with a central gap defined as overlap [21]. Previous studies were mostly conducted on the optimization of design parameters such as blade number, blade shape and overlap distances. Experimental studies carried out by Sheldahl et al. [22], Sivasegaram [23], Clayton [24] and Fujisawa et al. [25] all report varying power coefficients for Savonius rotors ranging from 0.14 to 0.33 within a TSR range of 0.8 to 1.0. Given the high solidity of this type of rotor, significant torque output was observed during static and rotational modes of operation making start-ability consistent at low wind speeds. Due to this high solidity/low speed design, the acoustic emission from this machine during normal operation is considerably less than the traditional HAWT described previously. With current UK planning legislation in mind this type of machine lends itself to installation in the built urban environment where noise restrictions are of primary concern [26].

One problem that was present in some machines was the large variation in rotor torque output due to the fixed two blade design. Upon detailed investigations into the flow fields across the machine it was found that blade interaction effects were present on the non-torque generating blade. It was identified that unfavourable pressure gradients were the primary cause which resulted in a counter-rotating torque which significantly reduced the efficiency of the rotor. These blade interaction effects have become one of the major limitations of this type of turbine given torque generation is only provided by one bucket each rotor cycle. Such limitations provide strong justification for exploring alternative reaction type devices which maintain similar high levels of starting torque and provide a more consistent power delivery.

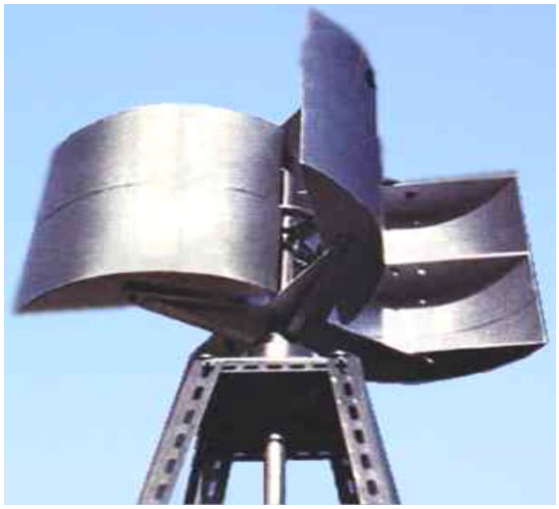

Figure 1.5 Savonius Vertical Axis Wind Turbines [20]

The Savonius rotor sweeps an area in vicinity to the ground, resulting in less effective overall energy extraction due to lower wind speed at lower heights. Buhtta et al. [27] states that the Savonius rotor is one of the several configurations that are useful in generating wind power. The Savonius VAWT is often employed in instances where reliability matters more than efficiency. Such applications include deep water buoys, advertising signs designed to draw attention to a message, and in the case of most anemometers.

This thesis focuses on the Savonius VAWT, since it is preferred when low wind speed tends to prevail in an environment. The major advantage of this, and other VAWTs, is that it can be used at any location and is a standalone system where the generator can be placed at ground level. The Savonious rotor is, however, only one of the available VAWTs for different operating environments.

1.4 Performance Characteristics of VAWTs

According to Colley et al. [28], the important performance parameters for wind turbines are the torque output and the tip speed ratio (TSR, λ). The tip speed ratio of a VAWT has been defined as:

$$\lambda = \frac{R\omega}{V} \tag{1.1}$$

where R is the radius of the rotor zone, ω is the rotational speed of the rotor and V is the wind velocity. In the present study, average annual wind speed in Huddersfield (UK) of 4m/sec has been considered for investigations, while the TSR of the VAWT is 0.4, which is the most practical one for such machines. The torque coefficient of the VAWT can be expressed as:

$$C_T = \frac{T}{0.5\rho V^2 AR} \tag{1.2}$$

where T is the torque output of the VAWT, ρ is the density of air and A is the frontal area of the VAWT. Once the torque output of the VAWT is known, the torque coefficient can be calculated. Rearranging the foregoing equation gives:

$$T = \frac{1}{2}\rho V^2 A R C_T \tag{1.3}$$

1.5 Motivation

Despite the fact that the operating principle of a VAWT is quite simple, the detailed aerodynamic and mechanical behaviour is quite difficult to understand, particularly in the desert environment where gusts of dusty winds are quite often experienced. The most serious issue with the wind turbines is the degradation in their performance, and the unpredictability of stall due to dust erosion and accumulation on airfoils/rotor blades. Dust cause problems for wind turbines operating in coastal areas and desserts, thus it is important to understand the dynamics of dusty winds on wind turbines since many countries embark on a very ambitious wind energy plan.

The present research seeks to provide a deep awareness into the physics of dust erosion over VAWT blades. A Computational Fluid Dynamics (CFD) based modelling approach has been employed in the present study in order to allow VAWT designers to extract several aerodynamic performance parameters like pressure fluctuations, velocity variations and instantaneous torque output from the VAWT. A numerical investigation has been conducted on the prediction of erosion by employing a commercial CFD code. This code has been used to model the sand particles interactions with the VAWT's blades. The study also demonstrates the viability of the CFD model in analysing the erosion rate variations w.r.t. the geometrical orientation of the VAWT.

1.6 Research Aims

The primary aim of this study is to investigate the effects of a dusty environment on the performance degradation of a vertical axis wind turbine (VAWT). The study is designed to carry out numerically using a commercial CFD code called ANSYS. Both local and global flow parameters will be computed and a detailed investigation into qualitative and quantitative parameters of interests will be carried out. A novel prediction model will be developed for the performance degradation of a VAWT under dusty environments. The research aims for this investigation are to:

1. Analyse the performance characteristics of a Vertical Axis Wind Turbine operating in a clean environment

2. Analyse the performance characteristics of a Vertical Axis Wind Turbine operating in dusty environments

1.7 Organisation of Thesis

Chapter 1 provides a general review on the wind energy as renewable source. Types of wind turbines have been discussed in detail, focusing on the Savonius type VAWTs. Advantages of VAWTs over HAWTs have been summarised is feature to pick this type of turbine. The operating principle of VAWTs has been discussed. The performance characteristic of VAWTs has also been mentioned. Furthermore, the motivation to acrry out this study has been reported.

Chapter 2 consists of a detailed review of the research that has been carried out in the area of performance evaluation of VAWTs in various environmental conditions. A critical review of the literature available for the erosion in VAWTs has been presented. Details of the scope of research are provided in the form of specific research objectives. Chapter 3 documents the fundamental principles of Computational Fluid Dynamics. It includes the CFD modelling of the VAWTs, including the solver settings and the appropriate boundary conditions that have been specified to solve the flow domain. The meshing technique that has been used for the flow domain has been discussed. A detailed discussion on the sliding mesh technique used for the rotation of the rotor blades has been presented. The erosion modelling employed in the CFD solver is the highlight of the chapter.

Chapter 4 includes the mesh independence testing, time step size independence testing and the validation of the CFD results. Furthermore, transient and instantaneous performance of a VAWT has been evaluated under clean environmental conditions. Furthermore, this chapter sheds light on the flow structure in the vicinity of the VAWT through analysing and investigating the pressure fields, velocity fields and the flow pathlines. A generic semi-empirical prediction tool that accounts for the variations in the geometric configurations of the VAWT.

Chapter 5 is related to the erosion in VAWTs. This is of particular importance to VAWT designers who wish to install VAWTs in dusty environments, such as desserts, where wind velocities are significantly higher than in urban areas. Various dusty environmental conditions have been numerically created, comprising of different sand particle sizes and mass flow rates. Their effects on the performance degradation has been critically analysed in this study. Furthermore, erosion rates on rotor blades of the VAWT have been recorded. The results obtained have then been used in order to develop a novel semi-empirical prediction model for the torque generation from the VAWT that takes into account various sand particles' parameters.

Chapter 6 concludes the findings of this study, clearly mentioning the goals achieved and additions to the existing knowledge about VAWTs in terms of both the optimal design and the condition monitoring of VAWTs. Recommendations for future work have also been included.

CHAPTER 2
LITERATURE REVIEW

The following chapter provides a detailed review of the available literature in the field of wind engineering with emphasis on the performance characteristics of Vertical Axis Wind Turbines operating in various environmental conditions. The main areas addressed in this chapter are associated to the flow diagnostics of VAWTs that form the basis of this thesis. Within each of these areas, specific limitations have been identified which have been used to define the scope of the research. From the scope, specific research objectives of this thesis are provided such that efforts are made to provide novel contributions in each of the areas investigated.

2.1 Introduction

Energy is a part of everyday life. Diminishing reserve of fossil fuel and the concern about the pollution caused by this fuel, the demand of sustainable renewable energy becomes greater every year. There are many on-going researches to find suitable renewable and environment friendly sources such as solar, wind, hydro energies etc. Renewable energy remains in the developmental stages with a strong focus on wind power. Wind power is widely recognized by various researchers, including Mohammed et al. [29], as a cost-effective, clean, renewable and sustainable source of energy.

Wind power involves converting the kinetic wind energy into electrical energy using wind turbine. Since 5000BC, people have been using wind power via windmill to pump water and grind grains. While wind turbines are recognised as providing a viable alternative source of energy, wind farms are being developed and employed in various environmental conditions. In general, a wind turbine consists of number of blades. Performance of these blades defines the performance of the wind turbine.

Working environment has a great impact on the performance and the life span of wind turbines. In different environment and operating conditions, the performance of blades varies. Urban environment, contaminated with various chemical components may corrode the blade. In the coastal area humidity in the air can also have impact on the blade life span. Moreover, in dusty environments, like in desserts, the constant impingement of sand particles on the blades of a wind turbine can cause erosion on the blades, which significantly degrades its performance output. Blackwell [30] drew concerns regarding the impact erosion had on the blades that emanate from the rotor, which centres the turbine. Tabassum-Abbasi et al. [1] pointed out that despite the widespread enthusiasm for the potential of wind energy, there are concerns relating to the degradation of performance due to dust accumulation on blade surface areas. The blade erosion and the dust accumulation on the blade surface concerns highlighted significant elements towards this research study.

An examination of the effects of erosion on the surface of wind turbine blades based upon a review of relevant literature is presented. Khalfallah et al. [31] pointed out that a number of studies have investigated the effect of erosion on rotor blades with a focus on horizontal axis wind turbines. However, the present study explores sand erosion on the blades of a Vertical Axis Wind Turbine (VAWT). Examining the effects of erosion on blades provide an opportunity to analyse erosion on leading edges, as well as the tools and techniques that can be employed to diminish this effect. Furthermore, a Computational Fluid Dynamics (CFD) model has been developed to predict performance degradation in VAWTs operating in Sahara Desert; an environment in which erosion due to sand and dust storms is common.

This chapter of the study starts with a critical review of the published literature regarding the performance evaluation of VAWTs in clean environments, extending to the effects of dusty environments on VAWT's performance. A variety of analytical, experimental and numerical studies has been presented here that discuss both the qualitative and quantitative evaluation of erosion on wind turbine blades.

2.2 Performance Evaluation of Vertical Axis Wind Turbines operating in Clean Environments

Blades are a critical component of a VAWT and have been the focus of many recent researches in this field. Park et al. [32] focused on blade faults, noting that most of the available studies in the literature presuppose a single fault in the blades of wind turbines, such as a missing blade, a deformed blade etc. Using two different faulty conditions simultaneously, Park et al. estimated the contribution of each fault on the performance output of a VAWT. It has been found that the presence of faults in rotor blades have adverse impacts on torque output of VAWTs. Furthermore, CFD based analysis has demonstrated that as faults multiplies, performance output decreases substantially. Park [33] has further researched on the development of a performance prediction model for the VAWT that takes into account the effects of the geometric parameters of the VAWT. These geometric parameters are the blade angles, the number of blades in the VAWT and the size of the rotor/stator sections of the VAWT. It has been concluded that CFD based solvers can detect various faults, like slits in blades, with reasonable accuracy.

Park et al. [34] carried out numerical studies on the performance of vertical axis turbines by modifying their geometric features. According to their findings, the optimum operating condition for a vertical axis turbine occurs at a tip speed ratio of 0.17, which corresponds to maximum turbine power output. Figure 2.4 depicts the effect of TSR (Tip Speed Ratio) on the average torque and power output of a vertical axis turbine for one complete revolution of the turbine. The torque output decreases with increasing TSR. On the other hand, the average power output initially increase upto a certain value (optimal operating condition). After that, the power output starts to decrease as the value of TSR keeps on increasing along with the reduction of torque output.

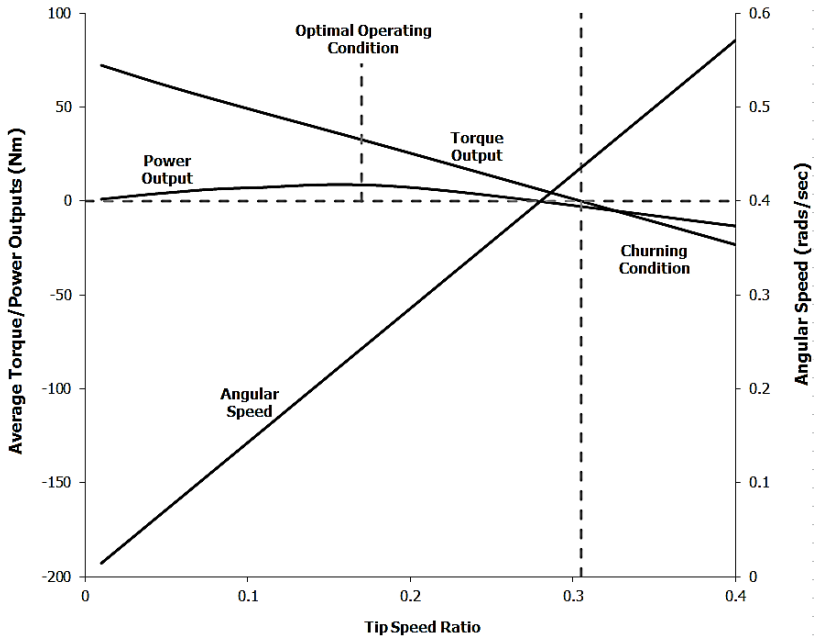

Figure 2.1 Average torque/power output variations w.r.t. tip speed ratio [34]

Where Park et al.'s research focuses on the rotor blades, Asim et al. [35] found that the flow field near the vertical axis turbines is considerably affected by the design and the shape of stator blades. Asim et al. [35] examined the effects of the shape of stator blades on the performance output of a vertical axis turbine, demonstrating that curved stator blades' performance output is higher as compared to straight stator blades. Hence, the study has explored the effects of the shape of guide vanes (stator blades) on a turbine's performance.

A number of studies have examined various aspects of the performance of VAWTs. Specifically, Shahzad et al. [36] examined the VAWT's performance under accelerating and decelerating flows, observing that the acceleration/deceleration of the wind changes the nature of the flow field in the vicinity of the VAWT, potentially degrading its life cycle. VAWT's performance has been evaluated using numerical simulations, based on advanced CFD tools, under accelerated and decelerated wind gusts of $1.09 m/s^2$ corresponding to change in flow velocity from 4m/sec to 10m/sec. It has been found that instantaneous torque output varies significantly under gusting conditions. Furthermore, it has been concluded that abrupt changes in instantaneous torque output of a wind turbine are linked to heavy stresses on the turbine structure, which can cause structural failure in extreme conditions.

Shahzad et al. [37] have also explored aspects of condition based monitoring in VAWTs. Effects of cracks in wind turbine blades have been numerically investigated and their impact on the performance of the VAWT has been evaluated. It has been observed that the cracks in VAWT's blades affect the aerodynamic performance of the blades, and the flow field around it. Cracks may also cause vibrations in the VAWT, which can further degrade VAWT's performance. It has been concluded that cracks of different shapes and sizes had different, and ultimately unpredictable, impact on the amplitude of the torque output of a VAWT.

Colley [38] focused on the design, operation and diagnostics of vertical axis wind turbines, both numerically and experimentally, in order to determine its operational characteristics. The study quantified the overall performance of Darrieus-type VAWTs to have a maximum torque coefficient of 1.7, and a power coefficient of 0.24. Furthermore, it has also been found that the stator blades' number, as a geometrical parameter, has a great impact on the torque and power outputs of the VAWTs.

Rotor blade position has been the focus of research by Colley et al. [39], who examined the performance output of three VAWT configurations using CFD. An inlet velocity of 4m/sec has been specified along with tip speed ratios ranging from zero to 0.6. The effects of varying rotor blade position on global performance parameters and local flow fields have been quantified. Results reported by Colley et al. indicate that within a typical rotor blade passage, maximum torque is obtained at a unique rotor angle. Furthermore, torque output of a turbine decreases with an increase in rotor tip speed ratio for all rotor blade positions.

A related study by Colley et al. [40] examines performance characteristics of a novel VAWT designed for urban settings. Using a full-scale prototype and CFD package Fluent, a turbine located at the exit of a 0.6m x 0.6m wind tunnel section has been investigated for its performance characteristics. Results obtained indicate that Multiple Reference Frame (MRF) modelling

technique under–predicts rotor torque at high rotor speeds, and hence cannot predict rotor suction effects. Colley et al. concluded that the primary factor affecting rotor's torque output might be the variations between experimental and computational velocity fields.

Colley et al. [41] further conducted a theoretical study on the performance evaluation of three different cross-flow VAWT configurations using a two dimensional CFD model and a quasi-steady MRF approach. The three variants were subject to an inlet velocity of 4m/sec and tip speed ratios in the range of 0 to 0.6. Results indicate a clear reduction in torque output as the number of stator and rotor blades in the VAWT reduced.

Aforementioned studies primarily focus on VAWT's performance with variables such as blade shape, blade faults, tip speed ratios etc. More attention has been paid onto the torque/power outputs of the VAWT, rather than a critical understanding of the complex flow phenomena occurring within and in the vicinity of VAWTs. Furthermore, most of the studies are based on simplified modelling techniques, such as quasi-steady MRF approach. Hence, the author feels convinced that a more rigorous flow field analysis needs to be carried out, based on advanced transient modelling techniques, such as Sliding Mesh. Furthermore, although the literature does include torque prediction tools accounting mostly the geometric variations in the VAWT, however, a generic torque prediction model needs to be developed that depends on the instantaneous geometrical positioning of the rotor blades within the VAWT, where this prediction model can be used as a basis to develop further prediction models that can quantify the effects of varying geometrical features of the VAWT.

2.3 Performance Evaluation of Vertical Axis Wind Turbines operating in Dusty Environments

Erosion is one of the problems that have a direct impact on the performance of wind turbine blades in dry dusty environments, leading up to 50% of power losses per year. It causes roughness on wind turbines via airborne dirt, debris and insects causing significant negative impact on wind turbine performance. Such effects are primarily observed on the leading edge surfaces of the blades. Generally, these impacts wear the leading edge surface by creating a rough and pockmark.

Gharali et al. [42] conducted studies examining a range of erosion characteristics on NACA profiles, in which erosion has been simulated with two thicknesses (12% and 25%; $t_A/t=t_B/t=0.12$ and $t_C/t=0.25$) and two lengths (4% and 14%; $h_A/C=0.14$ and $h_B/C=h_C/C= 0.04$). Authors have found that the eroded areas usually have sharp edges. Three different conditions have been modelled to study the effects of the length and the thickness of the erosion. These models of leading edge blades are shown in figure 2.2.

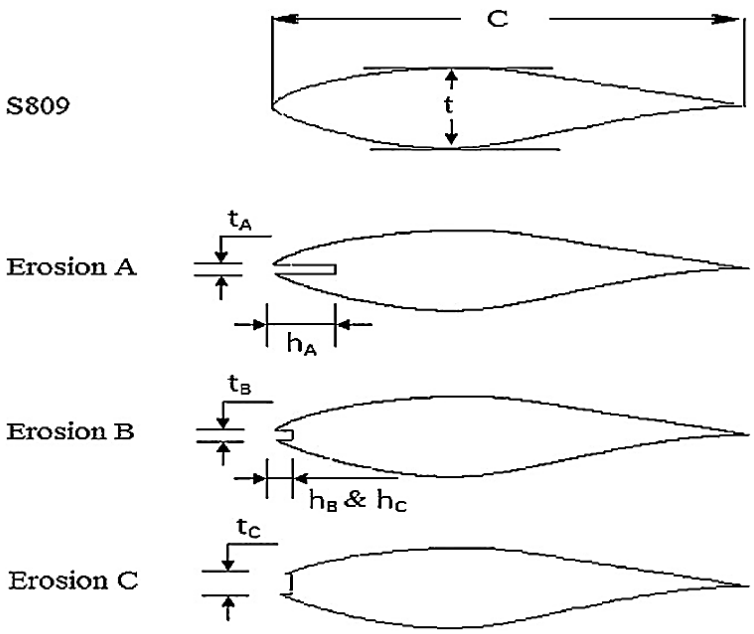

Figure 2.2 Models of Leading Edge Blade Erosion [42]

Only the leading edge area of the affected blades presents some indication of erosion. According to erosion simulation results, authors found that the lift coefficient decreases when $Re=10^6$, as shown in figures 2.3 and 2.4. The average/maximum values of the reduction in lift for erosions A, B and C are 17/48%, 20/51% and 34/76% respectively, as compared to smooth S809 profile. The erosion thickness affects the aerodynamic performance of the profiles substantially. Subsequently, it has also been identified that the erosion primarily decreases the lift coefficient when the blade is travelling leewards.

The results illustrate that the erosion thickness has significant influence on the lift coefficient as compared to the length of the erosion. The erosion depicted at the leading edge alters the standard shape of the blades, and when significant erosion occurs, the characteristics of the dynamic action of the wind turbine are impacted. Overall, the results of the investigation demonstrate that a reducing lift coefficient is derived from the erosion thickness, rather than the length of the eroded surface, leading to a significant decrease in efficiency. One consequence identified by Gharali et al. is the dynamic stall phenomena, based on the smooth S809, which can no longer be predicted. The average/maximum lift coefficient decrease has been observed at 34%/76% for the thickest erosion assumed. These variations in lift demonstrate that under extreme erosion, the performance of the wind turbine blades is highly affected.

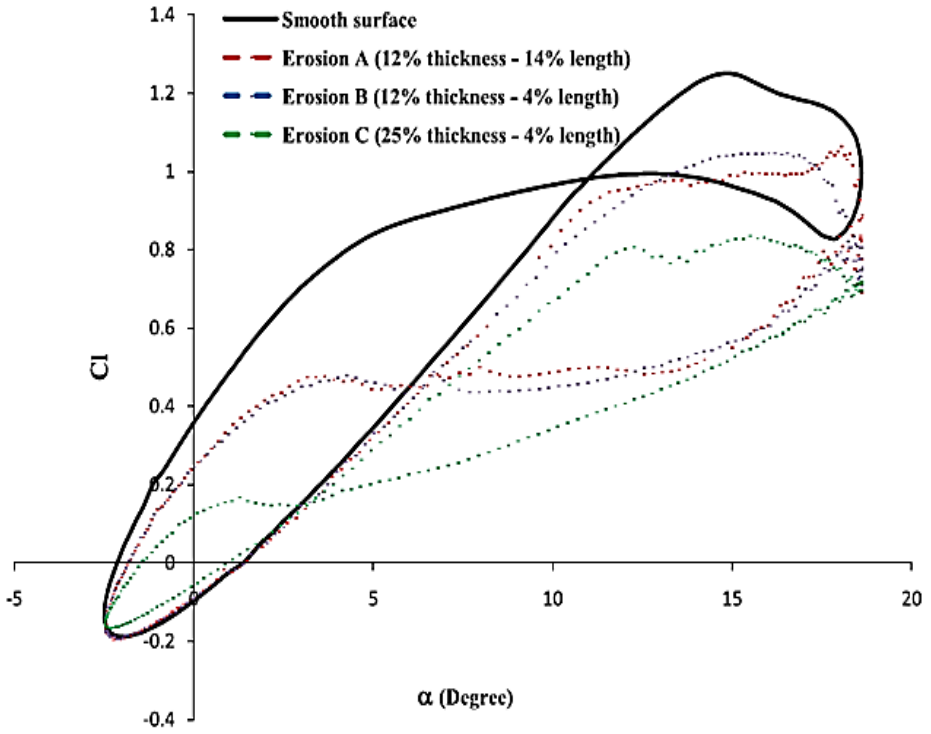

Figure 2.3 Lift Coefficients for Smooth and Eroded S809 for Reduced Stall, Re=106 [42]

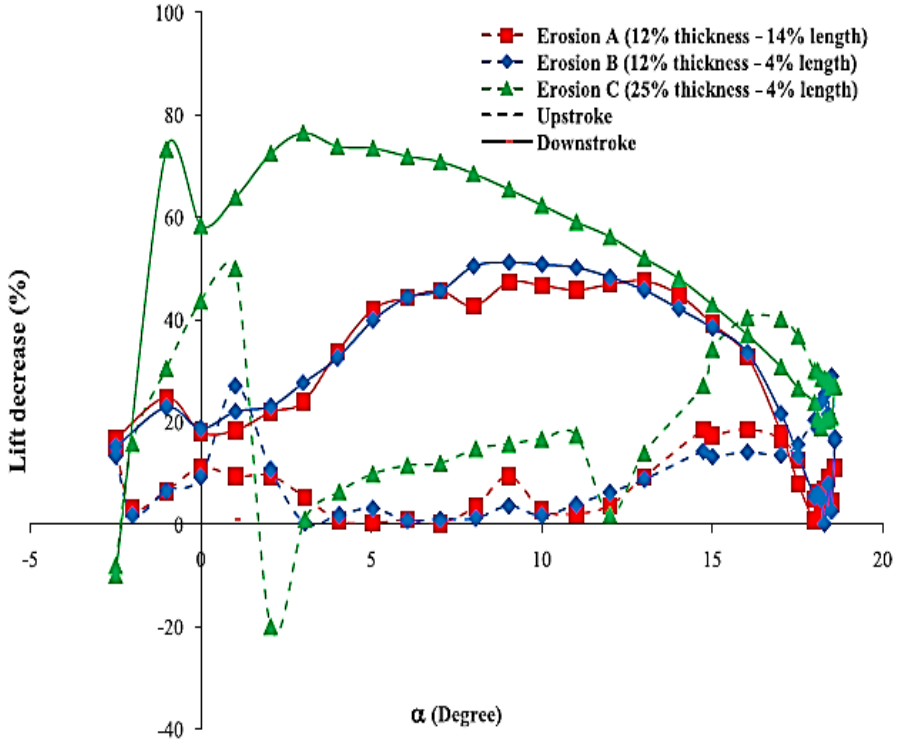

Figure 2.4 Lift decrease for Smooth and Eroded S809 for Reduced Stall, Re=106 [42]

Research by Hameed et al. [18] examines a number of scholarly studies on erosion and deposition, and their effects on turbomachines, as well as their association in degradation of engine performance linked to particulate matter ingestion. There are several mechanisms described that are known to contribute to particle ingestion in gas turbine engines. Solid as well as molten particles are often produced during the combustion process via the burning of heavy oils or synthetic fuels. Aircraft engines are known to encounter and experience negative effects from particles transported by sandstorms into the upper atmosphere. Thus, when turbomachines are located at lower levels or in proximity to the surface, it is likely that erosion will occur since the particulate impact will be greater. According to Hameed et al. [18] it has been observed that erosion on turbomachines, including wind turbines, are influenced by various factors such as particle characteristics, gas flow path, blade geometry, operating conditions and blade material. The coatings applied to the material of the components are also linked to various erosion related effects.

Erpul et al. [43] investigated the effects of wind driven rain on the erosion processes. Rain falls with a vertical velocity component, however, with the influence of wind acting on the rain, raindrops gain some degree of horizontal velocity component as well. Therefore, when the rain strikes the soil, particles shear off. The same effect occurs on the wind turbine blades. As the sand particles strike the blades, the velocity magnitude of the wind sheds material off the blade. This phenomena must occur continuously on the same region/s of the blades for erosion to take place.

Keegan et al. [2] pointed out that the unpredictable and potentially volatile operating environmental conditions present great challenges to the development in wind technology, with respect to erosion issues on the leading edge of the wind turbine blades. Rain droplets and hailstones have been identified by Keegan as a prime focus in the research area on the erosion of the wind turbine blades.

Other studies, such as that of Ren et al. [44] have investigated the effect of dust particles interaction with wind turbine blades' performance, and so as by Salem et al. [3]. The following explores these studies in further detail, demonstrating how vulnerable wind turbine blades are to numerous eroding particles, which varies according to the external environment and the position of the wind turbine itself.

It is of special significance that the rotor blades airfoil designs are examined rigorously for erosion. This is in order to obtain and provide a better understanding of the blade surface roughness effect, originating due to erosion, on the performance of wind turbines with thick airfoils. In general, researchers assert that roughness is a direct consequence of erosion, due to dust and other particulates, since they have a substantial effect on the entire dynamic flow process. Hence, for this reason, it is necessary to analyse strategies for overcoming such effects and creating more efficient designs for wind turbine blades.

Airfoils are crucial to the rotor design of wind turbines. One of the most critical problems for all wind turbine rotors, regardless the environment in which they are found in, is the accumulation of dust particles on blade surface areas resulting degradation of performance and the

unpredictability of stall. Ren et al. [44] studied the dust accumulation effect and the resulting performance degradation of NACA 63-430 airfoils under different operational periods. It has been concluded that numerical simulations provide economical investigative tools in order to analyse the effects of dust on the performance of wind turbines.

A number of studies focus on dusty environments and the degradation of wind turbine airfoils. Ren et al. conducted investigations on incompressible viscous flow past the wind turbine's two-dimensional airfoil under clean and rough surface conditions. NACA 63-430 airfoil, which is widely used in wind turbines, has been chosen for analysis. Generally, this airfoil is positioned at the mid-span of the blade with a thickness to chord length ratio of 0.3. The findings indicate that the roughness brought about by particulate impact promoted premature transition to turbulence and flow separation, thereby reducing the performance efficiency of wind turbines.

The work carried out by Salem et al. [3] sought to employ the Computational Fluid Dynamics (CFD) based modelling approach to enable wind turbine designers to predict energy losses under harsh operating conditions. The research is particularly relevant in the context of the harsh desert environment found in the countries of the MENA (Middle East and North Africa) region. After the wind turbines have been installed in such environments, their rotors have been observed to suffer significant performance degradation and unpredictability of stall, because of erosion and dust accumulation. Dust has been identified as causing problems and inefficiencies for wind turbines that operate in coastal areas, such as Hurghada and Zafarana in Egypt, where wind energy is being embraced as a cost effective alternative to fossil fuels.

The study carried out by Khakpour [45] explored the effects of sand particles, in dusty environments, on the performance evaluation of wind turbines. This work is useful in demonstrating how sand particles impact upon drag and lift coefficients of the airfoils. Much of the literature tends to focus on horizontal rather than vertical axis wind turbines, the reason being insufficient attention given to vertical axis wind turbines, and the effects of dust on their performance. This has motivated the author of this study to carry out detailed numerical investigations on the erosion effects in VAWTs.

Although on an annual basis, it has been observed in eroded blades and airfoils, that there are power losses of up to 50%; limited research focuses on this critical issue. There are a limited number of studies dealing with the impact of dust erosion on wind turbines. Considering that the majority of wind turbines are installed in northern countries, where dust does not pose significant problems to wind turbines' operations, the problem of dust contamination has been given limited attention in the empirical research as well. A number of studies, however, have dealt with the accumulation of ash particles and powder deposits on turbine blades, particularly with the use of low-grade fuels.

An experimental study by Khalfallah et al. [31] on the impact of blade surface roughness due to dust accumulation has been carried out. For continuity of the data collection, the experimental data has been recorded in the operational period only. Hence, the dust accumulation and energy output data has been recorded from May to November 1999. Analysing the dust accumulation data from the experiments revel that with increase of dust accumulation on the blades, the drag

force on the airfoil increases, and lift force decreases, leading to reduction in turbine's power output. Moreover, it has also been found out that the dust particle size has significant impact on the blade's surface roughness over time. With increase in dust particles size, the power output of wind turbine decreases.

A study carried out by Khakpour [45] reports that the performance of wind turbines are affected by environments in which sand concentration over the surface of the blade is brought about by airflows. Previously, the effects of monitoring parameters such as sand dimensions, sand/air drift velocity and sand/air mass flow rate ratios have been studied. These results have been compared against uniform performance, under other less invasive and damaging conditions. This research has been conducted employing numerical simulations. Pressure distribution over the blade surface, drag and lift coefficients, and the erosion due to the collision of sand particles with the blade surface for several angles of attack has been studies. Khakpour concluded that the computational model is a useful instrument for assessing erosion in wind turbines.

According to El Batsh [46], modelling is useful for identifying particle deposition on compressor and turbine blade surface. The effects of ash particle deposition on the performance of turbine cascade blades has been studies using the deposition model. The model includes three principle processes i.e. particle transport to the blade surface, particles sticking to the surface and particle separation from the surface. The study calculated the deposition model in three periods of 12 hours each. After each period, the fouled blade profile has been calculated, and the flow field has been analysed. The particle deposition calculations are repeated to account for the unsteady conditions. The flow field has been calculated for the blade that had fouled after 36 operating hours to investigate the effects of deposition on the performance of the blades. The surface velocity and the downstream total pressure have also been analysed.

Work by El Batsh reveals that the particles smaller than 100μm, stick to the surface upon impact. For larger particles, the probability of sticking depends on particle size, particle impact velocity and temperature. The particle thermal response time relates the time required for a particle to respond to the changes in the fluid temperature. The sticking coefficient is the mass fraction of the incident ash, which remains on the surface. When the dependence of the sticking coefficient on the thermal response time was studied, three regions were distinguished i.e. perfect sticking region, cooling affected-region and cooling unaffected-region.

According to El Batsh, a new grid has been generated for the fouled blade after 12 operating hours. The deposition model predicted a thick deposit on the blade pressure surface in the vicinity of the leading edge. It has been stated that the thick deposit is unrealistic, and will be removed by the fluid flow due to gross detachment of particles. Hence, it has not been considered in this study. Figure 2.5 depicts the new structured two-dimensional grid that was generated for the fouled blade with a total number of approximately 17,000 cells.

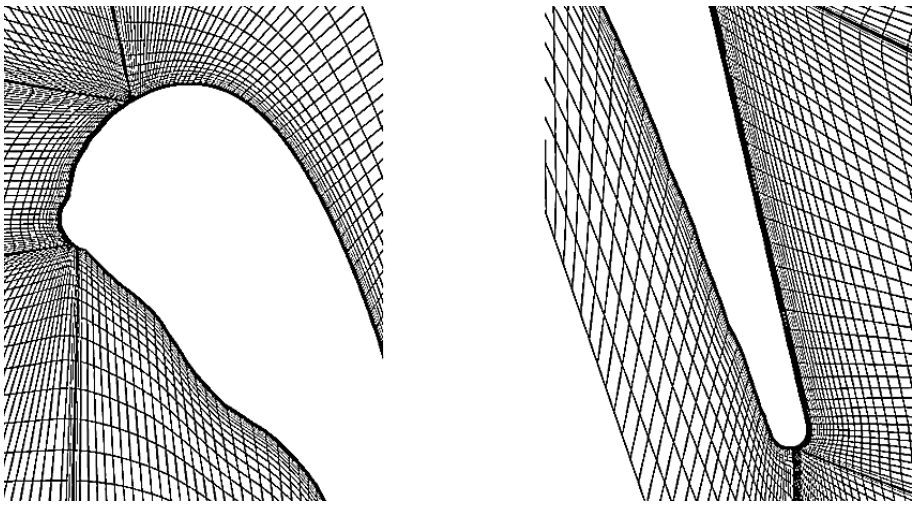

Figure 2.5 Computational Grid [46]

The deposition model has been used to study the effect of particle deposition on turbine blades' performance. The majority of the previous deposition models are based on the assumption of perfect-sticking of the particles at the surface without deposit detachment. These are theories of particle transport whereby the approach does not consider sticking behaviour due to the physical and the chemical characteristics of the gas, the entrained particles and the surface. Hence, these are inadequate and generally results in over-predicted deposition rates.

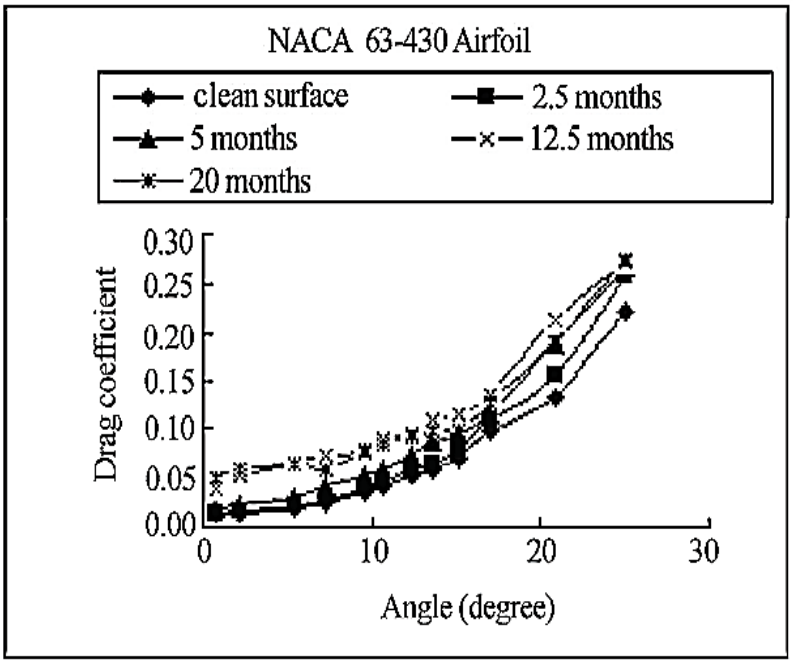

Figure 2.6 Comparison of Drag Coefficient Curves during Different Operation Periods [46]

2.4 Scope of Research

The literature review presented in this chapter has shown that erosion is serious issue in Vertical Axis Wind Turbines that causes roughness on the blades via airborne dirt, debris and insects. Erosion has been shown to degrade the performance characteristics of a VAWT significantly. A number of different strategies have been employed to analyse erosion in VAWTs, and with the advent of powerful and advanced computational methods, it has become possible to investigate erosion at microscopic levels. Hence, this study is based on the predictions from numerical simulations performed using a Computational Fluid Dynamics based solver.

The first aspect of this study comprises of detailed numerical investigations on the performance evaluation of VAWTs operating in clean environments. Although many numerical studies are available in this particular area, however, most of these studies use rather simplified modelling techniques. The results presented in this study are based on transient modelling approaches, where instantaneous pressure and velocity fields have been computed and analysed. Furthermore, instantaneous torque output of the VAWT has been recorded in order to develop a generic semi-empirical prediction tool that accounts for the variations in the geometric configurations of the VAWT.

The second aspect of this study is related to the erosion in VAWTs. This is of particular importance to VAWT designers who wish to install VAWTs in dusty environments, such as desserts, where wind velocities are significantly higher than in urban areas. Various dusty environmental conditions have been numerically created, comprising of different sand particle sizes and mass flow rates. Their effects on the performance degradation has been critically analysed in this study. Furthermore, erosion rates on rotor blades of the VAWT have been recorded. The results obtained have then been used in order to develop a novel semi-empirical prediction model for the torque generation from the VAWT that takes into account various sand particles' parameters.

2.5 Research Objectives

Based on the research aims presented in the previous chapter, and after conducting a detailed literature review, the following objectives have been formulated which will aid the research aims and address the issues in the existing knowledge:

1. Flow diagnostics and Performance Characteristics evaluation of the VAWT operating in a clean environment

2. Flow diagnostics and Performance Characteristics evaluation of the VAWT operating in various dusty environments

3. Development of a novel semi-empirical torque prediction tool accounting a range of different operating environments for the VAWT

In order to satisfactorily achieve the aforementioned research objectives, this study uses Computational Fluid Dynamic tools to numerically simulate the flow within and in the vicinity of a VAWT. The next chapter presents the numerical modelling techniques being incorporated in this study.

CHAPTER 3
NUMERICAL MODELLING OF VERTICAL AXIS WIND TURBINES

In order to investigate the research objectives of this study that have been identified in the previous chapter, advanced CFD techniques have been used to computationally simulate the transient flow of air in the vicinity of a VAWT. Sliding mesh technique has been used in order to rotate the rotor blades of the VAWT with respect to the stator blades. For this purpose, appropriate solver settings and boundary conditions needs to be specified, that are discussed in this chapter. Furthermore, Discrete Phase Modelling and Erosion Modelling for creating different environmental scenarios have been discussed in detail, and are the highlights of this chapter.

3.1 Introduction to Computational Fluid Dynamics

Computational Fluid Dynamics or CFD is the analysis of systems involving fluid flow, heat transfer and associated phenomena such as chemical reactions by means of computer-based simulation. The technique is very powerful and spans a wide range of industrial and non – industrial application areas. From the 1960s onwards, the aerospace industry has integrated CFD techniques into the design, R&D and manufacture of aircraft and jet engines. More recently, the method has been applied to the design of internal combustion engines, combustion chambers of gas turbines and furnaces. Furthermore, motor vehicle manufacturers now routinely predict drag forces, under – bonnet air flows and the in – car environment with CFD. CFD is becoming a vital component in the design of industrial products and processes.

The variable cost of an experiment, in terms of facility hire and/or person – hour costs, is proportional to the number of data points and the number of configurations tested. In contrast, CFD codes can produce extremely large volumes of results at no added expense, and it is very cheap to perform parametric studies, for instance, to optimise equipment performance.

3.2 Working of CFD Codes

There are three distinct streams of numerical solution techniques. They are finite difference, finite element and spectral methods. Finite volume method, a special finite difference formulation, is central to the most well established CFD codes. The numerical algorithms include integration of the governing equations of fluid flow over all the control volumes of the domain, discretisation or conversion of the resulting integral equations into a system of algebraic equations and the solution of these equations by an iterative method.

CFD codes are structured around the numerical algorithms that can tackle fluid flow problems. In order to provide easy access to their solving power, all commercial CFD packages include sophisticated user interfaces to input problem parameters and to examine the results. Hence, all codes contain three main elements. These are:

- Pre – Processor
- Solver Execution
- Post – Processor

Pre – processing consists of the input of the flow problem to a CFD programme by means of an operator – friendly interface and the subsequent transformation of this input into a form suitable for use by the solver. The user activities at the pre – processing stage includes definition of the geometry of the region of interest. It is called the computational domain. Grid generation is the sub – division of the domain into a number of smaller, non – overlapping sub – domains. It is

also called Mesh. Selection of the physical or chemical phenomena that needs to be modelled, definition of fluid properties and the specification of appropriate boundary conditions at cells, which coincide with or touch the domain boundary, are also included in pre – processing [47].

The solver primarily consists of setting up the numerical model and the computation/monitoring of the solution. The setting up of the numerical model includes the following:

- Selection of appropriate physical models. These included turbulence, combustion, multiphase etc.
- Defining material properties like the fluid, solid, mixture etc.
- Prescribing operating conditions
- Prescribing boundary conditions
- Prescribing solver settings
- Prescribing initial solution
- Setting up convergence monitors

The computation of the solution includes:

- The discretised conservation equations are solved iteratively. A number of iterations are required to reach a converged solution.
- Convergence is reached when change in solution variables from one iteration to the next is negligible. Residuals provide a mechanism to help monitor this trend.
- The accuracy of the converged solution is dependent upon problem setup, grid resolution, grid independence, appropriateness and accuracy of the physical model.

Figure 3.1 describes the working of the solver.

Post processing comprises the examination of the results obtained and revision of the model based on these results. These can be further elaborated into:

- Examine the results to view solution and extract useful data.
- Visualization tools can be used to extract the overall flow pattern, separation, shocks, shear layers etc.
- Numerical reporting tools are used to calculate quantitative results like forces, moments, and average heat transfer co-efficient, flux balances, surface and volume integrated quantities.
- Are physical models appropriate?
- Are boundary conditions correct?
- Is the grid adequate?

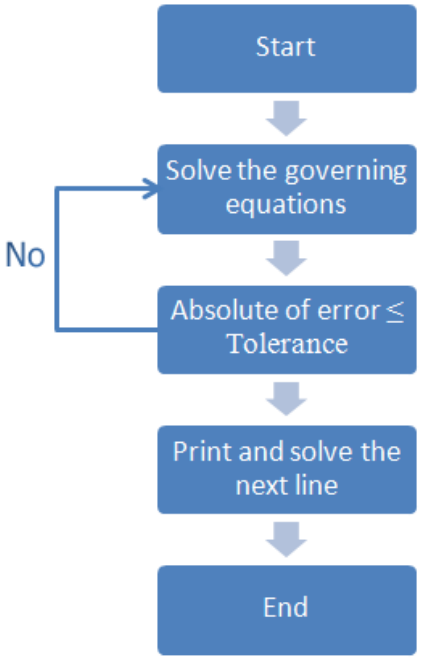

Figure 3.1 CFD Solver

- Can grid be adapted to improve results?
- Does boundary resolution need to be improved?
- Is the computational domain large enough?

Due to the increased popularity of engineering workstations, many of which have outstanding graphic capabilities, the leading CFD packages are now equipped with versatile data visualisation tools. These include domain geometry, grid display, vector plots, line and shaded contour plots, 2D and 3D surface plots, particle tracking, view manipulations, colour post – script output etc. more recently these facilities may also include animation for dynamic result display, and in addition to graphics, all codes produce trusty alphanumeric output and have data export facilities for further manipulation external to the codes. As in many other branches of CAE, the graphics output capabilities of CFD codes have revolutionised the communication of ideas to the non – specialists. An overview of CFD modelling is presented in figure 3.2.

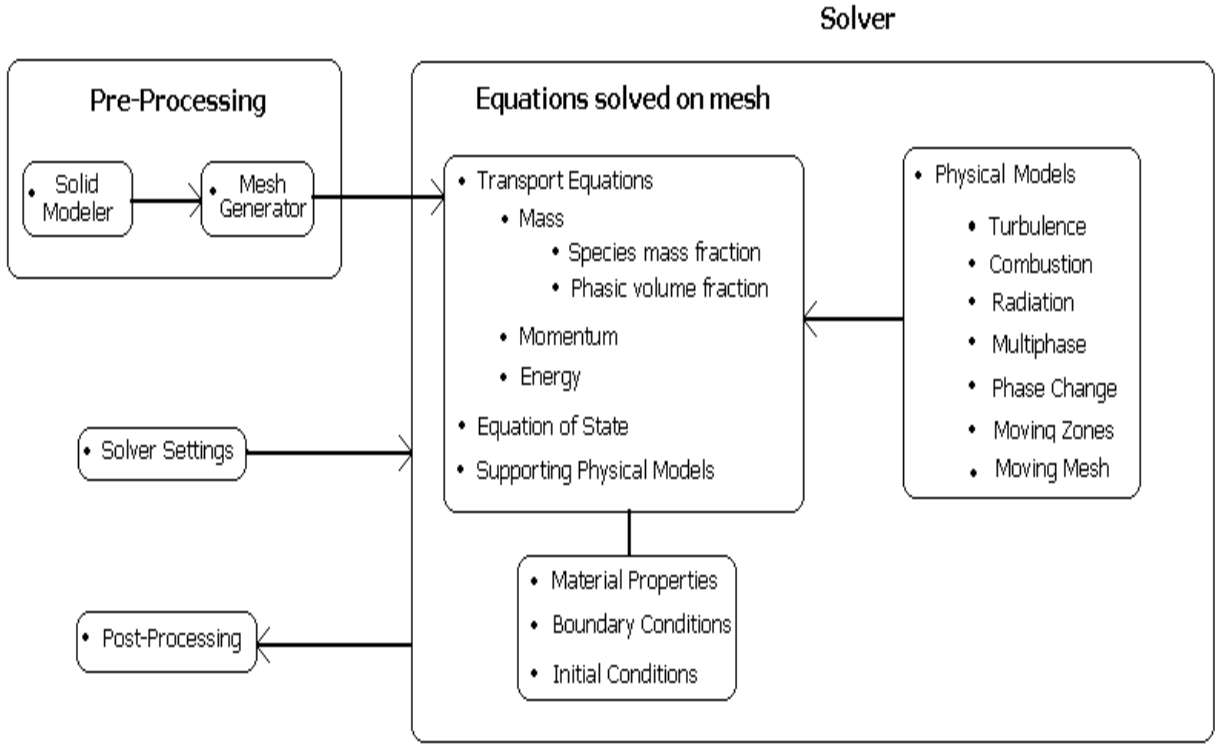

Figure 3.2 Overview of CFD Modelling [48]

3.3 Numerical Formulation of Fluid Flow

The governing equation of fluid flow represents mathematical statements of the conservation laws of Physics:

- The mass of a fluid is conserved.

- The rate of change of momentum equals the sum of the forces on a fluid particle. (Newton's second law)

- The rate of change of energy is equal to the sum of the rate of heat addition to and the rate of work done on a fluid particle. (First law of thermodynamics)

The fluid is regarded as a continuum. For the flow diagnostics at macroscopic length scales, the molecular structure of matter and molecular motions may be ignored. The behaviour of the fluid is described in terms of macroscopic properties such as velocity, pressure, density and temperature etc. These are averages over suitably large numbers of molecules. A fluid particle or point in a fluid is then the smallest possible element of fluid whose macroscopic properties are not influenced by individual molecules.

3.3.1 Conservation of Mass

The mass balance equation for the fluid element can be written as [49]:

$$\begin{matrix} Rate\ of\ increase\ of\ mass\ in \\ fluid\ element \end{matrix} = \begin{matrix} Net\ rate\ of\ flow\ of\ mass\ into \\ fluid\ element \end{matrix} \tag{3.1}$$

For liquids, as the density is constant, the mass conservation equation is:

$$Div\ V = 0 \tag{3.2}$$

This equation describes the net flow of mass out of the element across its boundaries. The above equation in longhand notation can be written as:

$$\frac{\partial u}{\partial x} + \frac{\partial \mathrm{v}}{\partial y} + \frac{\partial w}{\partial z} = 0 \tag{3.3}$$

This equation represents the steady, three dimensional mass conservation of the fluid or continuity at a point in an incompressible fluid.

3.3.2 Conservation of Momentum

Newton's second law states that the rate of change of momentum of a fluid particle equals the sum of the forces on the particle [50]:

$$\begin{matrix} Rate\ of\ increase\ of\ Momentum\ of \\ the\ fluid\ particle \end{matrix} = \begin{matrix} Sum\ of\ forces\ acting\ on\ the \\ fluid\ particle \end{matrix} \tag{3.4}$$

There are two types of forces on fluid particles. These are surface forces and the body forces. Surface forces include pressure, viscous and gravity forces while body forces include centrifugal,

coriolis and electromagnetic forces. It is a common practice to highlight the contributions due to the surface forces as separate terms in the momentum equations and to include the effects of body forces as source terms.

The x – component of the momentum equation is found by setting the rate of change of x – momentum of the fluid particle equal to the total force in the x – direction on the element due to surface stresses, plus the rate of increase of x – momentum due to sources. The equation is as follows:

$$\rho g_x + \frac{\partial \sigma_{xx}}{\partial x} + \frac{\partial \tau_{yx}}{\partial y} + \frac{\partial \tau_{zx}}{\partial z} = \rho \left(\frac{\partial u}{\partial t} + u \frac{\partial u}{\partial x} + v \frac{\partial u}{\partial y} + w \frac{\partial u}{\partial z} \right) \quad (3.5)$$

The y and z – component of momentum equation are given by:

$$\rho g_y + \frac{\partial \tau_{xy}}{\partial x} + \frac{\partial \sigma_{yy}}{\partial y} + \frac{\partial \tau_{zy}}{\partial z} = \rho \left(\frac{\partial v}{\partial t} + u \frac{\partial v}{\partial x} + v \frac{\partial v}{\partial y} + w \frac{\partial v}{\partial z} \right) \quad (3.6)$$

$$\rho g_z + \frac{\partial \tau_{xz}}{\partial x} + \frac{\partial \tau_{yz}}{\partial y} + \frac{\partial \sigma_{zz}}{\partial z} = \rho \left(\frac{\partial w}{\partial t} + u \frac{\partial w}{\partial x} + v \frac{\partial w}{\partial y} + w \frac{\partial w}{\partial z} \right) \quad (3.7)$$

3.3.3 Navier – Stokes equations

In a Newtonian fluid, the viscous stresses are proportional to the rates of deformation. Liquids are incompressible; the viscous stresses are twice the local rate of linear deformation times the dynamic viscosity. The Navier – Stokes equations are [51]:

$$\rho g_x - \frac{\partial p}{\partial x} + \mu \left(\frac{\partial^2 u}{\partial x^2} + \frac{\partial^2 u}{\partial y^2} + \frac{\partial^2 u}{\partial z^2} \right) = \rho \left(\frac{\partial u}{\partial t} + u \frac{\partial u}{\partial x} + v \frac{\partial u}{\partial y} + w \frac{\partial u}{\partial z} \right) \quad (3.12)$$

$$\rho g_y - \frac{\partial p}{\partial y} + \mu \left(\frac{\partial^2 v}{\partial x^2} + \frac{\partial^2 v}{\partial y^2} + \frac{\partial^2 v}{\partial z^2} \right) = \rho \left(\frac{\partial v}{\partial t} + u \frac{\partial v}{\partial x} + v \frac{\partial v}{\partial y} + w \frac{\partial v}{\partial z} \right) \quad (3.13)$$

$$\rho g_z - \frac{\partial p}{\partial z} + \mu \left(\frac{\partial^2 w}{\partial x^2} + \frac{\partial^2 w}{\partial y^2} + \frac{\partial^2 w}{\partial z^2} \right) = \rho \left(\frac{\partial w}{\partial t} + u \frac{\partial w}{\partial x} + v \frac{\partial w}{\partial y} + w \frac{\partial w}{\partial z} \right) \quad (3.14)$$

3.4 Pre-Processing

Further details about computational fluid dynamics and difference turbulence models can be found in any good CFD book. For reader's interest, some books regarding CFD are recommended here [47-52]. The following sections provide details of the numerical modelling that has been used in the present study. The CFD package that has been used to achieve this is known as Ansys [53]. The pre-processing in CFD is subdivided into two main categories, i.e.

creation of the geometry and the meshing of the flow domain. This section provides details of the geometric modelling and the meshing of the hydraulic capsule pipelines.

3.4.1 Geometry of VAWT

A three dimensional vertical axis wind turbine model, similar to Colley [40], has been numerically created as shown in figure 3.3. The model has 12 rotor blades and 12 stator blades. The radius of the core region r_c=0.5m whereas the radius of the rotor and the stator regions i.e. r_r and r_s are 0.7m and 1m respectively. The height of the VAWT, h=1m.

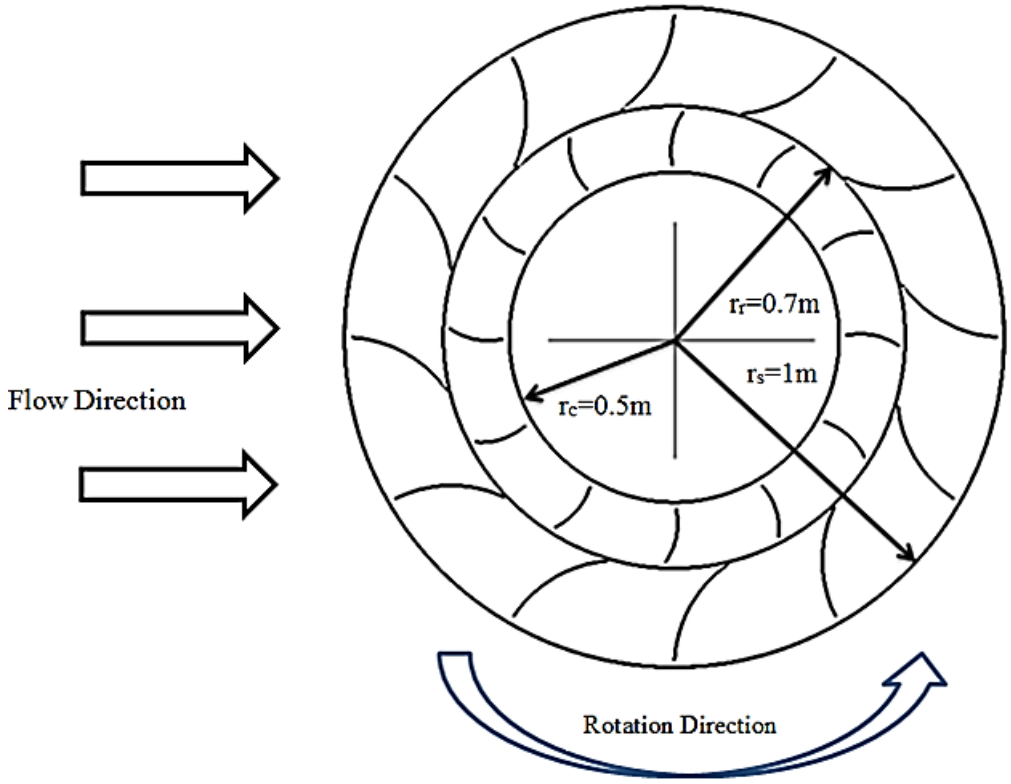

Figure 3.3 Geometry of the VAWT

Figure 3.4 shows the flow domain of the VAWT. The length, width and the height of the flow domain are 13m, 9m and 3m respectively. These dimensions have been taken from Colley and have been used here because the validation of the CFD results, presented in Chapter 4, will be carried out against the published results of Colley in the next chapter.

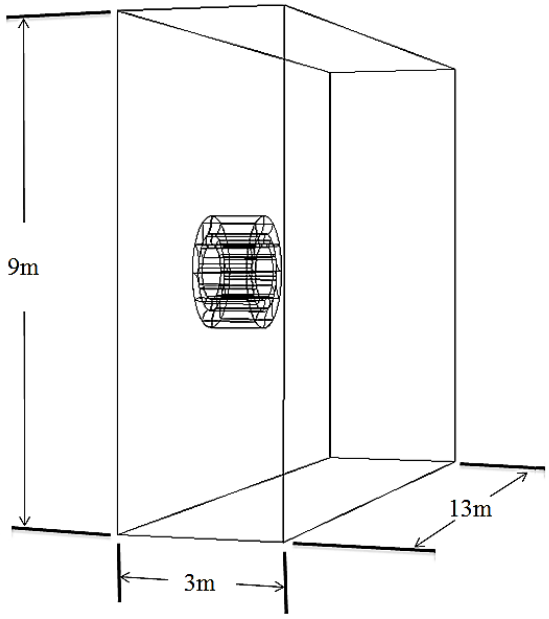

Figure 3.4 Flow Domain of the VAWT

3.4.2 Meshing of the Flow Domain

The mesh has been created in two different steps. Domain mesh has been controlled by global sizing function i.e. maximum size of 100mm and minimum size of 0.1mm. Stator, rotor and the core zones have been meshed for 30mm mesh sizing, whereas the rest of the flow domain has been meshed for 100mm mesh sizing. It has been observed that these mesh sizes give a balance between the accuracy of the results obtained, and time to simulate the flow around the VAWT. Figure 3.5 shows the mesh in the flow domain. Mesh independence testing has been carried out, and is discussed in Chapter 4.

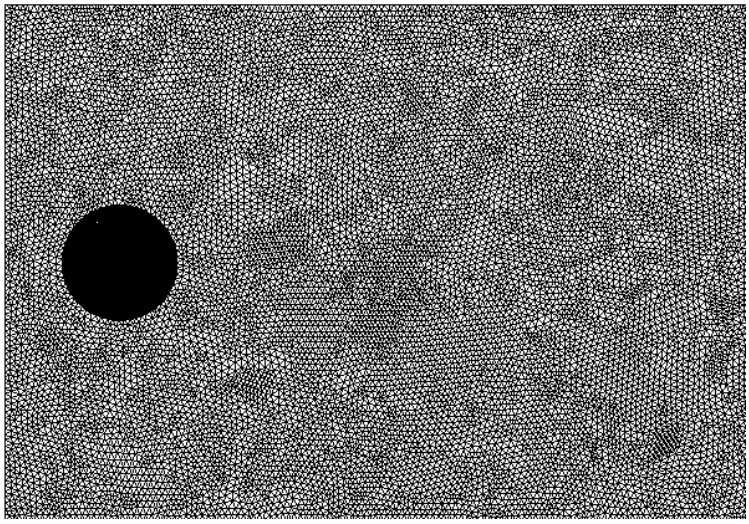

Figure 3.5 Mesh in the VAWT

3.5 Solver Execution

As the flow of air in the present study is at low speeds (4m/sec) which is the annual mean wind velocity in Huddersfield (UK), pressure based solver has been chosen for the flow diagnostics of VAWT. In this solver, the density of the fluid remains constant and the primary fluid flow parameter, that is being computed iteratively, is the pressure within the flow domain.

As the interaction between the stationary (stator) and rotating (rotor) frames of references is highly transient, an unsteady solver has been designed to simulate the flow of air. In addition to the aforementioned solver settings, there is a need to model the turbulence in the flow as well. This is because the investigations carried out in the present study focuses on the turbulent flow of air. The criteria for external flows (such as VAWT) to be turbulent is that the Reynolds number of the flow should be higher than 500,000. Furthermore, in practical applications of VAWTs, the velocity of the flow normally ranges from 2m/sec to 6m/sec. These velocities correspond to Reynolds number of 136,917 to 410,752 for the VAWT under consideration. Hence, the flow is turbulent and a turbulence model is required to predict the parameters of turbulence in the vicinity of the VAWT with reasonable accuracy.

There are many turbulence models available in the commercial CFD package that has been used in this study. Each one of these turbulence models has got its own advantages and disadvantages, which can be found out in any CFD text book. As far as VAWTs are concerned, due to the formation of a wake region downstream the VAWT, k-ω model has been chosen for the modelling of turbulence. The primary reason behind choosing k-ω model is its superiority in accurately modelling the wake regions and extreme pressure gradients. Most recent studies also show that k-ω turbulence model predicts the changes in the flow parameters in VAWTs with reasonable accuracy.

The k-ω is a two equation model that is further divided into two types. The first type is called Standard k-ω model whereas the second type is called Shear-Stress Transport (SST) k-ω model. In the present study, SST k-ω model has been chosen because it includes the following refinements:

- The standard k-ω model and the transformed k-ε model are both multiplied by a blending function, and both models are added together. The blending function is designed to be one in the near-wall region, which activates the standard k-ω model, and zero away from the surface, which activates the transformed k-ε model.

- The definition of the turbulent viscosity is modified to account for the transport of the turbulent shear stress.

These features make the SST k-ω model more accurate and reliable for a wider class of flows (e.g., adverse pressure gradient flows, aerofoils, transonic shock waves) than the standard k-ω model. Other modifications include the addition of a cross-diffusion term in the ω equation and a blending function to ensure that the model equations behave appropriately in both the near-wall

and far-field zones. Further details of SST k-ω model can be found in any turbulence modelling text book and hence have not been included here.

3.5.1 Boundary Conditions

The boundary types that have been specified are listed in the table 3.1. The incident flow velocity remains constant as 4m/sec throughout this study. Tip Speed Ratio (λ) is also kept constant at 0.4 because it represents the most common operating condition in real world practice [28]. Atmospheric conditions at pressure outlet boundary means that zero gauge static pressure has been prescribed, which again is expected in real world conditions. Furthermore, all the walls in the flow domain have been modelled as no-slip boundaries which mean that the flow does not slip on the surface of the walls. This is because, in real world, zero velocity gradient is observed between the walls and the flow layer adjacent to the wall.

Table 3.1 Boundary Types and Conditions

Boundary Name	Boundary Type	Boundary Condition
Inlet	Velocity Inlet	4m/sec
Outlet	Pressure Outlet	Atmospheric Conditions
Surrounding Sides	Stationary Walls	No-Slip
Rotor Blades	Rotating Walls	No-Slip
Stator Blades	Stationary Walls	No-Slip
Core & Passages	Interior	Interior

As the interactions between the rotor and the stator blades are highly transient, Sliding Mesh technique has been used to rotate the rotor blades corresponding to the stationary stator blades. The details of this technique are presented in the next section.

3.5.2 Sliding Mesh

When a time-accurate solution for rotor-stator interaction (rather than a time-averaged solution) is desired, sliding mesh model should be used to compute the unsteady flow field. The sliding mesh model is the most accurate method for simulating flows in multiple moving reference frames, but also the most computationally demanding. In the sliding mesh technique two or more cell zones are used. Each cell zone is bounded by at least one interface zone where it meets the opposing cell zone, as shown in figure 3.6 for VAWTs. The interface zones of adjacent cell zones are associated with one another to form a mesh interface. The two cell zones will move relative to each other along the mesh interface. During the calculation, the cell zones slide (i.e. rotate) relative to one another along the mesh interface in discrete steps. As the rotation takes place, node alignment along the mesh interface is not required. Since the flow is inherently

unsteady, a time-dependent solution procedure is required. The sliding mesh model allows adjacent meshes to slide relative to one another. In doing so, the mesh faces do not need to be aligned on the mesh interface. This situation requires a means of computing the flux across the two non-conformal interface zones of each mesh interface.

The flow domain is divided into sub-domains, each of which may be rotating and/or translating with respect to the inertial frame. The governing equations in each sub-domain are written with respect to that sub-domain's reference frame. At the boundary between two sub-domains, the diffusion and other terms in the governing equations in one sub-domain require values for the velocities in the adjacent sub-domain. The solver used in the present study enforces the continuity of the absolute velocity to provide the correct neighbour values of velocity for the sub-domain under consideration. When the relative velocity formulation is used, velocities in each sub-domain are computed relative to the motion of the sub-domain.

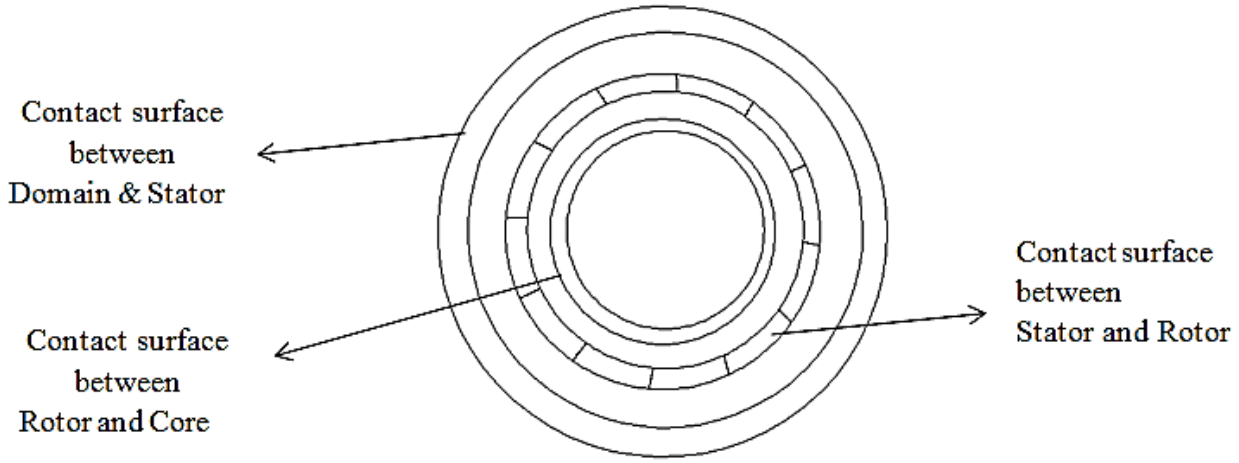

Figure 3.6 Interfaces between different zones

3.5.3 Discrete Phase Modelling

The flow of sand particles in the flow domain, for erosion studies, is quite complicated to model as the trajectory of the sand particles while passing through the VAWT cannot be known in advance. A novel modelling technique, called Discrete Phase Model (DPM), has been used in the present study to accommodate this. DPM solves transport equations for the continuous phase, i.e. air. It also allows simulating a discrete second phase in a Lagrangian frame of reference [54]. This second phase consists of spherical particles (having same diameter as sand particles) dispersed in the continuous phase. DPM computes the trajectories of these discrete phase entities. The coupling between the phases and its impact on both the discrete phase velocities and trajectories, and the continuous phase flow has been included in the present study. The discrete phase in the DPM is defined by defining the initial position (from inlet), mass flow rate and the size of the sand particles. These initial conditions, along with the inputs defining the physical properties of the discrete phase (sand particles), are used to initiate trajectory and velocity calculations. The trajectory and velocity calculations are predicted by integrating the force

balance on the particles, which is written in a Lagrangian reference frame. This force balance equates the particles' inertia with the forces acting on the particles, and can be written as:

$$\frac{dV_p}{dt} = F_D\,(V_w - V_P) + \frac{g\,(\rho_P - \rho_W)}{\rho_P} \tag{3.12}$$

where V_P and V_W are the velocities of particles and air respectively, ρ_P and ρ_W are the densities of particles and air respectively, t is time and g is the gravitational acceleration. $F_D(V_w\text{-}V_p)$ is the drag force per unit particles' mass, and can be re-written as:

$$Drag\ Force = \frac{1}{2}\,\rho_w\left(V_w - V_p\right)^2 A\,C_d \tag{3.13}$$

where C_d is the drag coefficient and A is the cross-sectional area of the particles:

$$Drag\ Force = \frac{1}{2}\,Re_p\left(V_w - V_p\right)\frac{\pi d\mu}{4}\,C_d \tag{3.14}$$

where d is the particle diameter.

$$Drag\ Force\ per\ unit\ particle\ mass = \frac{\frac{1}{2}Re_p\left(V_w - V_p\right)\frac{\pi d\mu}{4}C_d}{\frac{\pi d^3}{6}\rho_p} \tag{3.15}$$

$$F_D = \frac{3\,\mu\,C_d\,Re_p}{4\,\rho_p\,d^2} \tag{3.16}$$

where C_D is the drag coefficient of the particles and Re_p is their Reynolds number. In the present study, erosion rate due to shear has also been included in the study as an additional force acting on the particles, and is discussed in the next section.

3.5.4 Erosion Modelling

According to Edwards et al. [55], the ability to predict erosion has been added to the CFD code through a network of FORTRAN subroutines. Impingement information is gathered as particles impinge the walls of the geometry. As particle trajectories are computed, this impingement information is recorded and erosion is computed using empirical relations. Particle erosion can be monitored at wall boundaries. The erosion rate is defined as:

$$R_{erosion} = \sum_{p=1}^{N\ particles} \frac{\dot{m}_p\,C(d_p)\,f(\alpha)\,v^{b(v)}}{A_{face}} \tag{3.17}$$

where $\dot{m}_p$ is the mass flow rate of the sand particles, $C(d_p)$ is a function of sand particles' diameter, α is the impact angle of the particles with the wall face, f(α) is a function of impact angle, v is the relative particle velocity, b(v) is a function of relative particle velocity, and A_{face} is

the area of the cell face at the wall. These parameters are defined as boundary conditions to the VAWT's walls. Values of these parameters for sand eroding aluminium are given by Edwards as $C(d_p) = 2.388 \times 10^{-7}$ and b(v) = 1.73. The mass flow rate of the sand particles is a parameter that has been studies in Chapter 5. A_{face} is automatically computed by the solver, based on the mesh information. F(α) has been calculated as:

$$f(\alpha) = xcos^2\alpha \sin(\omega\alpha) + ysin^2\alpha + z \quad (3.18)$$

Edwards has given the values for the various constants required in equation (3.18), which are summarised in table 3.2.

Table 3.2 Erosion Model Constant for Aluminium

Constant	Value
w	5.202
x	0.147
y	-0.745
z	1.000

3.6 Solver Settings

Application based solver settings are required to accurately predict the fluid flow behaviour in the flow domain. These settings comprise:

- Pressure – Velocity Coupling
- Gradient
- Spatial Discretisation

The Navier-Stokes equations are solved in discretised form. This refers to the linear dependency of velocity on pressure and vice versa. Hence, a pressure – velocity is required to predict the pressure distribution in the flow domain with reasonable accuracy. In the present study, SIMPLE algorithm for pressure – velocity coupling has been incorporated because it converges the solution faster and is often quite accurate for flows in and around simple geometries such as spheres, cylinders etc. In SIMPLE algorithm, an approximation of the velocity field is obtained by solving the momentum equation. The pressure gradient term is calculated using the pressure distribution from the previous iteration or an initial guess. The pressure equation is formulated and solved in order to obtain the new pressure distribution. Velocities are corrected and a new set of conservative fluxes is calculated.

Gradients are needed for constructing values of a scalar at the cell faces, for computing secondary diffusion terms and velocity derivatives. Green – Gauss Node – based gradient evaluation has been used in the present study. This scheme reconstructs exact values of a linear function at a node from surrounding cell – centred values on arbitrary unstructured meshes by solving a constrained minimization problem, preserving a second-order spatial accuracy.

The CFD solver stores discrete values of the scalars at the cell centres. However, face values are required for the convection terms and must be interpolated from the cell centre values. This is accomplished using an upwind spatial discretisation scheme. Upwinding means that the face value is derived from quantities in the cell upstream, or upwind relative to the direction of the normal velocity. In the present study, 2^{nd} order upwind schemes have been chosen for pressure, momentum, turbulent kinetic energy and turbulent dissipation rate. The use of 2^{nd} order upwind scheme results in increased accuracy of the results obtained.

3.7 Convergence Criteria

Getting to a converged solution is often necessary. A converged solution indicates that the solution has reached a stable state and the variations in the flow parameters, w.r.t. the iterative process of the solver, have died out. Hence, only a converged solution can be treated as one which predicts the solution of the flow problem with reasonable accuracy.

The default convergence criterion for the continuity, velocities in three dimensions and the turbulence parameters in Ansys 16 is 0.001. This means that when the change in the continuity, velocities and turbulence parameters drops down to the fourth place after decimal, the solution is treated as a converged solution. However, in many practical applications, the default criterion does not necessarily indicate that the changes in the solution parameters have died out. Hence, it is often better to monitor the convergence rather than relying on the default convergence criteria.

In the present study, torque output of the blades of the VAWT has been monitored throughout the iterative process. The solution has been considered converged once it has become statistically steady i.e. the variations in the torque output become negligibly small between two consecutive rotations of the VAWT.

After numerically simulating the flow of air in the vicinity of VAWT, various results have been gathered from CFD. Detailed discussions on these results are presented in the proceeding chapters, where the next chapter deals with the optimisation of VAWT based on blade angles.

3.8 Scope of Work

Based on the aims and objectives of this study, the scope of the work has been defined, and is presented in table 3.3.

Table 3.3 Scope of Work

Environmental Condition	Mass Flow Rate of Sand Particles, ṁ	Diameter of Sand Particles, d
	(kg/sec)	(μm)
Clean	N/A	N/A
Dusty	1	125
		250
		500
	2	125
		250
		500

The next chapter presents the numerical results on the performance characteristics of the VAWT operating in a clean environment.

CHAPTER 4
PERFORMANCE ANALYSIS OF A VERTICAL AXIS WIND TURBINE

Performance analysis of a vertical axis wind turbine has been carried out, in the present chapter, based on the VAWT design discussed in chapter 3. Recent studies have shown that the transient analysis of various types of turbomachines has provided valuable insight into the complex flow phenomena in such machines. Hence, a thorough qualitative and quantitative analysis has been carried out that makes use of local flow parameters such as flow velocity and static pressure. The transient analysis of blades has been carried out both on the global output parameters such as torque output and the local flow features. Furthermore, a novel semi-empirical expression for the torque coefficient has been developed that takes into account the transient behaviour and geometrical configuration of the VAWT.

4.1 Mesh Independence Testing

Three different meshes with 2.2, 3.5 and 4.5 million mesh elements were chosen for spatial discretisation. The results obtained, shown in table 4.1, depict that the difference in the average torque output of the VAWT is 3.36% between 2.2 and 3.5 million mesh elements, whereas, the difference between 3.5 and 4.5 million mesh elements is 2.84%. It can therefore be concluded that the mesh with 3.5 million elements is capable of accurately predicting the complex flow features in the vicinity of the VAWT, and hence has been chosen for further analysis.

Table 4.1 Mesh Independence Testing

Number of Mesh Elements	Average Torque Output	Difference w.r.t. 2.2million
(Million)	(N-m)	(%)
2.2	7.74	N/A
3.5	8.00	3.36
4.5	7.96	2.84

4.2 Time Step Independence Testing

Three different time step sizes, corresponding to 1°, 2° and 3° rotation of the rotor blades, were chosen for temporal discretisation. It can be seen in figure 4.1 that the variations in the instantaneous torque output of the VAWT reduces as the time step size increases, hence capturing the flow features accurately. Furthermore, the results summarised in table 4.2 depict that the difference in the average torque output of the VAWT is 1.43% between 1º and 2ºe step sizes, whereas, the difference between 2º and 3º step sizes is 3.25%. It can therefore be concluded that the time step size of 3º is capable of accurately predicting the fast changing flow phenomena in the vicinity of the VAWT, and hence has been chosen for further analysis.

Table 4.2 Time Step Independence Testing

Time Step Size	Average Torque Output	Difference w.r.t. 1°
(°)	(N- m)	(%)
1	7.69	N/A
2	7.80	1.43
3	7.94	3.25

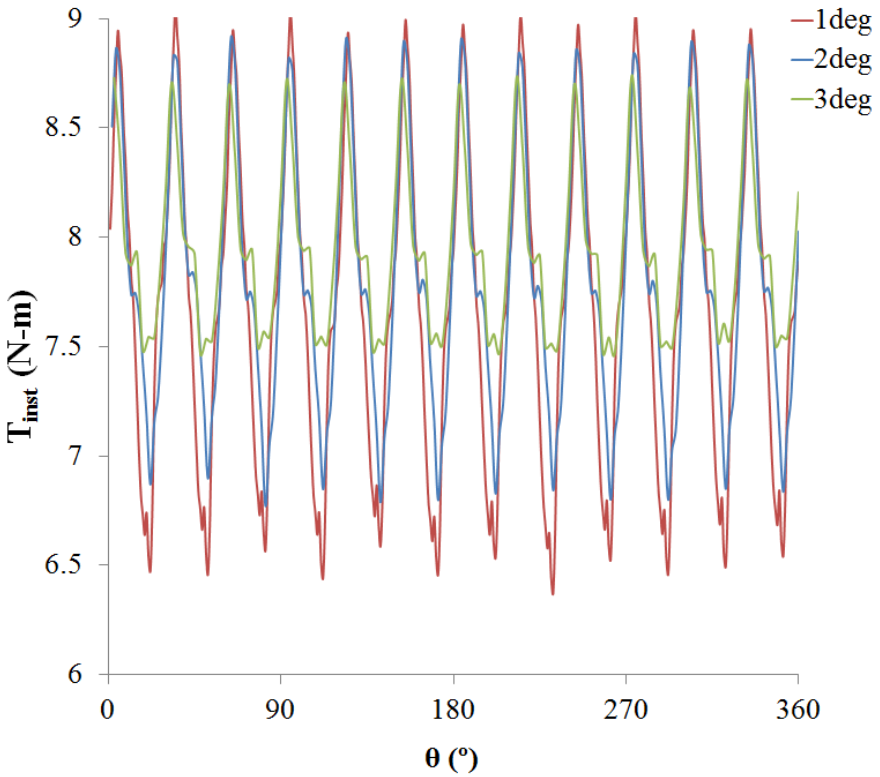

Figure 4.1 Time Step Independence Testing

4.3 Validation of CFD Results

One of the most important steps while conducting numerical studies is the validation of the results. This means that the results obtained from the numerical simulations are compared against experimental findings to confidently authorise that the numerical model represents the physical model of the real world. Hence, all the geometric, flow and solver-related parameters/variables become important in validation studies.

For the present study, the numerical model has been validated against the experimental findings for the average torque output of a VAWT considered by Colley [28]. The size of the VAWT and the blade angles, from Colley's work, has been noted to accurately validate CFD results. The geometric details of the VAWT are shown in table 4.3:

Table 4.3 Geometric Details of the VAWT

Geometric Entity	Symbol	Value
Height of the VAWT	h	1m
Radius of Stator	r_s	1m
Radius of Rotor	r_r	0.7m
Radius of Core	r_c	0.5m
Stator Blade's inlet angle	β	90º
Stator Blade's outlet angle	α	11.689º
Rotor Blade's outlet angle	γ	28.2º
Rotor Blade's inlet angle	δ	32.357º

In order to accurately validate the CFD model, same flow conditions have been specified as in Colley's study i.e. λ=0.5 and v=4m/sec. Figure 4.2(a) depicts the variations in the coefficient of pressure (C_p) between angular positions of 270º and 360º of the VAWT at a radius of 1.025m. C_p is defined here as:

$$C_p = \frac{P - P_\infty}{0.5\rho {v_\infty}^2} \tag{4.1}$$

In equation (4.1), P is the local pressure, P_∞ is the free stream pressure (averaged at inlet boundary), ρ is the density of air and v_∞ is the free stream flow velocity (averaged at both inlet and outlet boundaries). It can be seen in figure 4.2(a) that the CFD model considered in the present study predicts the performance of a VAWT with reasonable accuracy. The average difference between the experimental and CFD results have been calculated to be less than 10%. Furthermore, figure 4.2(b) depicts the variations in the normalised flow velocity, where the velocity has been normalised with average flow velocity value between angular positions of 270º and 360º of the VAWT at a radius of 1.025m. It has been shown that the velocity variations predicted by the CFD model closely match with that measured experimentally.

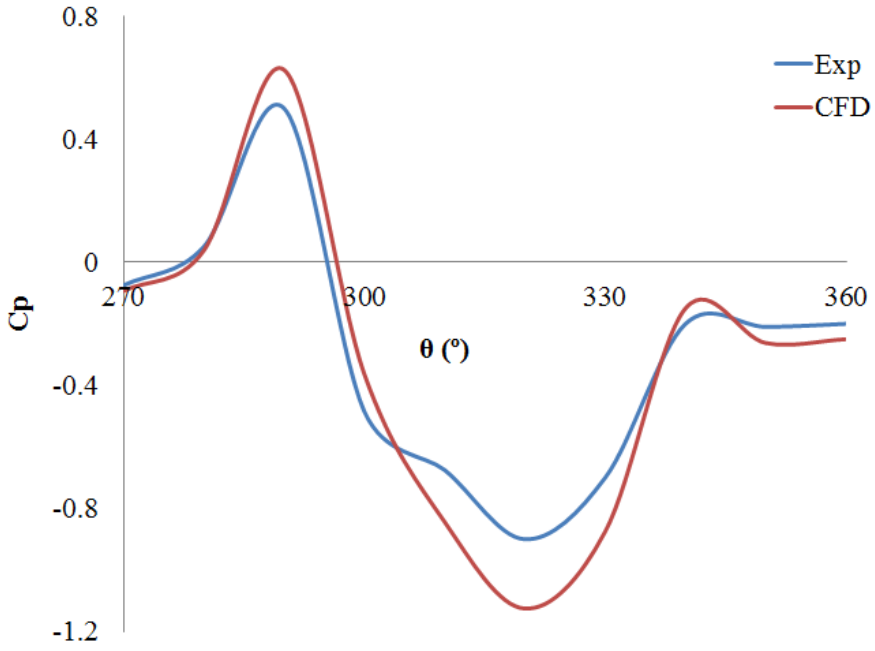

(a)

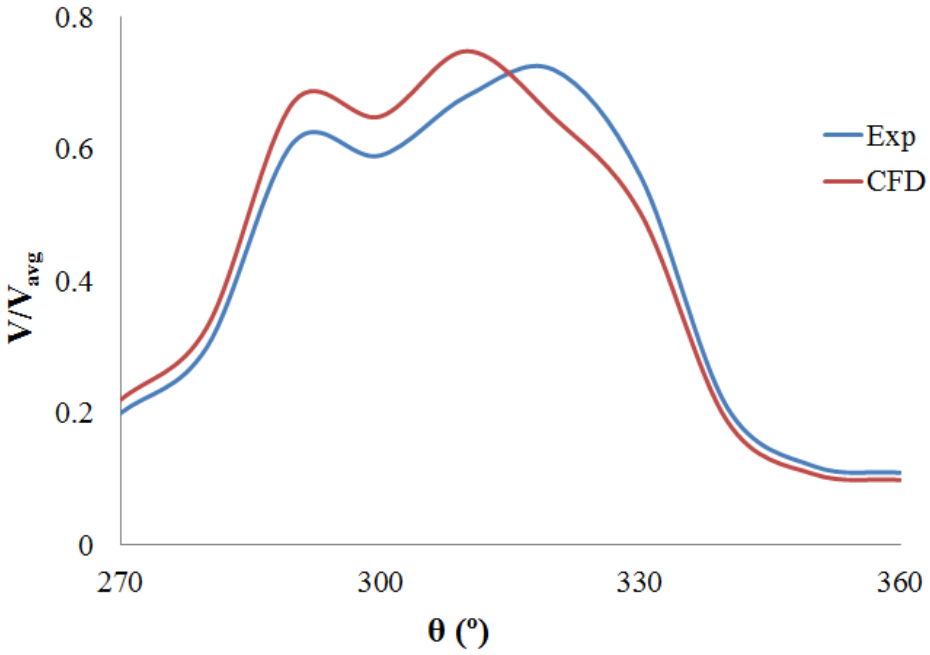

(b)

Figure 4.2 Validation of CFD results (a) variations in Cp, and (b) variations in normalised flow velocity

4.4 Performance Output of the VAWT

It has been discussed in chapter 3 that sliding mesh technique has been used in the present study in order to analyse the transient behaviour of the VAWT. In this approach rotor blades change their position with respect to the stator blades, and hence the geometrical configuration of the VAWT constantly varies. This leads the author to carry out performance analysis of the VAWT such that it covers a wide range of transient analysis. Furthermore, it is also known that the VAWT considered in the present study comprises of 12 rotor and 12 stator blades, each at an angle of 30º with respect to each other. Hence, the flow behaviour is cyclic after periods of 30º. Therefore, the analysis presented in the present study, related to the flow phenomena, covers one such period. This has been achieved by choosing four different geometrical configurations of the VAWT as shown in figure 4.3. The first VAWT configuration corresponds to the occasion when a rotor blade is perfectly aligned with a stator blade (see figure 4.3(a)). The second VAWT configuration corresponds to the occasion when a rotor blade has crossed a stator blade by 3º, or one time step (see figure 4.3(b)). The third VAWT configuration corresponds to the occasion when a rotor blade is in the centre of two stator blades (see figure 4.3(c)). The last VAWT configuration corresponds to the occasion when a rotor blade is approaching a stator blade, and is 3º off it (see figure 4.3(a)). For convenience, rotor blade number 2 (RB2) has been chosen as a reference in the present study.

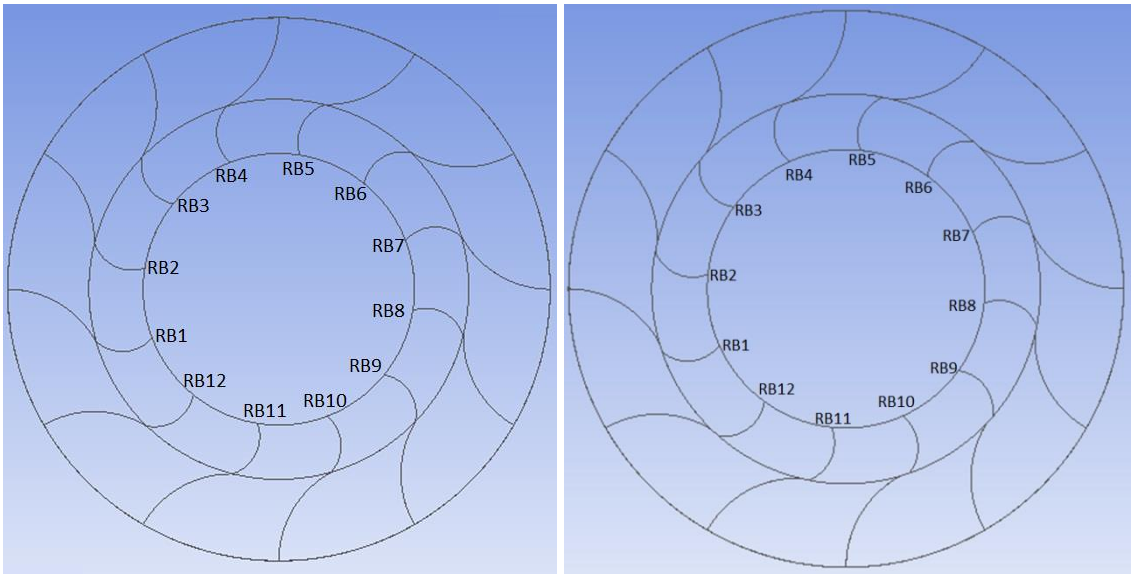

(a) (b)

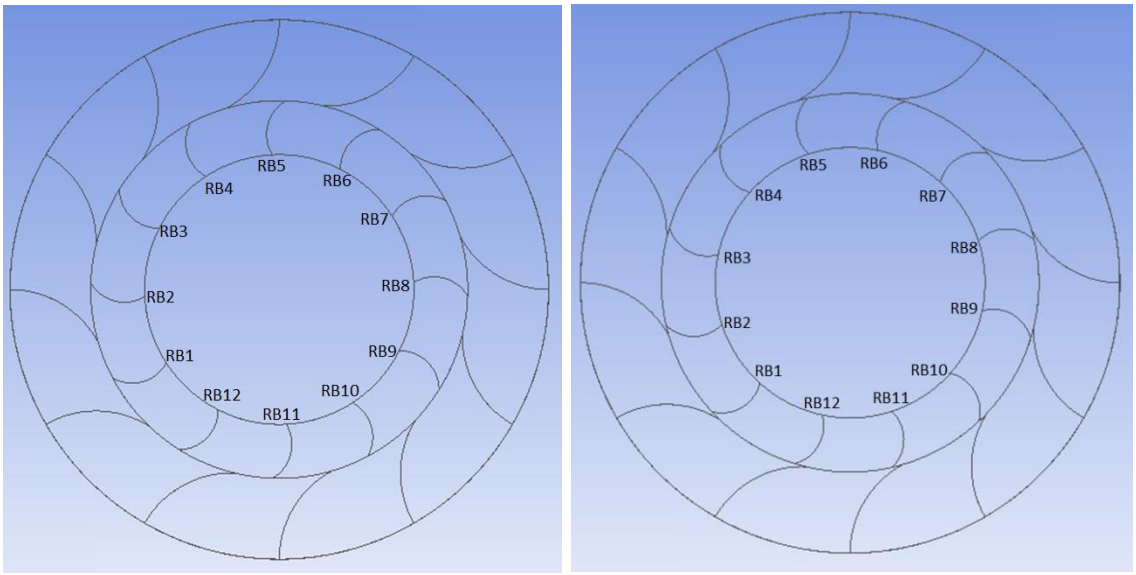

(c) (d)

Figure 4.3 Instantaneous evaluation of the VAWT's performance at (a) 0º (b) 3º (c) 15º (d) 27º

In order to effectively analyse the performance of the VAWT, the following flow and performance parameters have been critically analysed in the present study:

1. Static gauge pressure in the vicinity of the VAWT
2. Flow velocity magnitude in the vicinity of the VAWT
3. Flow pathlines in the vicinity of the VAWT
4. Sand particle tracks (for erosion studies in chapter 5 only)
5. Instantaneous torque output of the VAWT
6. Contribution of individual rotor blades to the overall torque produced by the VAWT
7. Instantaneous erosion rate on a rotor blade (for erosion studies in chapter 5 only)

Figure 4.4 depicts the variations in the static gauge pressure in the vicinity of the VAWT for the four different geometrical configurations discussed above. The scale of the contours has been kept constant throughout this study for effective comparison purposes. It can be seen in figure 4.4(a) that the high pressure regions are either on the windward side of the VAWT, or in the vicinity of rotor blades 7 and 8. Similarly, the low pressure regions occur primarily on the upper and lower sections of the VAWT. The general trend remains the same for all the different geometrical configurations of the VAWT considered here. However, there are significant local variations in the static gauge pressure distribution for different geometrical configurations.

When a rotor blade crosses a stator blade (figure 4.4(b)), the windward section of the VAWT depicts lower pressure. The high pressure regions in the vicinity of the rotor blades also shrink. Hence, it is expected that the performance (torque production capability) of the VAWT reduces when there is some degree of misalignment between rotor and stator blades. When a rotor blade comes exactly in-between two stator blades, it has been noticed (in figure 4.4(c)) that more number of rotor blades exhibit higher pressure zones, whereas the low pressure zones shrink. This behaviour of the VAWT hints towards a possible increase in the performance (as compared

to slight misalignment between rotor and stator blades). Possible reasons for this behaviour of the VAWT can be attributed to the fact that in this particular geometrical configuration of the VAWT, there exist two equal passages between a rotor and two stator blades, as compared to two unequal passages formed when the rotor blades are only slightly misaligned with the stator blades.

It can be further observed in figure 4.4(d) that the higher pressure regions grow considerably when a rotor blade approaches a stator blade, but there still exist a small degree of misalignment between the two. This behaviour of the VAWT is of particular interest as it is completely different from the one observed in figure 4.4(b). Hence, the VAWT behaves differently when a rotor blade leaves a stator blade and when a rotor blade approaches a stator blade, where the degree of misalignment between the two is the same. One possible reason for this behaviour of the VAWT could be because of the curvature of the stator blades. As the stator blades considered in the present study are concave to the approaching flow, and are primarily used to direct the flow towards the rotor blades, the effects of a rotor blade leaving, and a rotor blade approaching a stator blade would be completely different, as observed here.

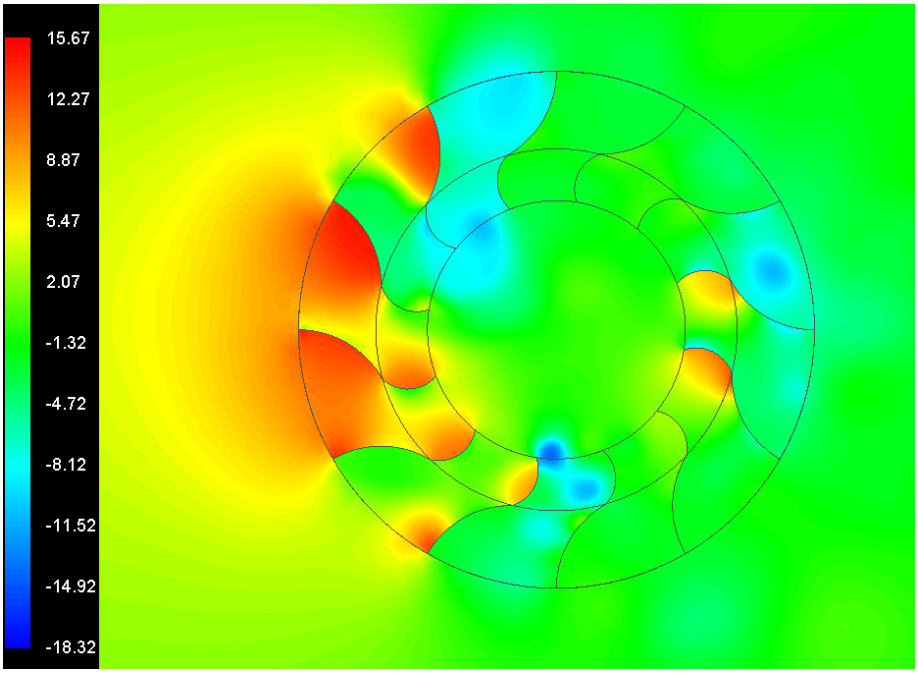

(a)

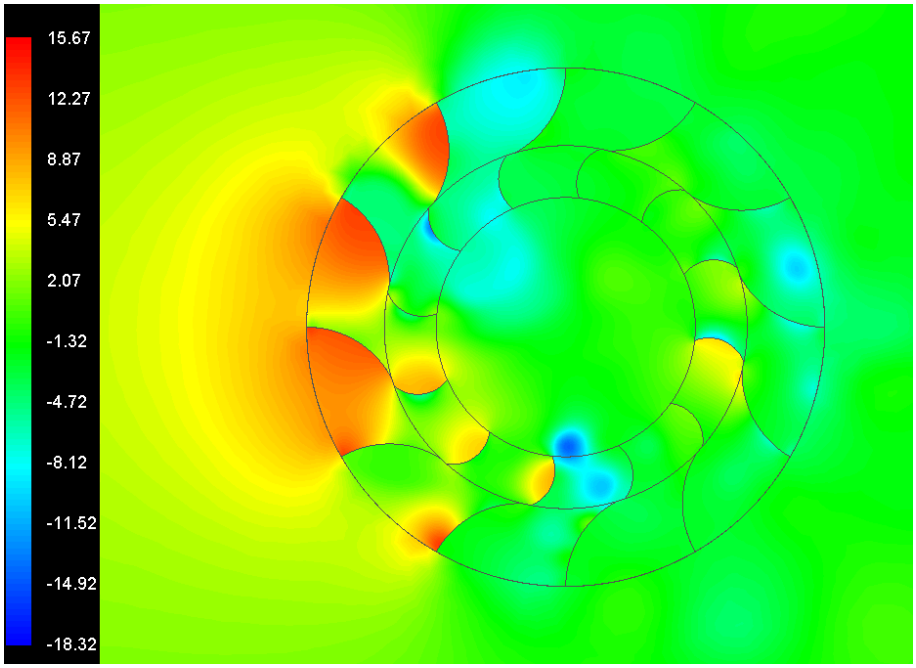
15.67
12.27
8.87
5.47
2.07
-1.32
-4.72
-8.12
-11.52
-14.92
-18.32

(b)

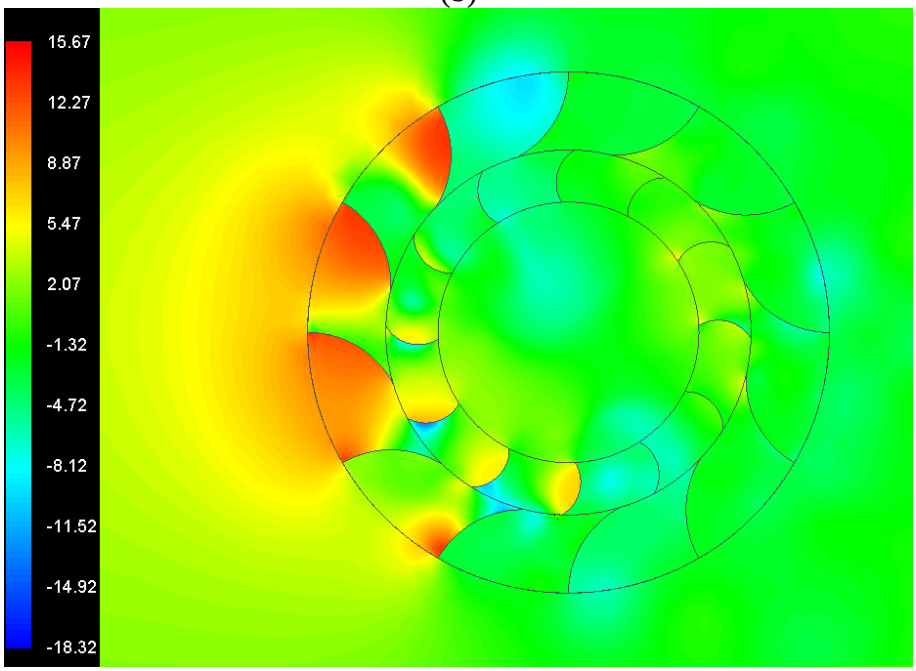
15.67
12.27
8.87
5.47
2.07
-1.32
-4.72
-8.12
-11.52
-14.92
-18.32

(c)

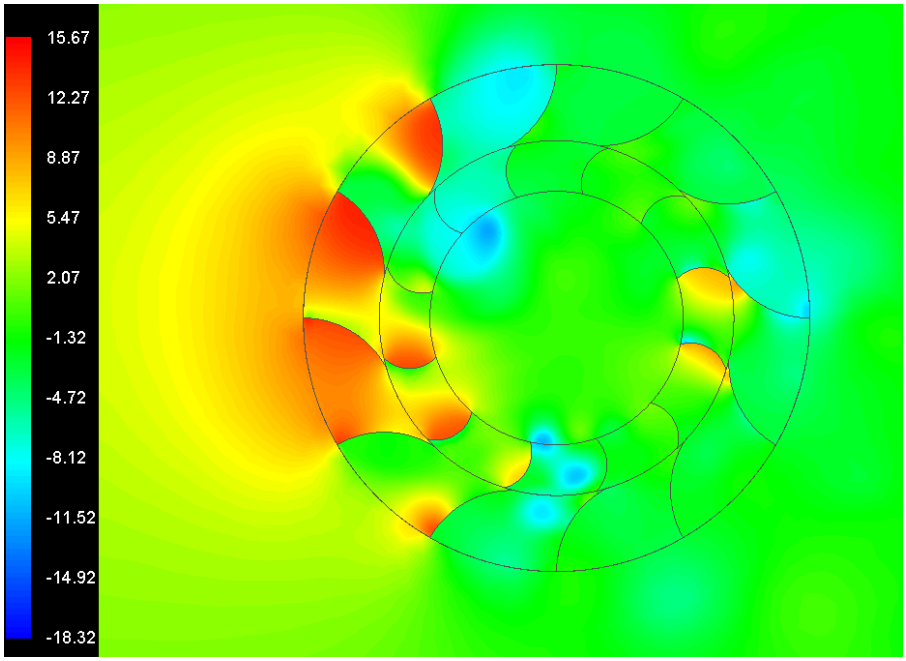

(d)

Figure 4.4 Static gauge pressure (Pa) variations in the vicinity of the VAWT at (a) 0º (b) 3º (c) 15º (d) 27º

Figure 4.5 depicts the variations in the flow velocity for the different geometrical configurations of the VAWT discussed above. Again, the scale of the contours has been kept constant throughout this study for effective comparison purposes. It can be seen in figure 4.5(a) that although the incident wind velocity is 4m/sec, it can increase up to 7.57m/sec within the VAWT. As expected, the flow velocity is high in the passages formed between stator and rotor blades, whereas it is considerable lower in the zones where there is more resistance to the flow path (such as the upper and lower sections of the VAWT). The effects of flow jets formed in the passages between the rotor and the stator blades can be noticed even within the core region of the VAWT.

As the rotor blades cross the stator blades, and there is some degree of misalignment between them, it has been observed (in figure 4.5(b)) that further jets appear in the core region. This is because of the unequal flow passages formed between the rotor and the stator blades. The smaller passages accelerate the flow, hence forming further jets. However, as the rotor blades rotate further, and arrive exactly in between two stator blades, equal passages are formed, and it can be noticed (in figure 4.5(c)) that the flow accelerates thorough these passages. Furthermore, figure 4.5(d) depicts that there isn't significant change in the flow velocity when the degree of misalignment between the rotor and the stator blades is the same, even if the rotor blades are approaching stator blades, or have just crossed them.

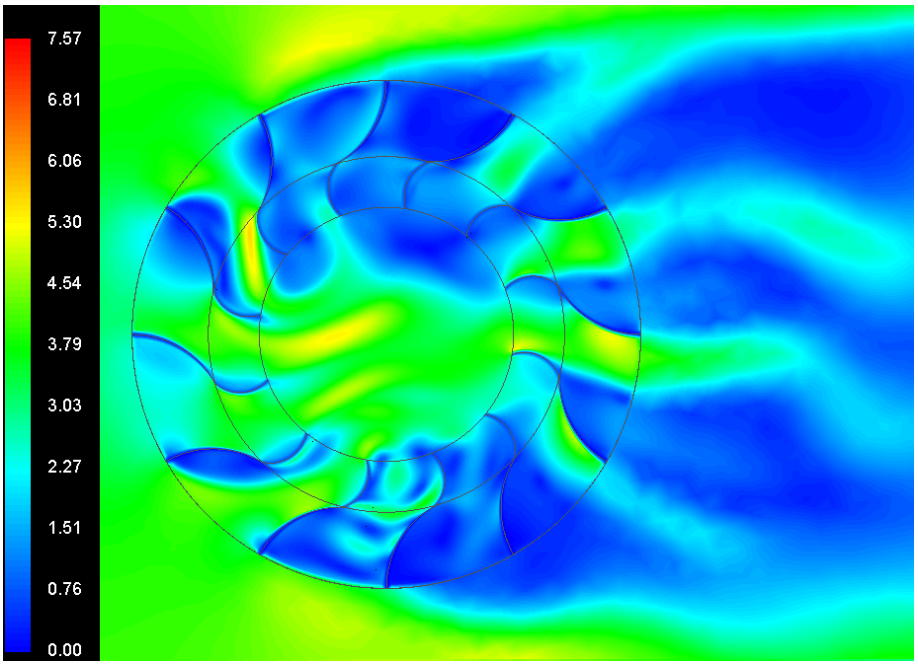
7.57
6.81
6.06
5.30
4.54
3.79
3.03
2.27
1.51
0.76
0.00

(a)

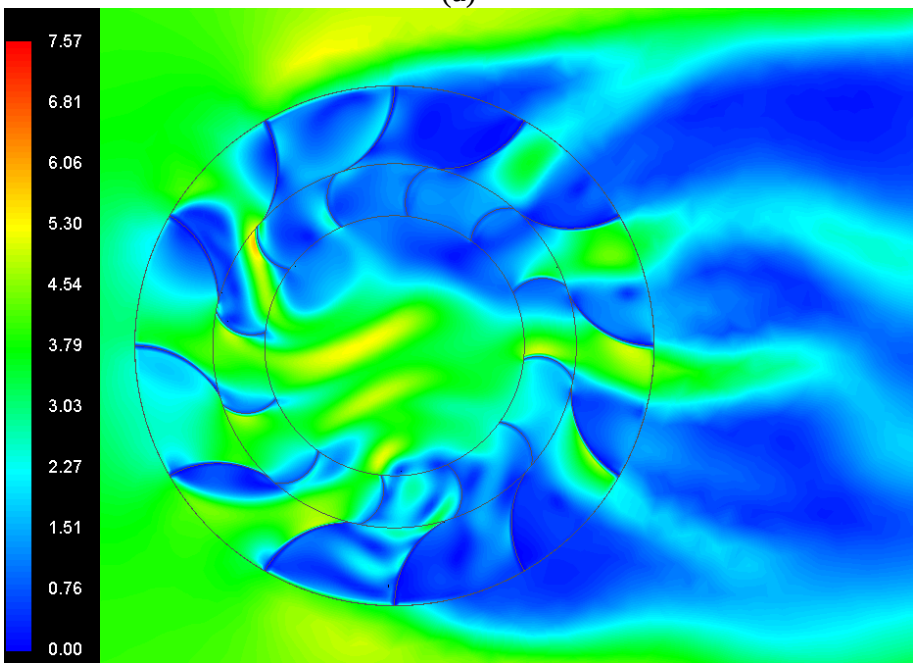
7.57
6.81
6.06
5.30
4.54
3.79
3.03
2.27
1.51
0.76
0.00

(b)

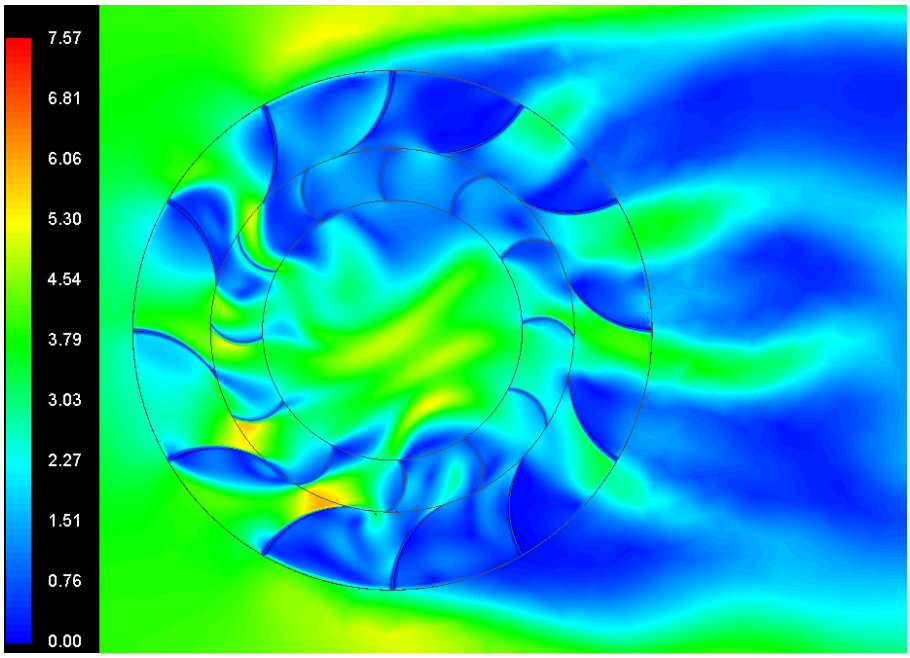

(c)

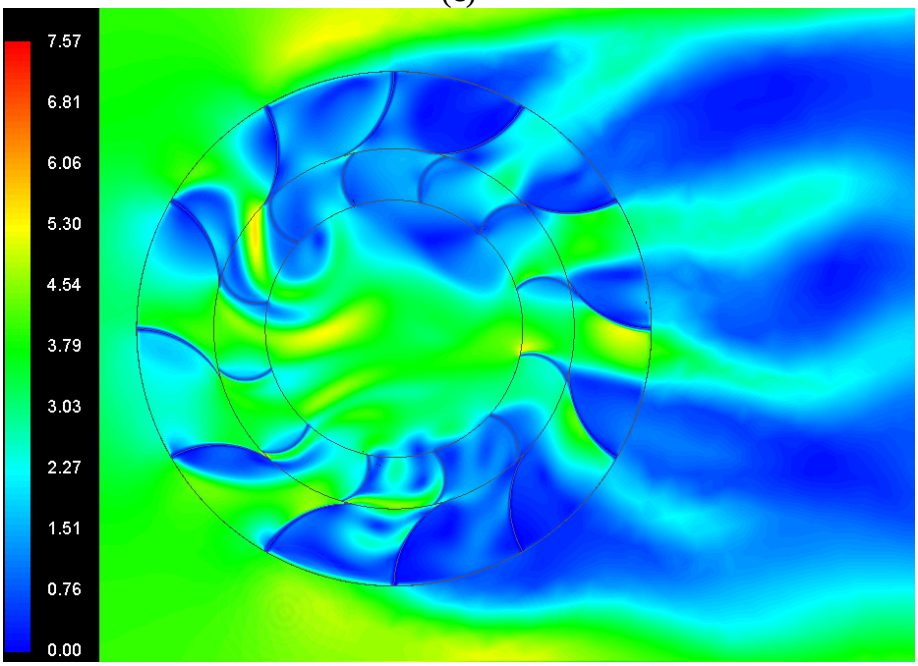

(d)

Figure 4.5 Velocity magnitude (m/sec) variations in the vicinity of the VAWT at (a) 0º (b) 3º (c) 15º (d) 27º

The flow velocity contours have shown some variations due to the geometrical variations within the VAWT; however a much clearer picture could be obtained by analysing the flow pathlines. This has been presented in figure 4.6, where the pathlines are coloured by flow velocity. The discussion presented here is focused on rotor blade number 2. It can be seen in figure 4.6(a) that when the rotor blades are inline with the stator blades, the flow smoothly propagates through the

passages formed in between the blades, following the line of the blade's curvature for those pathlines that are very close to them. However, as rotor blade 2 crosses the stator blade, opening up a small passage, the pathlines can now escape through this passage and travel upwards. This is because it has been observed in figure 4.4(a) that there exists a relatively low pressure region behind that particular stator blade. Then, the pathlines follow the general flow path i.e. through the core region and into the passages formed at the leeward side of the VAWT, or else sucked into pockets of lower pressure, if applicable.

Figure 4.6(c) depicts the same behaviour as observed in case of figure 4.6(a). However, in figure 4.6(d), when again there is some degree of misalignment between the rotor and the stator blades, focusing on rotor blade 3 now, air tries to propagate towards low pressure region (behind the stator blade), however, due to the presence of rotor blade 3 in its path now, the pathlines are forced to follow the curvature of the rotor blade and into the core region.

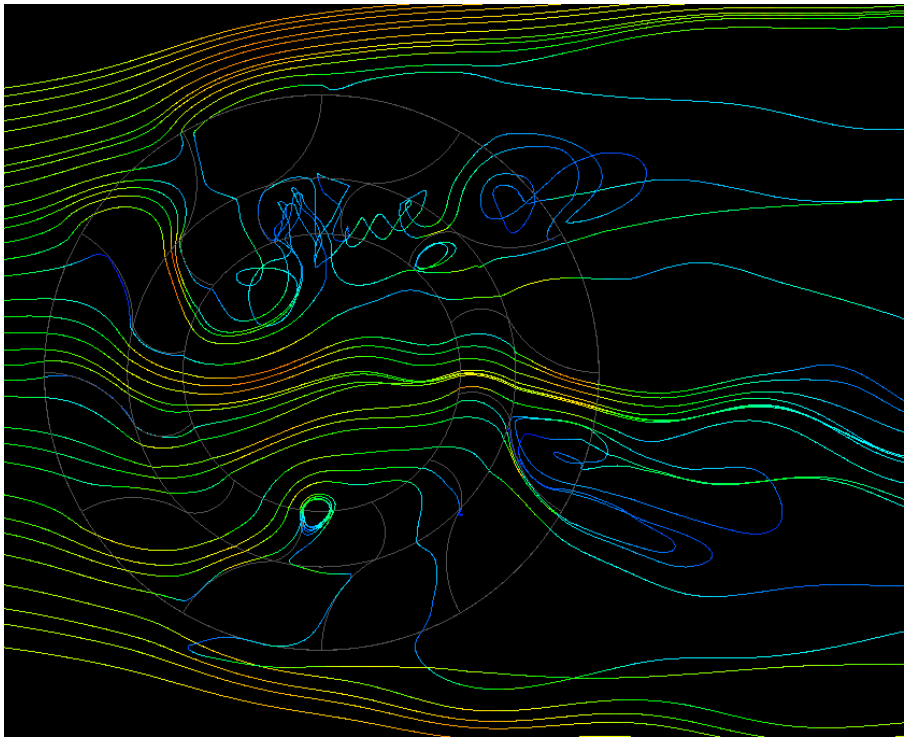

(a)

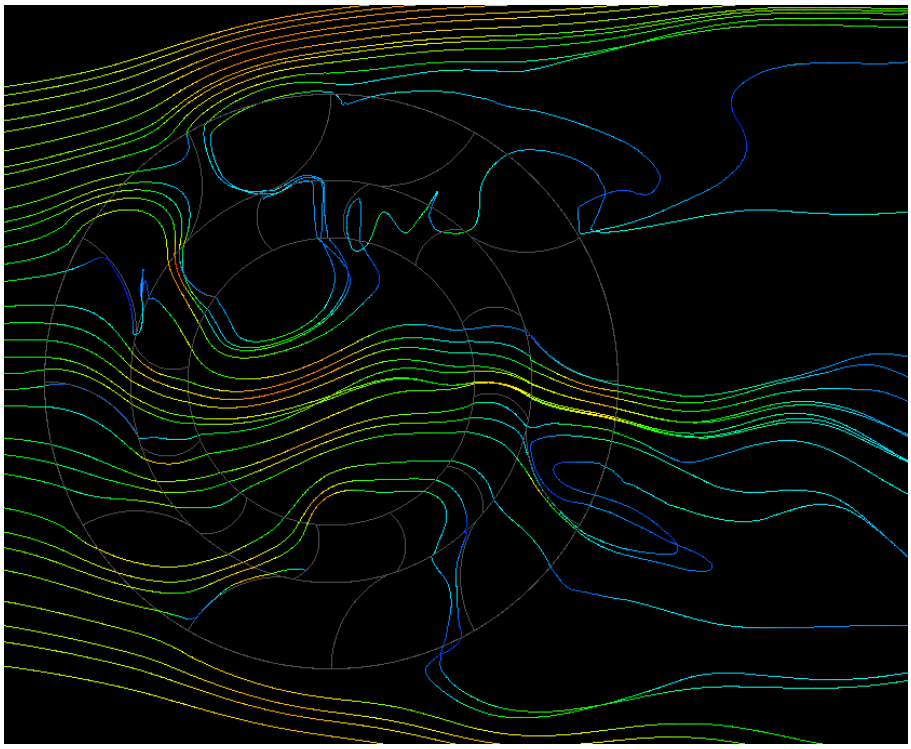

(b)

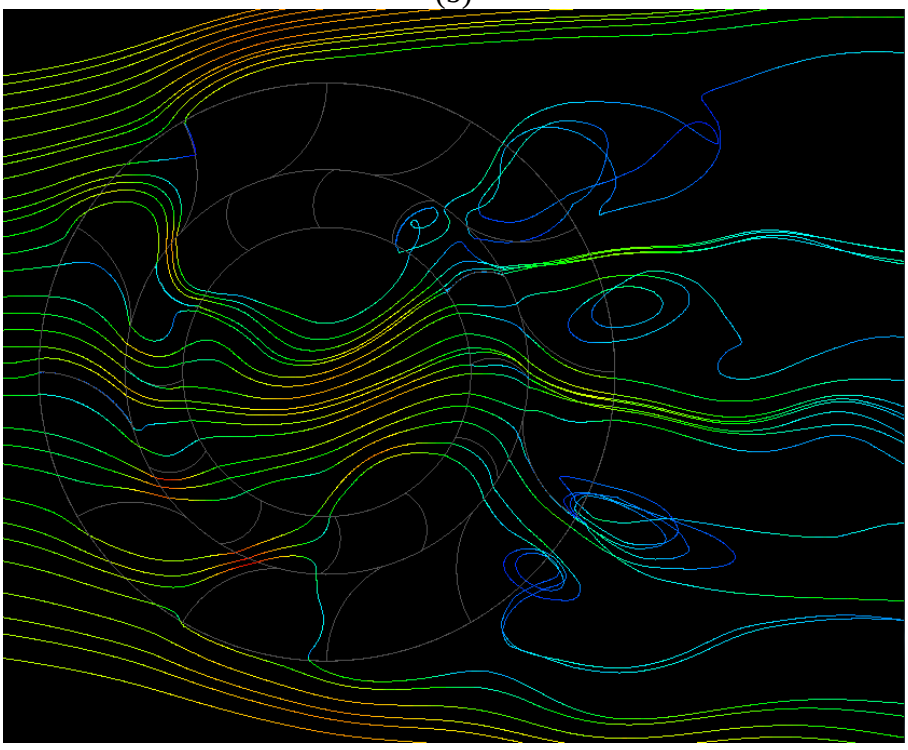

(c)

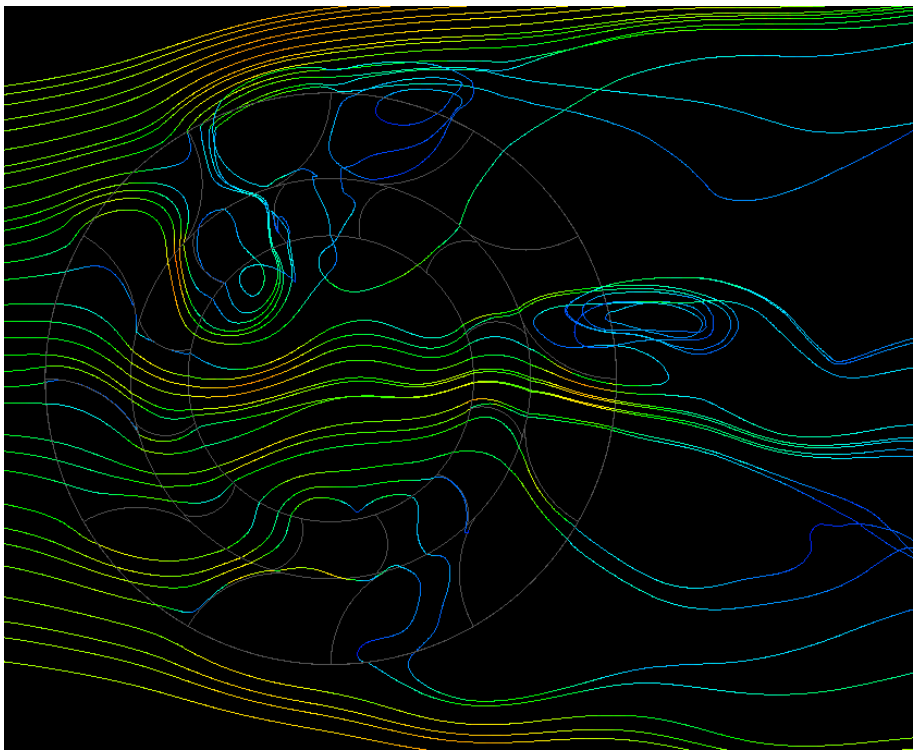

(d)

Figure 4.6 Flow pathlines, coloured by velocity, in the vicinity of the VAWT at (a) 0º (b) 3º (c) 15º (d) 27º

After carrying out detailed flow feature analysis in the vicinity of the VAWT, figure 4.7 depicts the variations in the instantaneous torque output generated by it in one revolution of its operation. The cyclic variations in the torque have been observed by many researchers [32-34] and [36-40] where the number of both positive and negative peaks are equal to the number of rotor blades of the VAWT. Each cycle (one wavelength) corresponds to the circular motion of a rotor blade from one stator blade to the next one. The torque variations shown in this figure corresponds to the overall torque generated by the torque. In order to analyse the contribution of each blade individually, to the total torque produced by the VAWT, torque generated by each blade has been recorded, as a function of its angular position, where the reference point corresponds to perfectly aligned rotor and stator blades. The recorded torque corresponds to one wavelength (30º) travel of the rotor blades only, because of its cyclic nature.

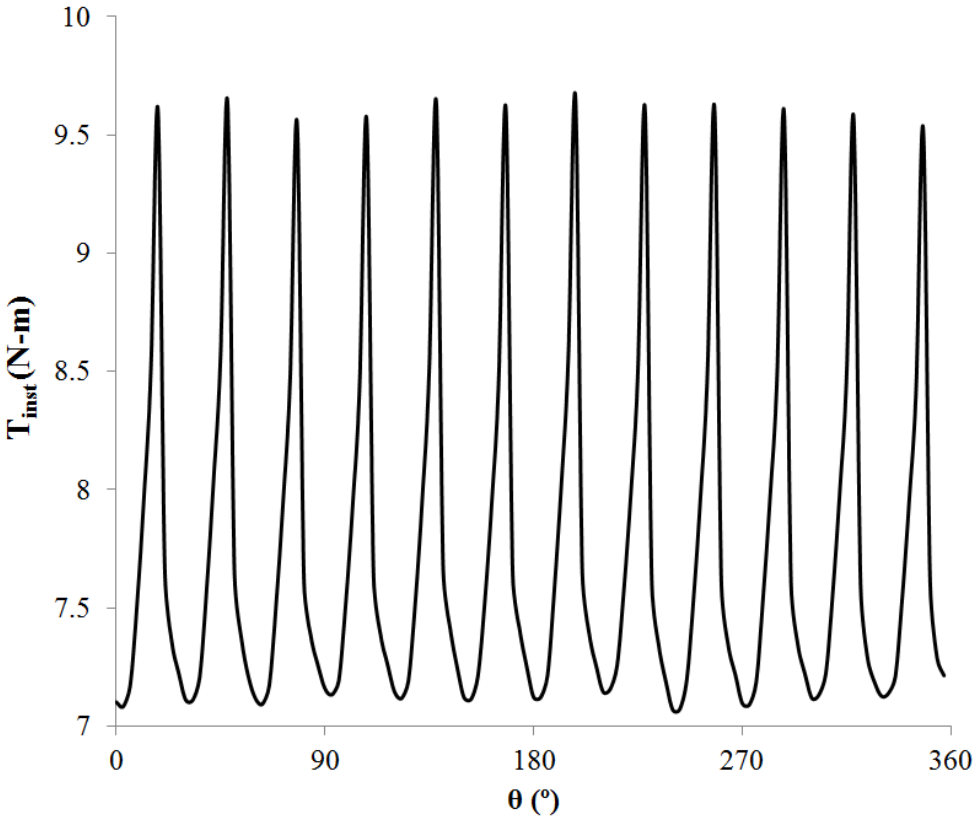

Figure 4.7 Instantaneous torque output from the VAWT

It can be seen in figure 4.8 that the torque generated by rotor blades on the windward side of the VAWT is generally higher as compared to the rotor blades present on the windward side of the VAWT at that particular instance.

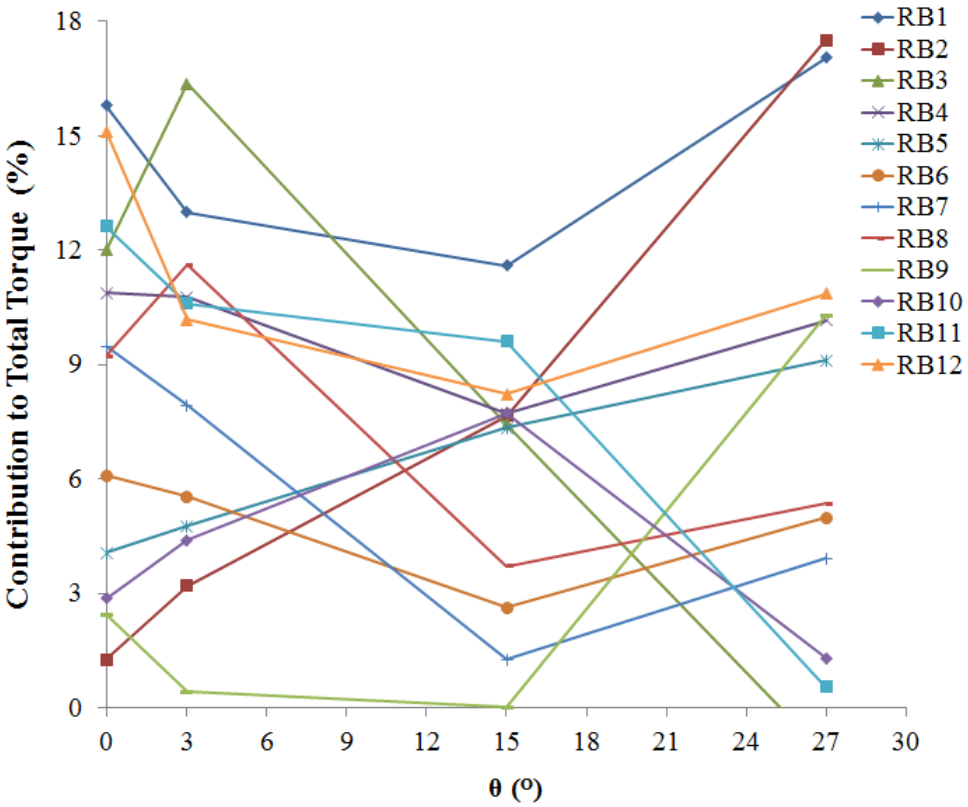

Figure 4.8 Contribution of each rotor blade to the overall torque generated by the VAWT

In order to quantitatively analyse the torque generation capability of the VAWT, a detailed statistical analysis has been carried out on the results presented in figure 4.7. It can be noticed that the peak-to-peak amplitude of the torque signals from the VAWT is 2.59N-m, whereas the average torque generated by the VAWT is 7.73N-m. The average torque generated by the VAWT is of great importance as this value can be compared against the average torque computed for VAWTs operating in dusty environments.

Table 4.4 Performance analysis of the VAWT

Torque Output (N-m)	
Max	9.66
Min	7.07
Max-Min	2.59
Average	7.73

Standard Deviation	0.75

It is well known fact that the torque output of a VAWT can be calculated by:

$$T = \frac{1}{2}\rho_f v^2 A R C_T \tag{4.2}$$

where T is the torque generated by the VAWT (N-m), ρ_f is the fluid density (1.225kg/m^3 in this study), v is the average freestream wind velocity (4m/sec in this study), A is the projected area of the VAWT (m^2), R is the radius of the rotor blades (0.7m in this study) and C_T is the torque coefficient. The torque coefficient can be expressed in terms of the angular position of the rotor blades, based on the results presented in this chapter, as:

$$C_T = 1.385\,\theta^{0.0012} - 1 \tag{4.3}$$

where θ is the angular position of the rotor blades (º). In order to valid equation (4.3) with the CFD predictions presented in this chapter regarding the torque generated by the VAWT, torque generated using this equation needs to be compared against the CFD results. It has been found that the average difference in the torque predicted by equation (4.3), and the torque obtained through the use of CFD, is 7% for 100% of the data, and 5% for 90% of the data. Hence, equation (4.3) can be sued to predict the instantaneous torque generated by a VAWT, operating in clean environment, with reasonable accuracy.

The next chapter will discuss in detail the dynamics of VAWT's performance, when it is working in a dusty environment, such as in desserts. Various flow conditions will be numerically created (such as sand particle diameters and mass flow rates of sand into the VAWT) and VAWT's performance will be analysed.

CHAPTER 5
PERFORMANCE ANALYSIS OF A VERTICAL AXIS WIND TURBINE OPERATING IN DUSTY ENVIRONMENTS

Performance analysis of a vertical axis wind turbine operating in dusty environments has been carried out in the present chapter. Recent studies have shown that the use of advanced Computational Fluid Dynamics based tools can provide reasonable estimates of the blade erosion, and the complex flow phenomena associated with it. Hence, a thorough qualitative and quantitative investigation has been carried out on the erosion characteristics of the VAWT. Furthermore, the effects of sand particles' diameters and mass flow rate have been analysed in detail. A novel semi-empirical expression for the torque coefficient has been developed that takes into account the effects of the aforementioned parameters.

5.1 Introduction

This chapter deals with the erosion phenomena within the VAWT, where the VAWT is operating in dusty environment. Various environments have been numerically generated, as discussed in the scope of the work in chapter 3, by varying the following parameters:

- Sand particles' diameter (125μm, 250μm and 500μm)
- Mass flow rate of sand particles (1kg/sec and 2kg/sec)

The analysis presented in this chapter follows from the analysis presented in chapter 4; focusing on the geometrical configurations of the VAWT shown in figure 4.3. Transient performance analysis of the VAWT has been presented here, and then using the results, a novel semi-empirical correlation has been formulated for the torque produced by the VAWT, taking into account the sand parameters discussed above. All the contours are on the same scale, matching with the one in chapter 4, for effective comparison purposes.

The first section of this chapter discusses the general erosion phenomena in a VAWT, with sand particles' diameter of 125microns and mass flow rate of 1kg/sec. The second section deals with the effect of sand particle size on the performance of the VAWT, whereas the third section focuses on the effect of mass flow rate of the sand particles on VAWT's performance. The last section of this chapter presents the novel predictor expression for the torque coefficient.

5.2 Performance evaluation of a VAWT operating in Dusty Environment

Figure 5.1 depicts the variations in the static gauge pressure in the vicinity of the VAWT for the four different geometrical configurations considered in the present study. It can be seen in figure 5.1(a) that the high pressure regions are on the windward and leeward sides of the VAWT, whereas the low pressure regions occur primarily on the upper and lower sections of the VAWT. The general trend remains the same for all the different geometrical configurations of the VAWT considered here. However, there are significant local variations in the static gauge pressure distribution for different geometrical configurations.

When a rotor blade crosses a stator blade (figure 5.1(b)), the windward section of the VAWT depicts lower pressure. The high pressure regions in the vicinity of the rotor blades also shrink. Furthermore, when a rotor blade comes exactly in-between two stator blades, it has been noticed (in figure 5.1(c)) that more number of blades exhibit higher pressure zones. It can be further observed in figure 5.1(d) that the higher pressure regions grow considerably when a rotor blade approaches a stator blade, but there still exist a small degree of misalignment between the two. The trends shown here are inline with the one observed in case of VAWT operating in a clean environment.

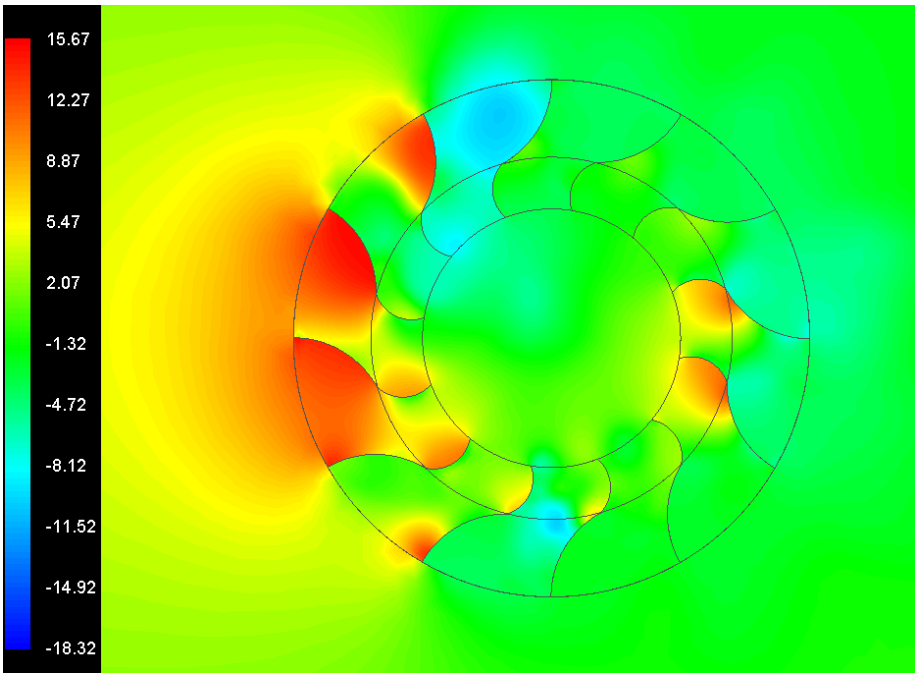
15.67
12.27
8.87
5.47
2.07
-1.32
-4.72
-8.12
-11.52
-14.92
-18.32

(a)

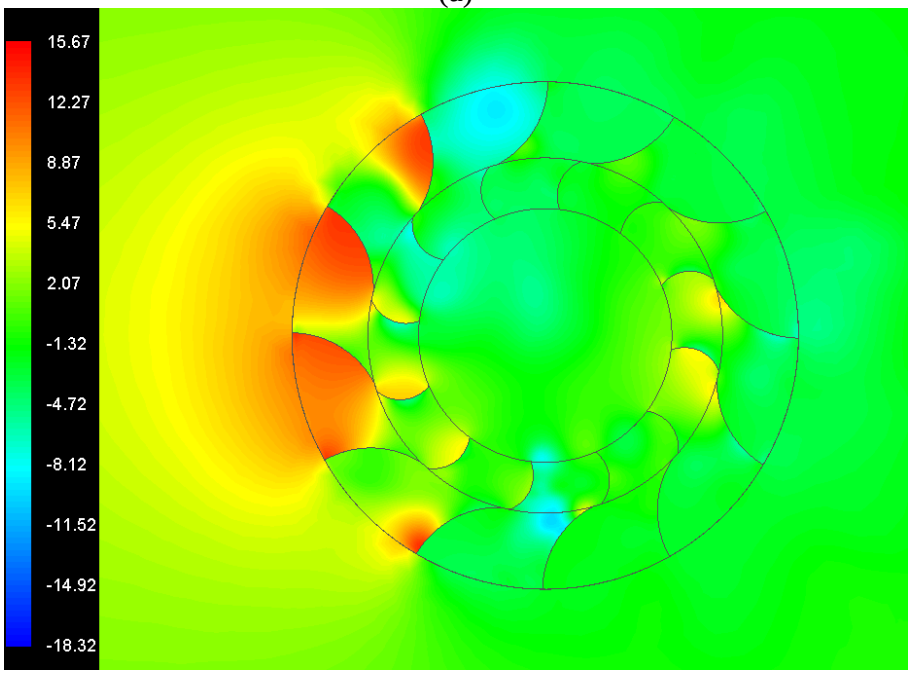
15.67
12.27
8.87
5.47
2.07
-1.32
-4.72
-8.12
-11.52
-14.92
-18.32

(b)

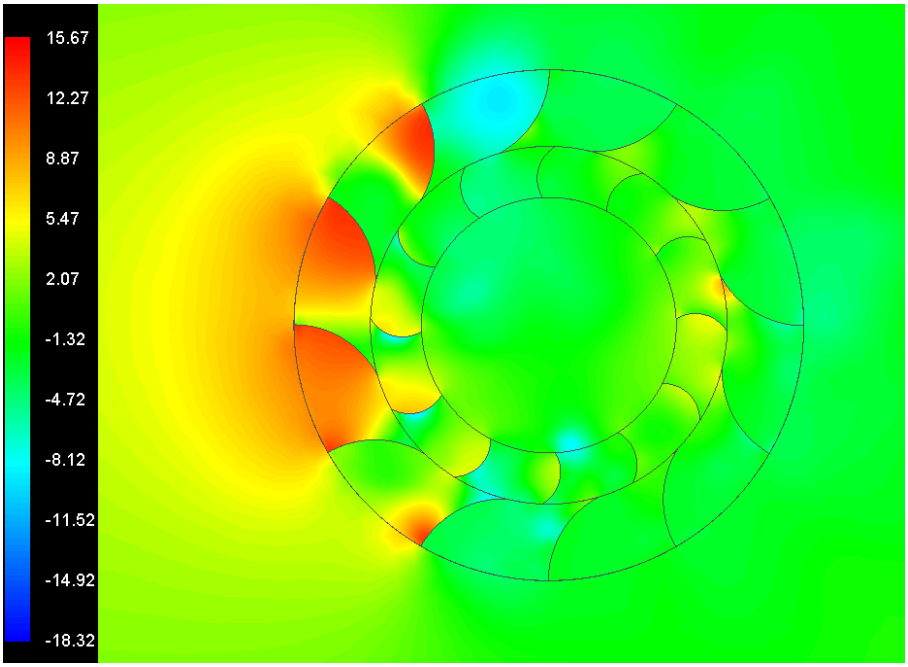

(c)

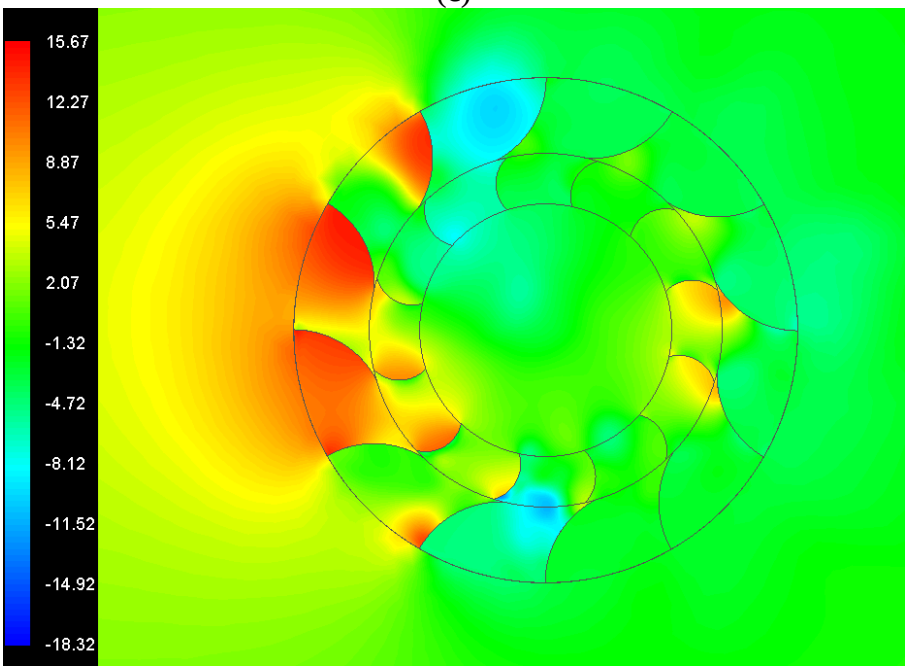

(d)

Figure 5.1 Static gauge pressure (Pa) variations in the vicinity of the VAWT at (a) 0º (b) 3º (c) 15º (d) 27º for sand particles' diameter of 125microns at 1kg/sec mass flow rate

Figure 5.2 depicts the variations in the flow velocity for the different geometrical configurations of the VAWT discussed above. It can be seen in figure 5.2(a) that the flow velocity is high in the passages formed between stator and rotor blades, whereas it is considerable lower in the zones where there is more resistance to the flow path (such as the upper and lower sections of the

VAWT. Moreover, due to the concave profile of the stator blades, the lower section of the VAWT depicts higher flow velocities as compared to the upper section of the VAWT. An important point to note over here is that, as compared to the VAWT operating in a clean environment (figure 4.5), the flow velocity is considerably lower throughout the flow domain.

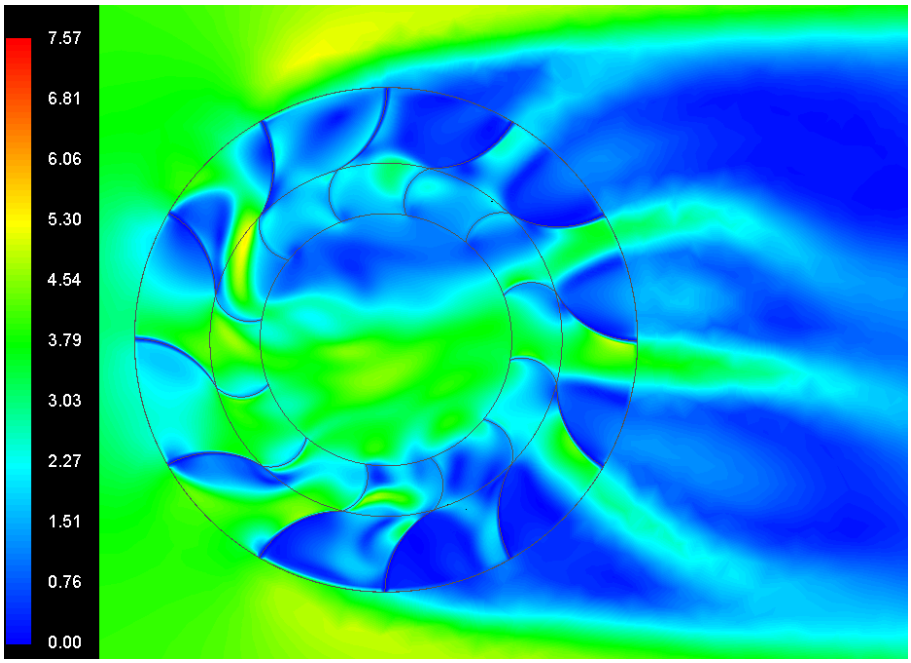

(a)

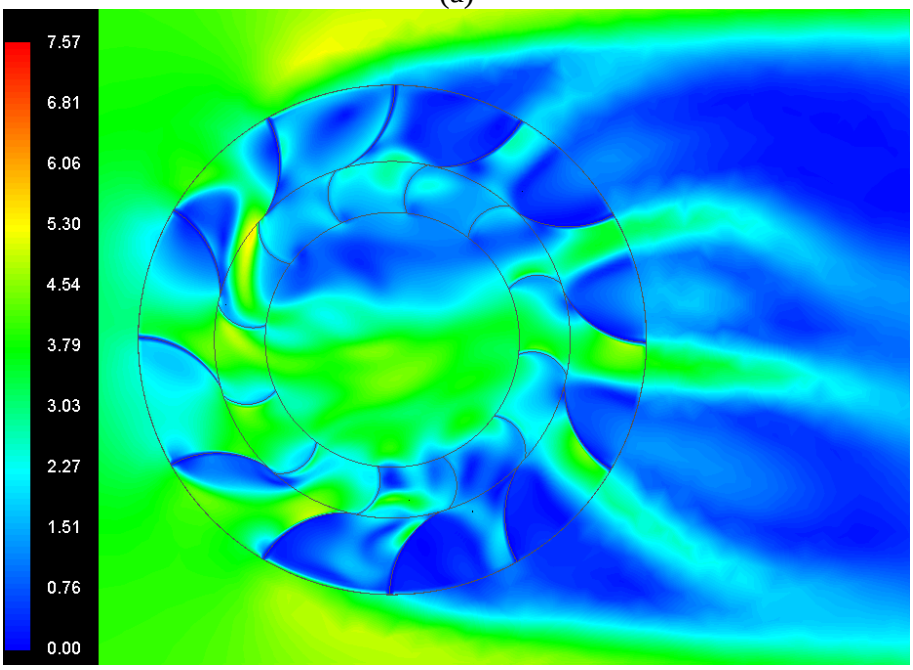

(b)

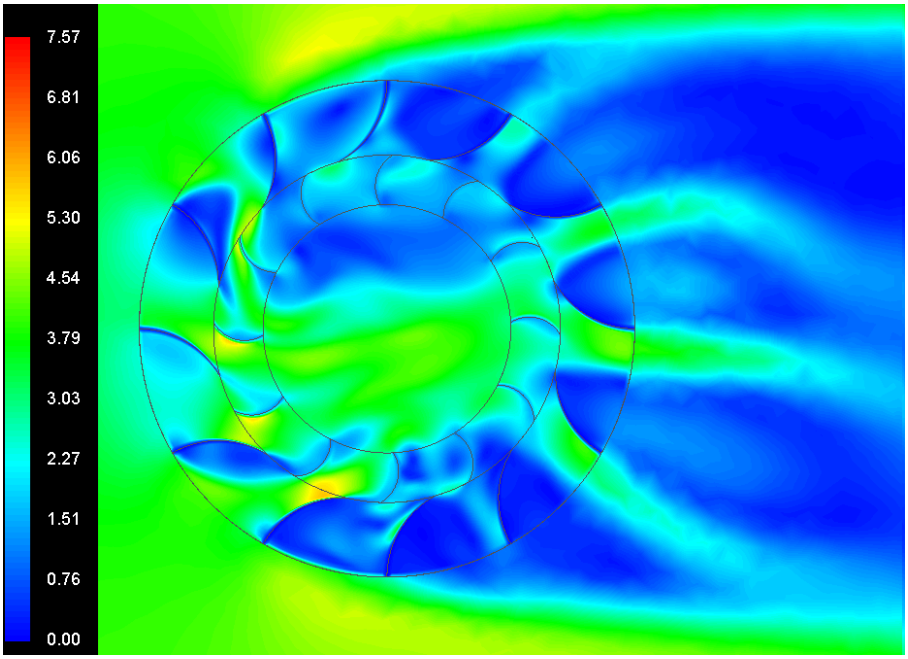

(c)

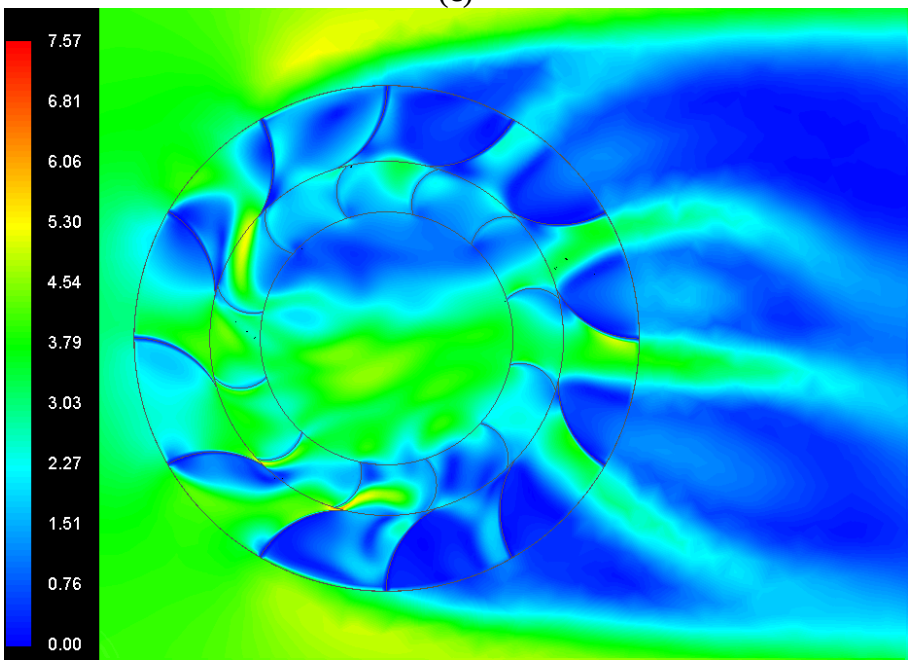

(d)

Figure 5.2 Velocity magnitude (m/sec) variations in the vicinity of the VAWT at (a) 0º (b) 3º (c) 15º (d) 27º for sand particles' diameter of 125microns at 1kg/sec mass flow rate

Figure 5.3 depicts the flow pathlines in the vicinity of the VAWT. It can be seen in figure 5.3(a) that when the rotor blades are inline with the stator blades, the flow smoothly propagates through the passages formed in between the blades, following the line of the blade's curvature for those pathlines that are very close to them. However, as rotor blade 2 crosses the stator blade, opening

up a passage, the pathlines can now escape through this passage and travel upwards. This trend is also inline with the one observed in case of the VAWT operating in clean environment.

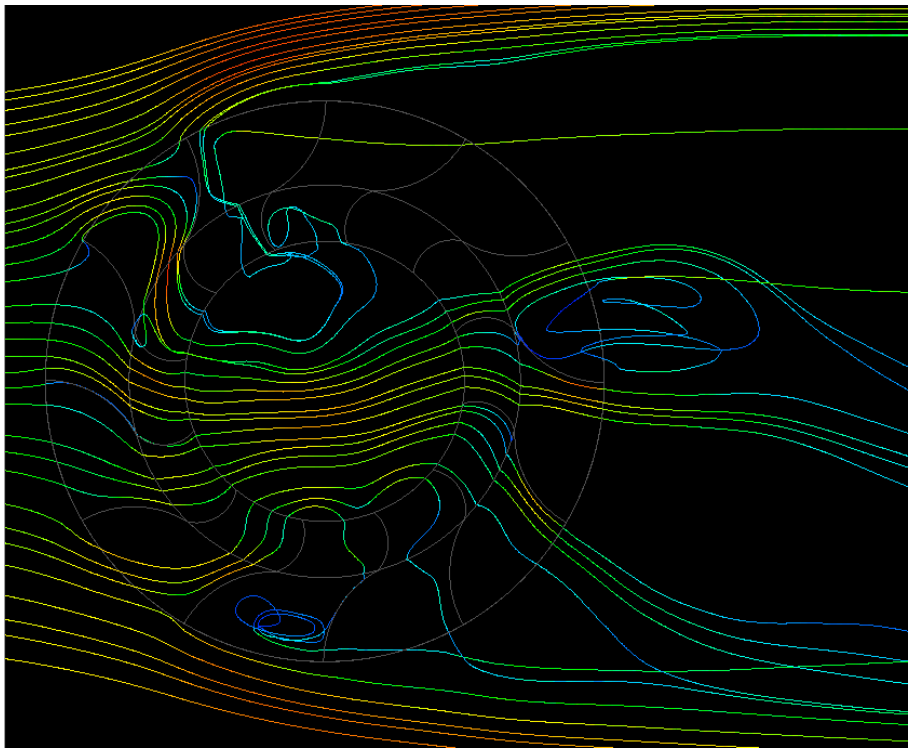

(a)

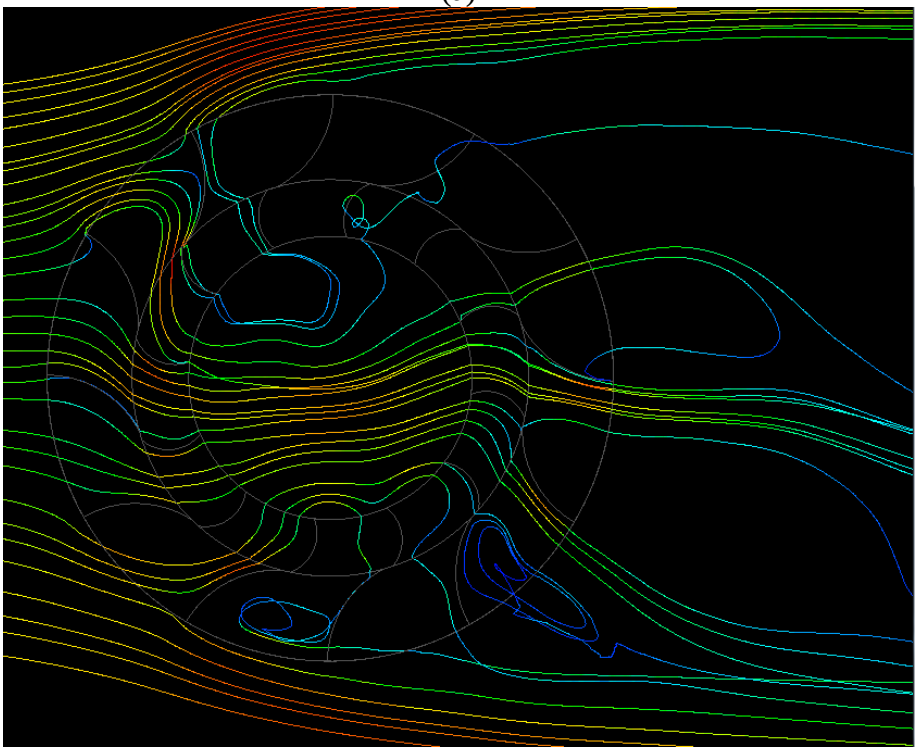

(b)

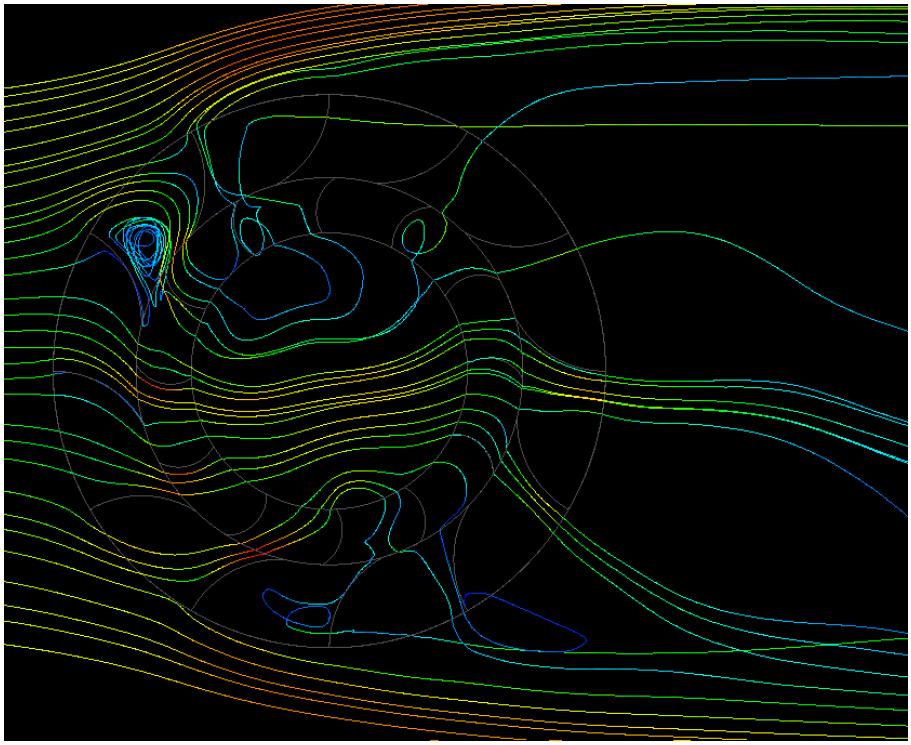

(c)

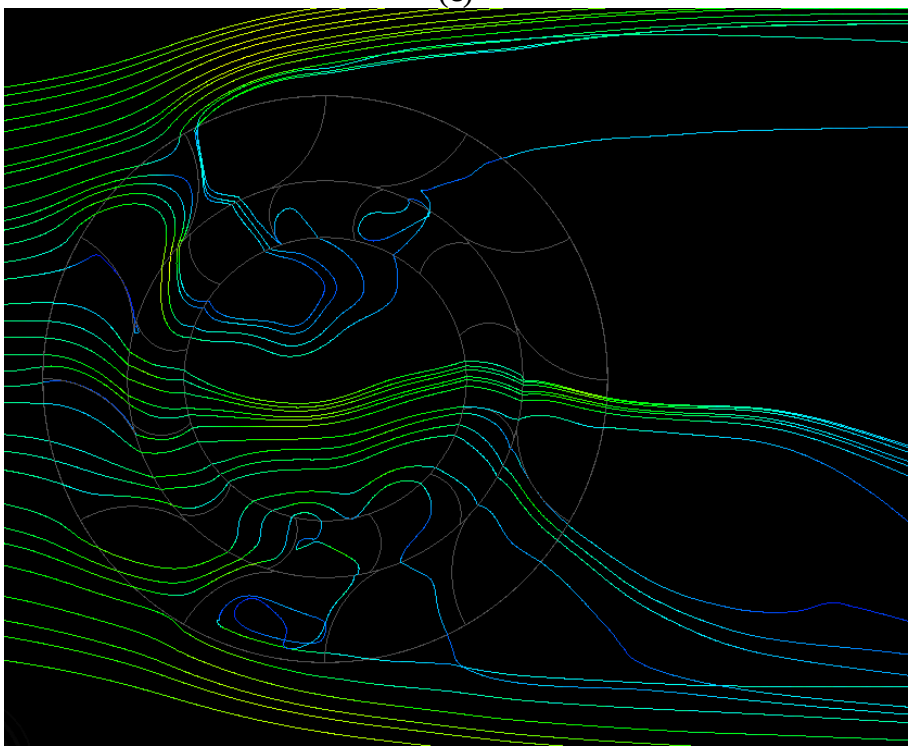

(d)

Figure 5.3 Flow pathlines, coloured by velocity, in the vicinity of the VAWT at (a) 0º (b) 3º (c) 15º (d) 27º for sand particles' diameter of 125microns at 1kg/sec mass flow rate

Figure 5.4 depicts the sand particles' tracks in the vicinity of the VAWT for the four geometrical configurations under discussion. The foremost observation from figure 5.4(a) is that most of the sand particles enter the VAWT through the passages formed between the rotor and stator blades on the windward side of the VAWT, where their velocity increases. However, due to a number of resistances in their path (in the form of blade walls), most of the sand particles get settled on these walls, whereas some particles escape the VAWT through the passages on the leeward side of the VAWT. Opening up of a small passage in figure 5.4(b) means that now a few sand particles can escape through these passages as well. However, they are more prone to settlement on the blade walls. Furthermore, in figure 5.4(c), when equal flow passages are formed, more sand particles escape the VAWT.

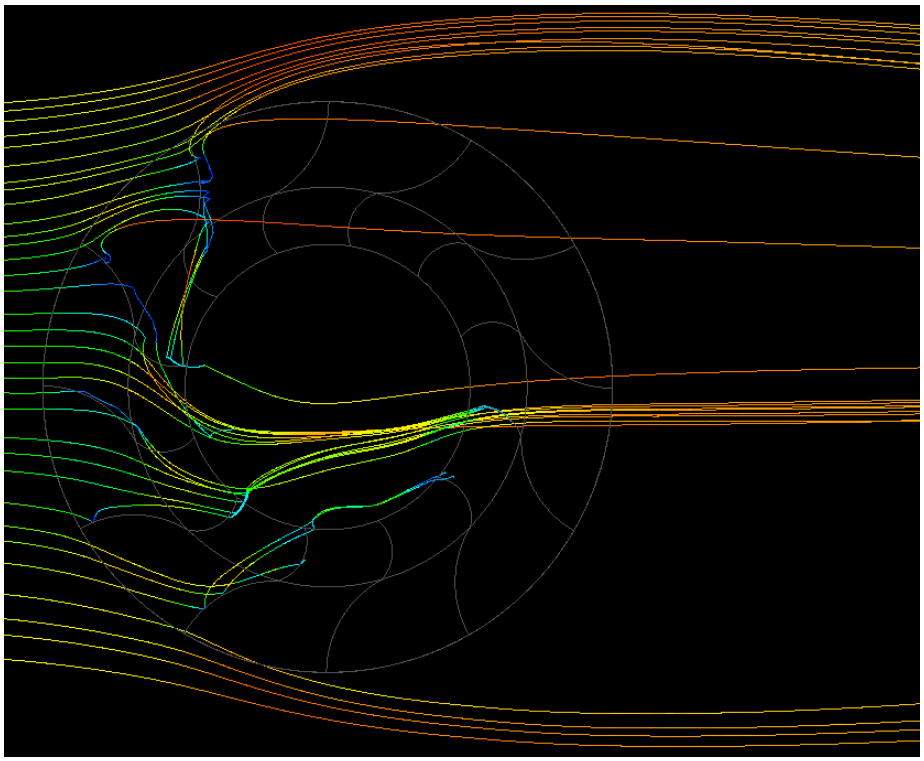

(a)

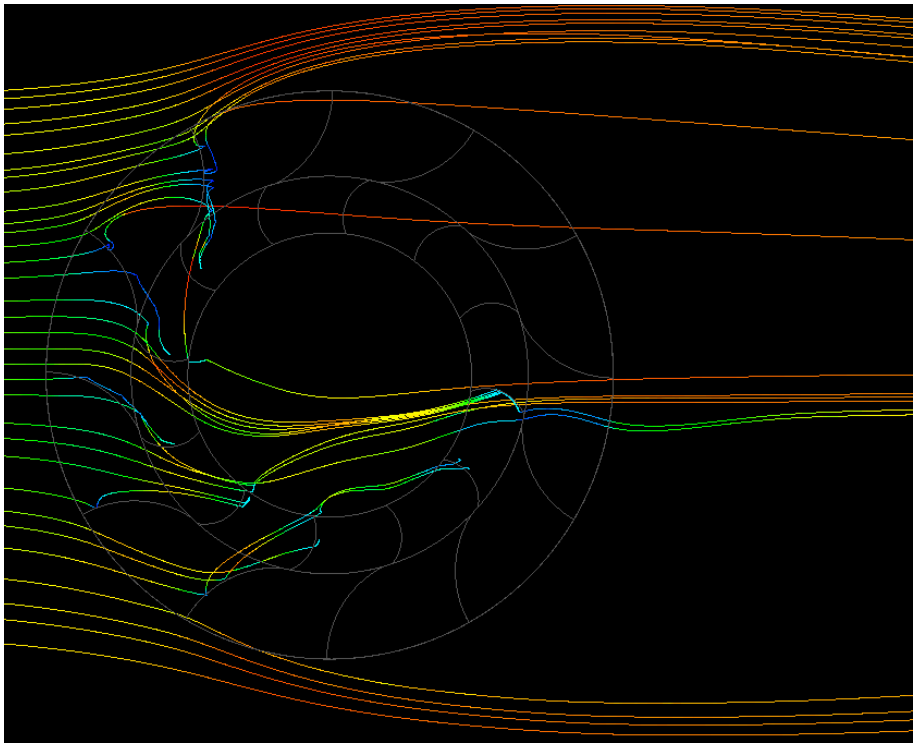

(b)

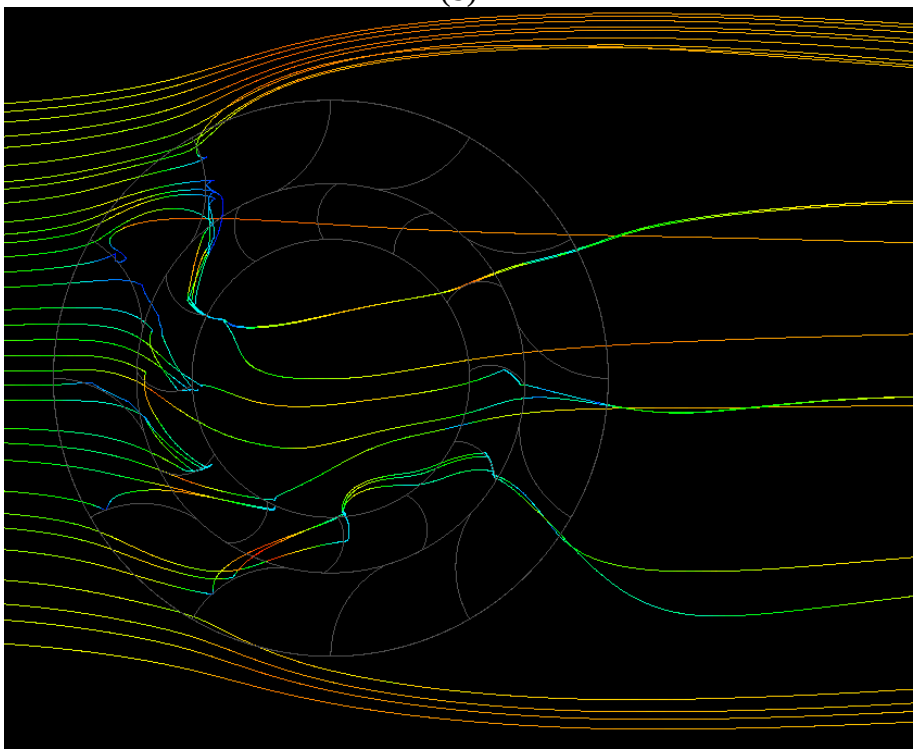

(c)

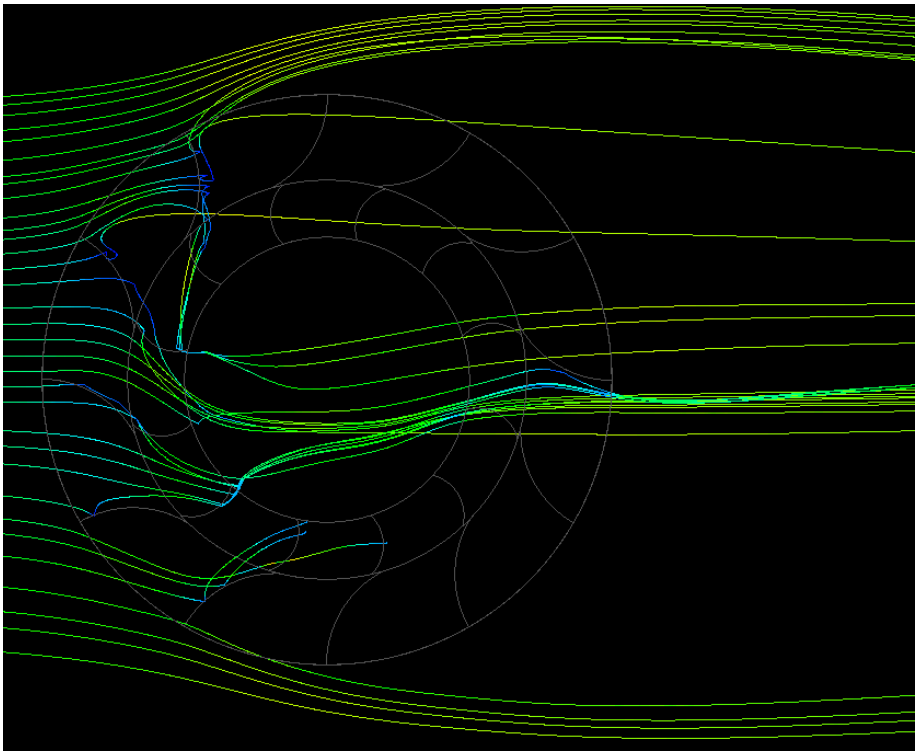

(d)

Figure 5.4 Sand particles' tracks, coloured by velocity, in the vicinity of the VAWT at (a) 0º (b) 3º (c) 15º (d) 27º for sand particles' diameter of 125microns at 1kg/sec mass flow rate

Figure 5.5 depicts the comparison of the instantaneous torque output from the VAWTs operating in clean and dusty environments, where the sand particles' diameter is 125microns with mass flow arte of 1kg/sec. It can be clearly seen that the presence of sand particles in the flow domain degrades the performance output of the VAWT by reducing its torque generating capabilities. The average torque generated by the VAWT under dusty conditions is 0.11% less than the VAWT operating in clean environment.

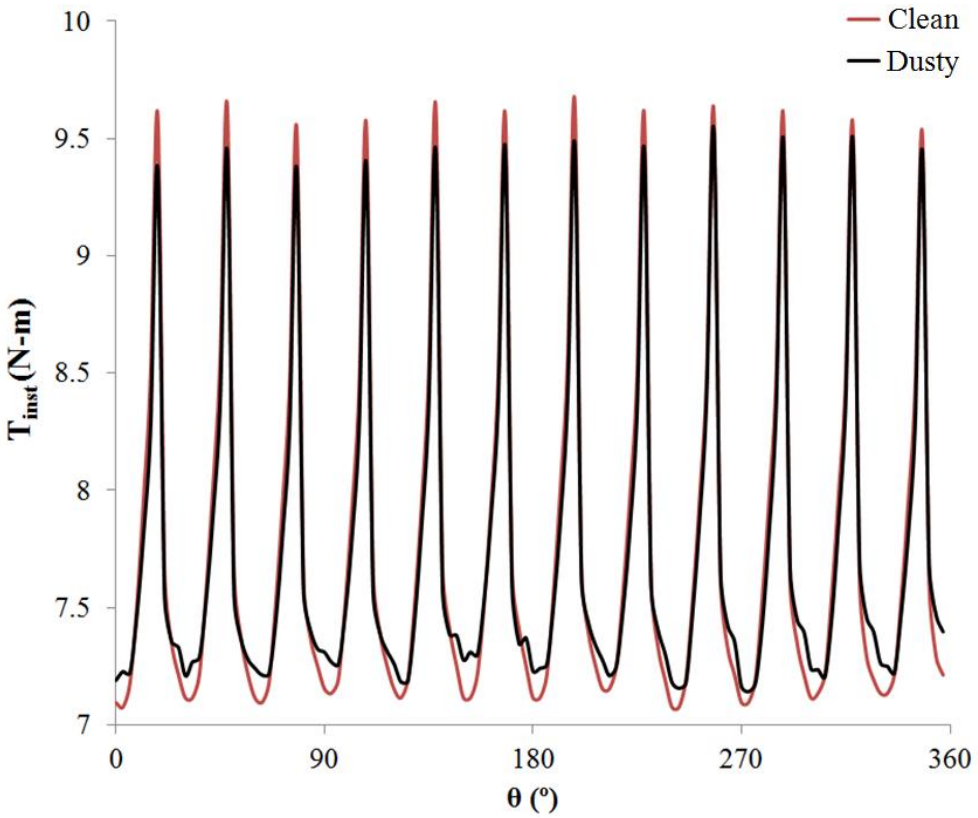

Figure 5.5 Instantaneous torque output comparison of the VAWTs operating in clean and dusty environments

Figure 5.6 depicts the contribution of individual rotor blades towards the total torque generated by the VAWT operating in dusty environment. In comparison with figure 4.8, it can be clearly seen that some rotor blades are in churning condition i.e. extracting energy from the flow rather than generating it.

Table 5.1 summarises the difference in the torque outputs from VAWTs operating in clean and dusty environments. It can be noticed that the peak-to-peak amplitude of the torque signals from the VAWT operating in dusty environment is 2.40N-m, which is 7.53% less than the VAWT operating in clean environment. Furthermore, there is a reduction of 0.11% in the average torque generation of the VAWT when it operates in dusty environments.

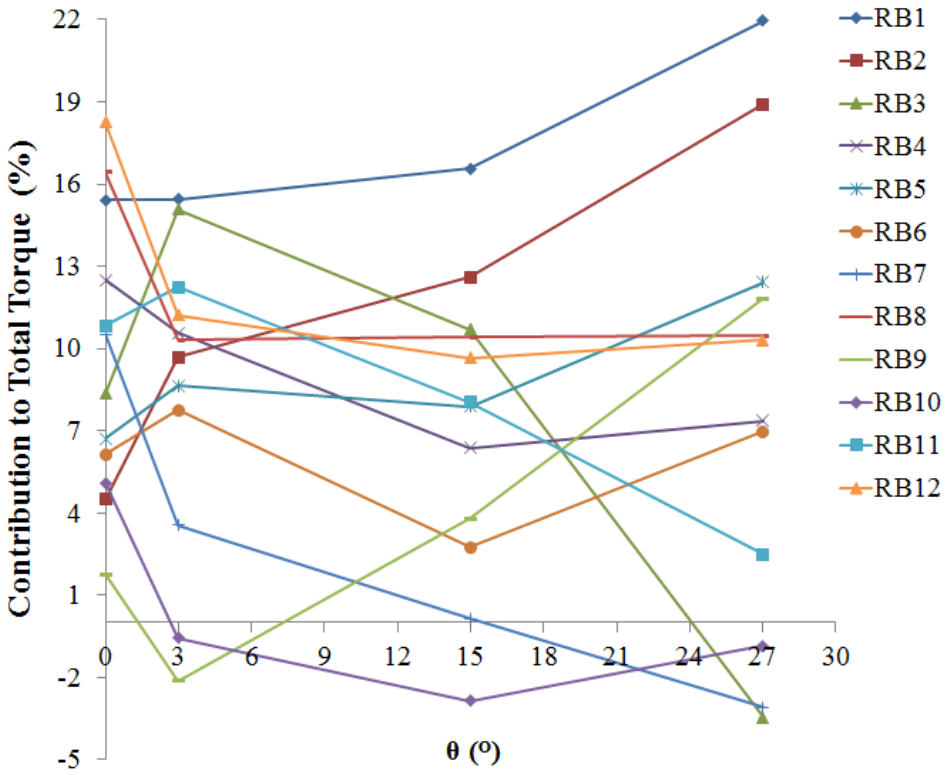

Figure 5.6 Contribution of each rotor blade to the overall torque generated by the VAWT operating in dusty environment with sand particle diameter of 125microns and mass flow rate of 1kg

Table 5.1 Performance analysis of the VAWT operating in dusty environment with sand particle diameter of 125microns and mass flow rate of 1kg

Torque Output (N-m)		Difference w.r.t. VAWT operating in clean environment (%)
Max	9.54	-1.27
Min	7.14	1.03
Max-Min	2.40	-7.53
Average	7.72	-0.11
Standard Deviation	0.67	-11.04

In order to quantitatively estimate the effects of dusty environment on the erosion characteristics of a VAWT, instantaneous erosion rate (in mm/yr) has been monitored on one of the rotor blades

(RB1) for one complete revolution of the VAWT, as shown in figure 5.7. It can be seen that the erosion rate is highest on the rotor blades when they are on either the windward side, or the leeward side of the VAWT. It has already been shown in figure 5.4 that most of the sand particles propagate through the passages formed at either the front, or the rear of the VAWT, hence eroding the rotor blades. The maximum erosion rate calculated for the case under discussion is 0.2mm/yr. Furthermore, it has also been noticed that apart from the windward and leeward sides of the VAWT, the rotor blades show negligible erosion rates as the sand particles either get deflected or settles on the blades present at other locations of the VAWT.

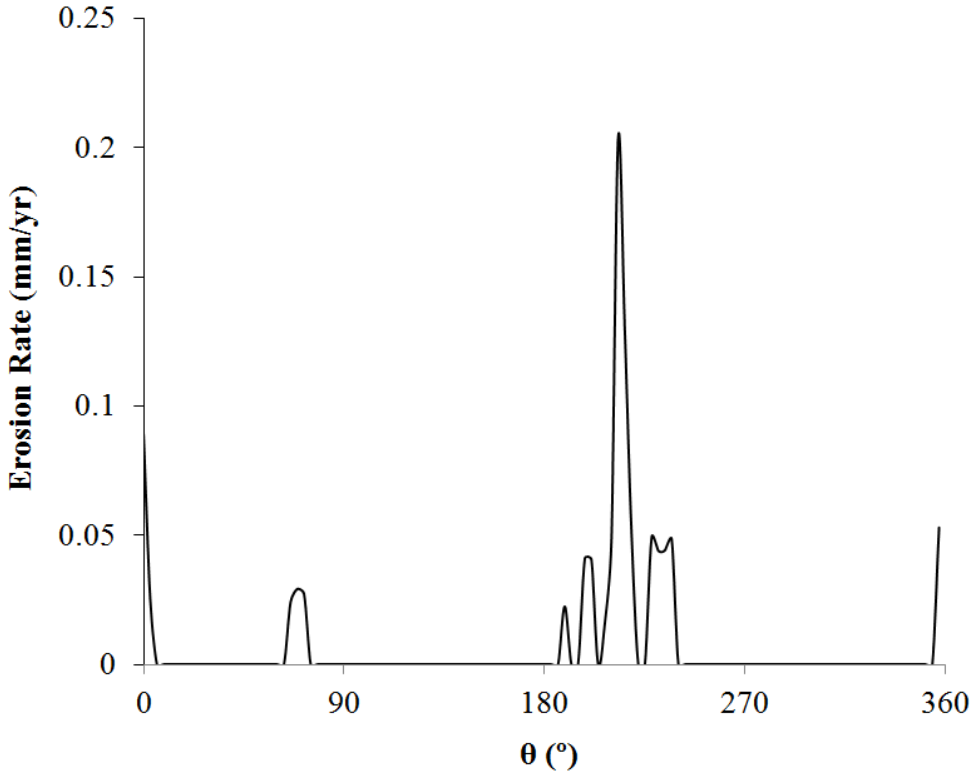

Figure 5.7 Instantaneous variations in the erosion rate (mm/yr) of a rotor blade for sand particles' diameter of 125microns at 1kg/sec mass flow rate

5.3 Effect of Sand Particles' Size on the Performance Output of a VAWT

Figure 5.8 depicts the variations in the static gauge pressure in the vicinity of the VAWT for the four different geometrical configurations when the diameter of the sand particles is 500microns. It can be seen in figure 5.8(a) that the high pressure regions are on the windward and leeward sides of the VAWT, whereas the low pressure regions occur primarily on the upper and lower sections of the VAWT. The general trend remains the same for all the different geometrical configurations of the VAWT considered here. However, there are significant local variations in the static gauge pressure distribution for different geometrical configurations.

When a rotor blade crosses a stator blade (figure 5.8(b)), the windward section of the VAWT depicts lower pressure. The high pressure regions in the vicinity of the rotor blades also shrink. Furthermore, when a rotor blade comes exactly in-between two stator blades, it has been noticed (in figure 5.8(c)) that more number of blades exhibit higher pressure zones. It can be further observed in figure 5.8(d) that the higher pressure regions grow considerably when a rotor blade approaches a stator blade, but there still exist a small degree of misalignment between the two. The trends shown here are inline with the one observed in case of VAWT with sand particles' diameter of 125microns.

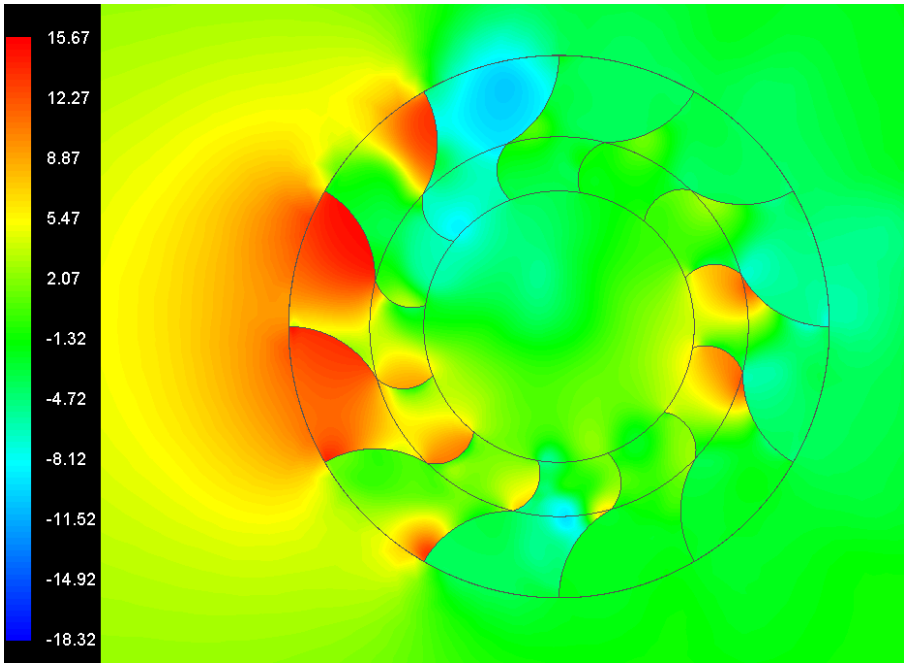

(a)

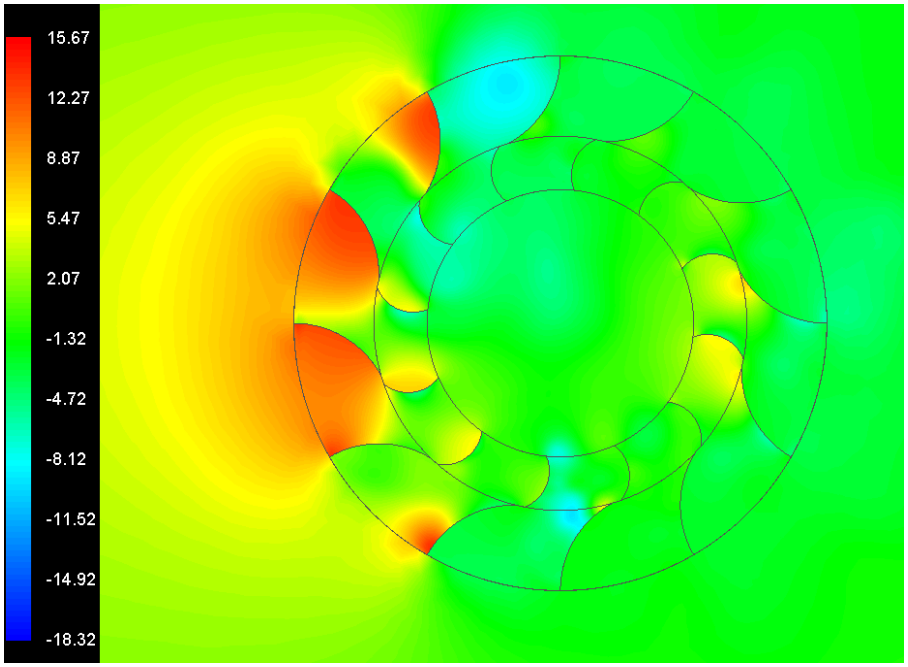
15.67
12.27
8.87
5.47
2.07
-1.32
-4.72
-8.12
-11.52
-14.92
-18.32

(b)

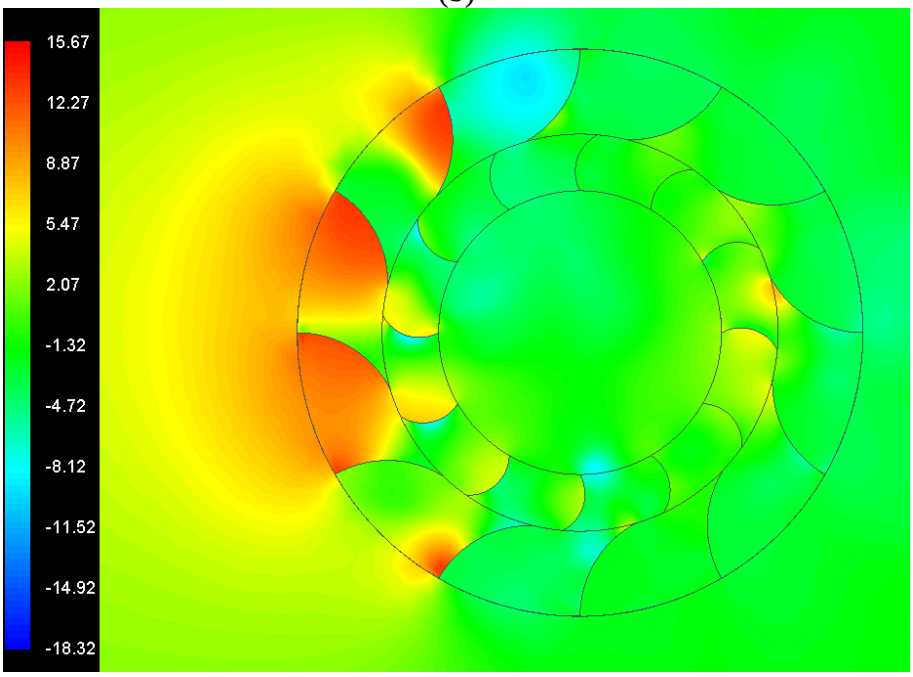
15.67
12.27
8.87
5.47
2.07
-1.32
-4.72
-8.12
-11.52
-14.92
-18.32

(c)

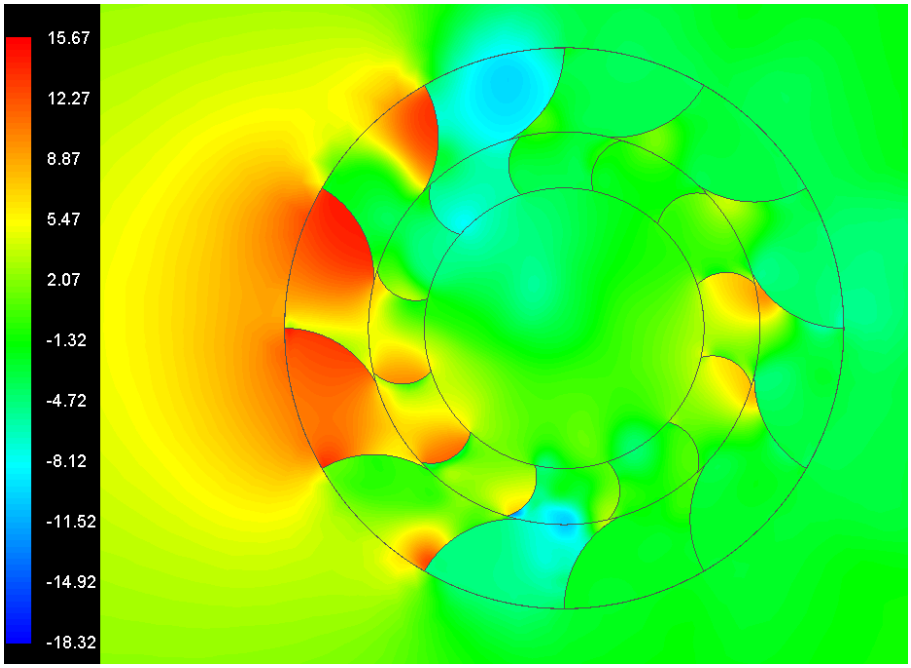

(d)

Figure 5.8 Static gauge pressure (Pa) variations in the vicinity of the VAWT at (a) 0º (b) 3º (c) 15º (d) 27º for sand particles' diameter of 500microns at 1kg/sec mass flow rate

Figure 5.9 depicts the variations in the flow velocity for the different geometrical configurations of the VAWT when the diameter of the sand particles is 500microns. It can be seen in figure 5.9(a) that the flow velocity is high in the passages formed between stator and rotor blades, whereas it is considerable lower in the zones where there is more resistance to the flow path (such as the upper and lower sections of the VAWT). Moreover, due to the concave profile of the stator blades, the lower section of the VAWT depicts higher flow velocities as compared to the upper section of the VAWT. An important point to note over here is that, as compared to sand particles' diameter of 125microns (figure 5.2), the flow velocity is lower throughout the flow domain.

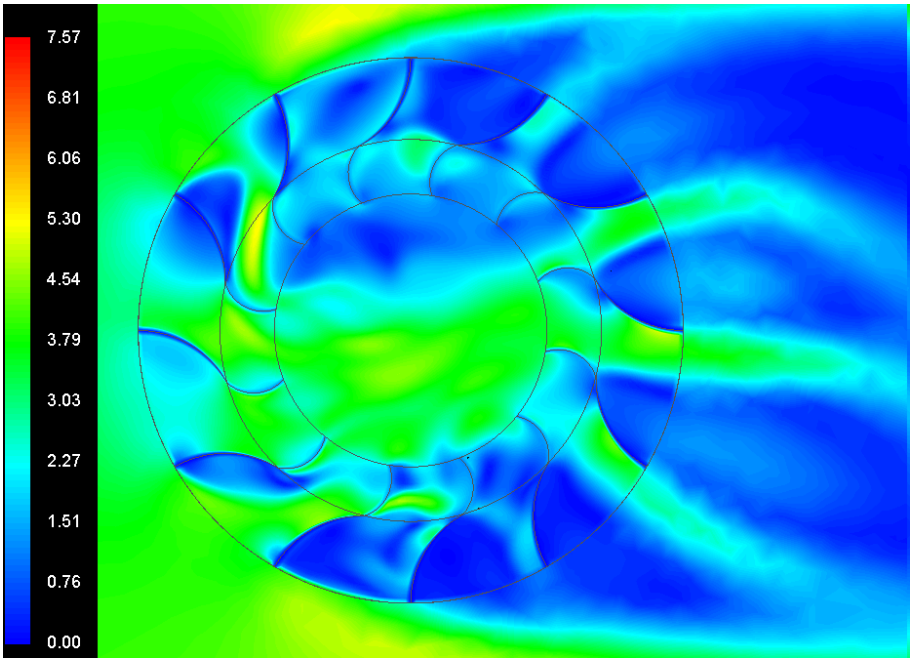
7.57
6.81
6.06
5.30
4.54
3.79
3.03
2.27
1.51
0.76
0.00

(a)

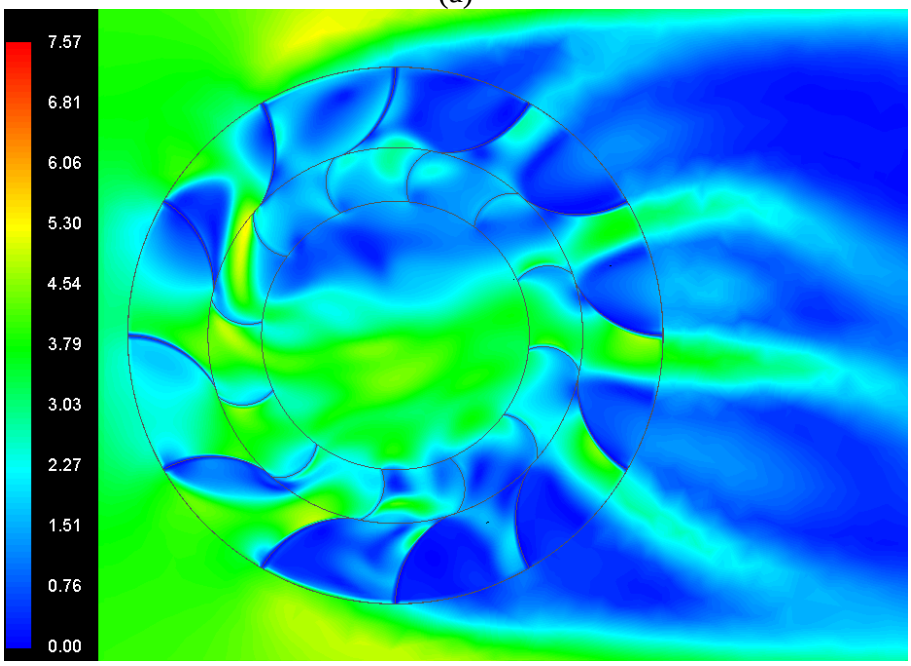
7.57
6.81
6.06
5.30
4.54
3.79
3.03
2.27
1.51
0.76
0.00

(b)

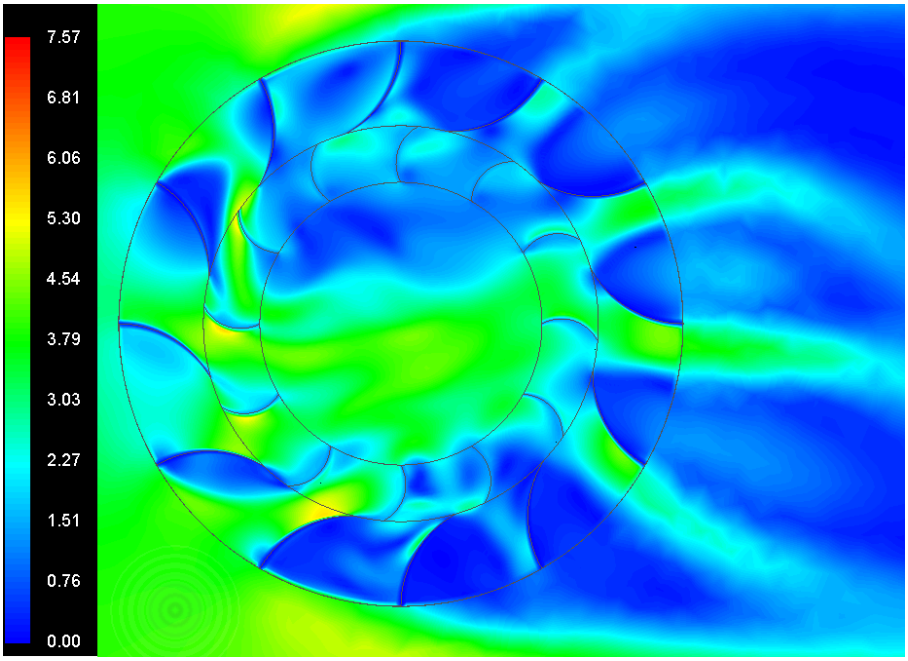

(c)

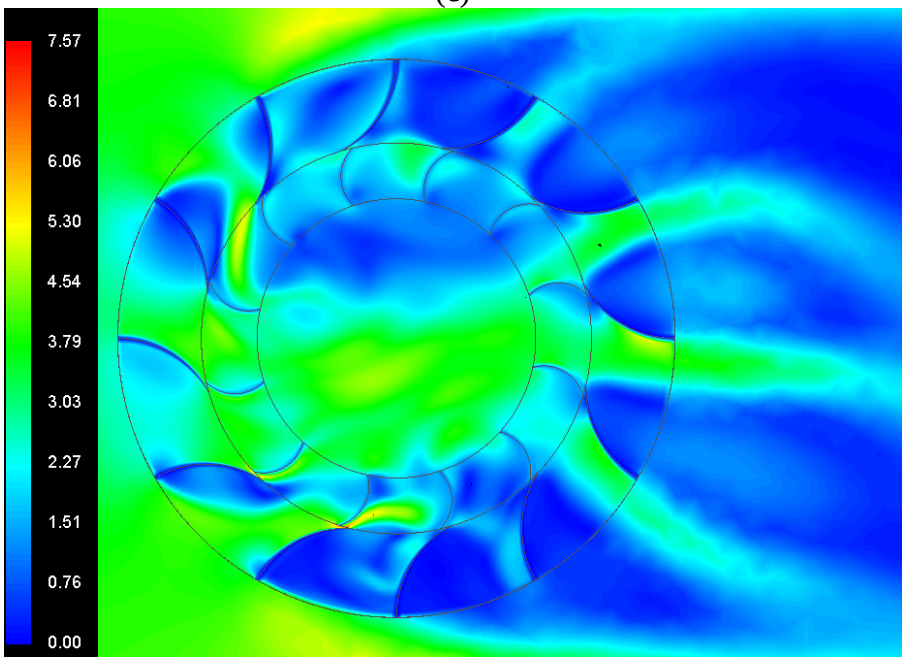

(d)

Figure 5.9 Velocity magnitude (m/sec) variations in the vicinity of the VAWT at (a) 0º (b) 3º (c) 15º (d) 27º for sand particles' diameter of 500microns at 1kg/sec mass flow rate

Figure 5.10 depicts the flow pathlines in the vicinity of the VAWT for sand particles' diameter of 500microns. Comparing figure 5.10 with figure 5.3 (125microns particles) it can be clearly seen that the disturbance in the flow domain is considerably higher for bigger sand particles. This is especially true at the leeward section of the VAWT. This is due to fact that bigger sand particles' tendency to settle down on the blades of the VAWT is significantly lower, due to their

higher inertia, and hence they cause more disturbances in the flow. Furthermore, the bigger sand particles offer more resistance to the flow of air through the VAWT, further increasing flow disturbances.

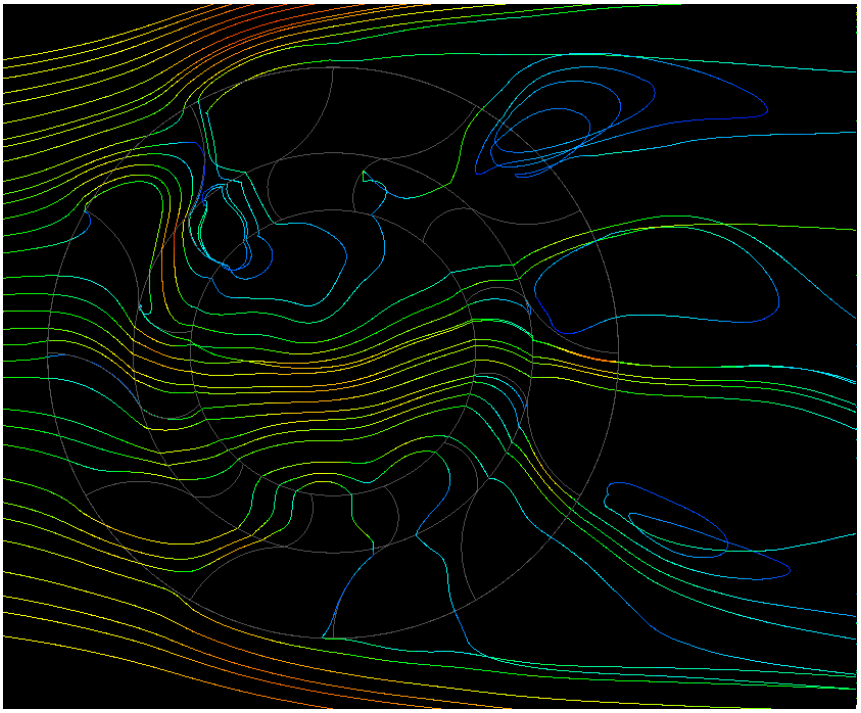

(a)

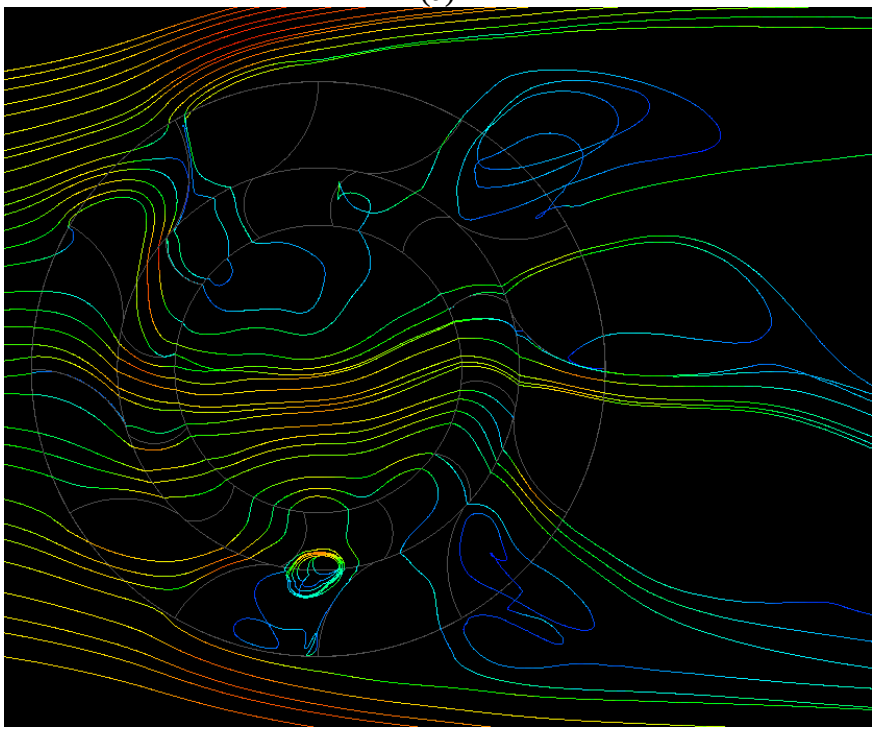

(b)

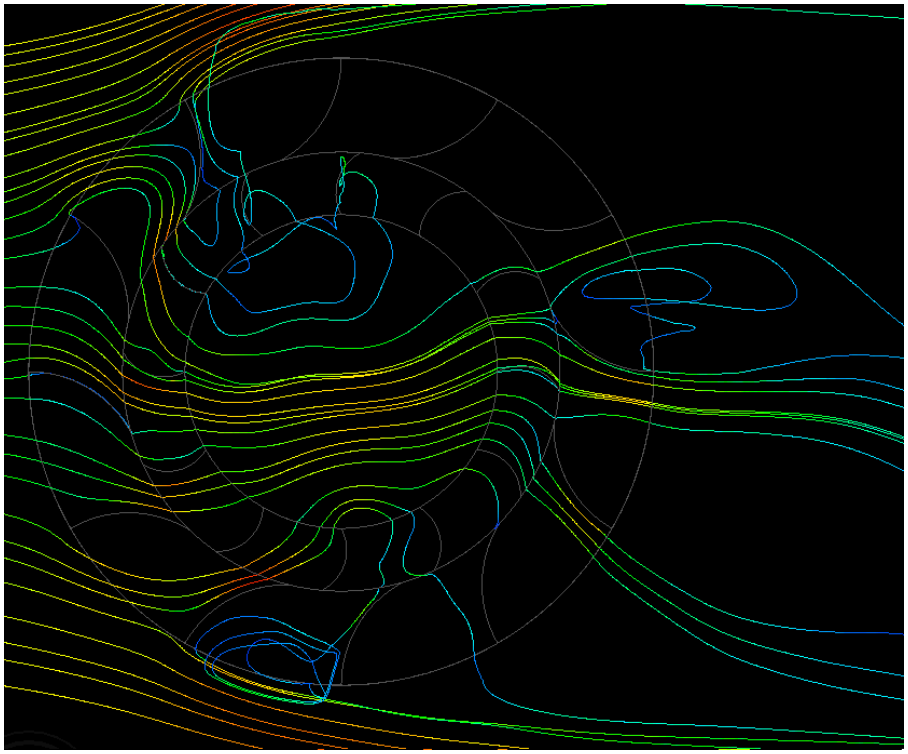

(c)

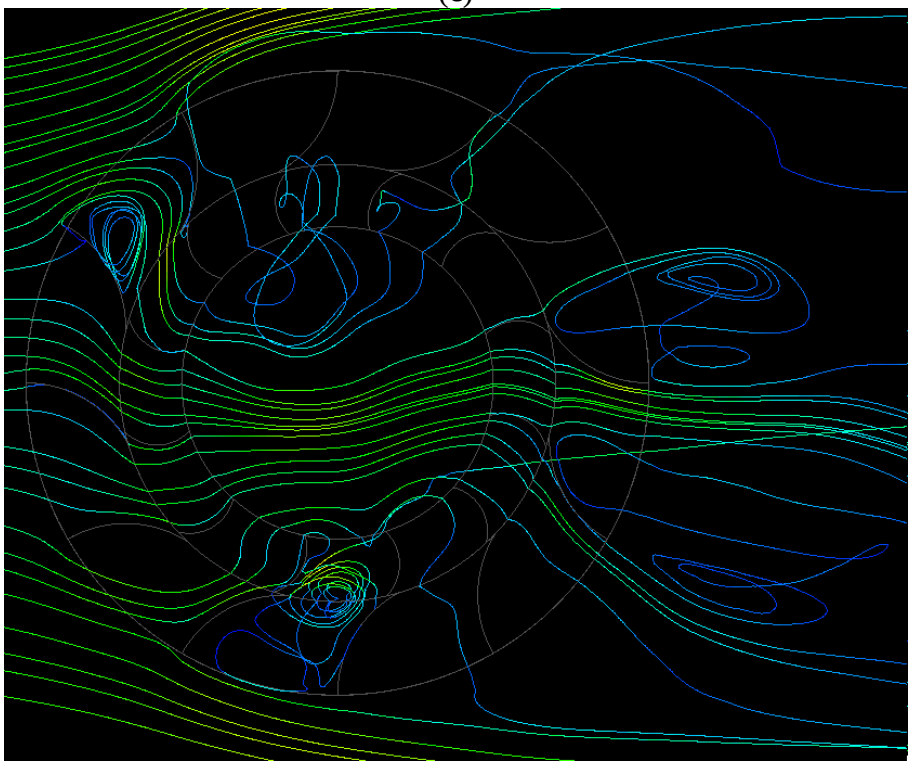

(d)

Figure 5.10 Flow pathlines', coloured by velocity, in the vicinity of the VAWT at (a) 0º (b) 3º (c) 15º (d) 27º for sand particles' diameter of 500microns at 1kg/sec mass flow rate

Figure 5.11 depicts the flow pathlines in the vicinity of the VAWT for sand particles' diameter of 500microns. In comparison with figure 5.4 (125microns), the most striking difference is the fact that in the present case, deflection of the sand particles from the blades of the VAWT on the windward side is significantly higher. Furthermore, more sand particles are escaping through the VAWT. This is because the size (and hence mass) of the sand particles is significantly higher as compared to 125microns, which means that the accretion capability of the sand particles reduces. As there are more deflections and more particles exiting the VAWT, it is anticipated that the erosion on the VAWT blades will be considerably higher for bigger sand particles.

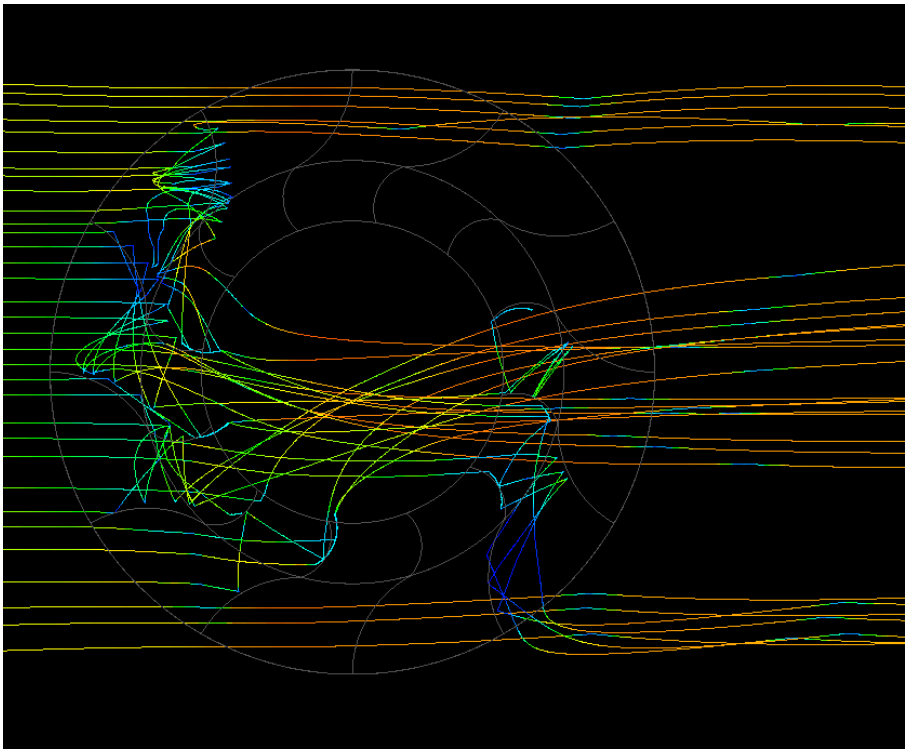

(a)

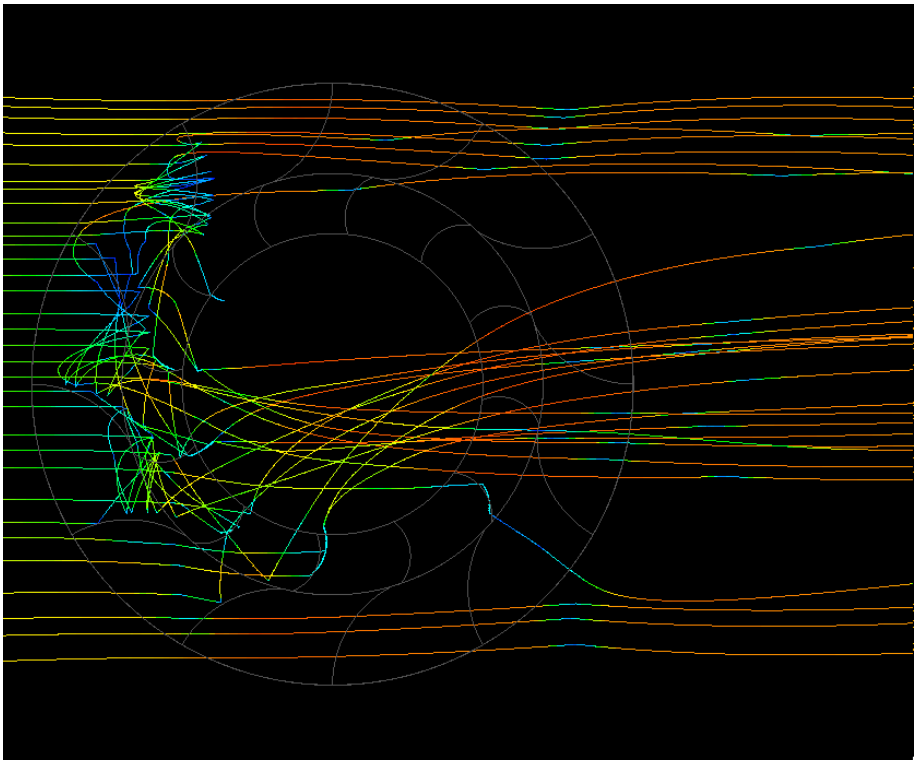

(b)

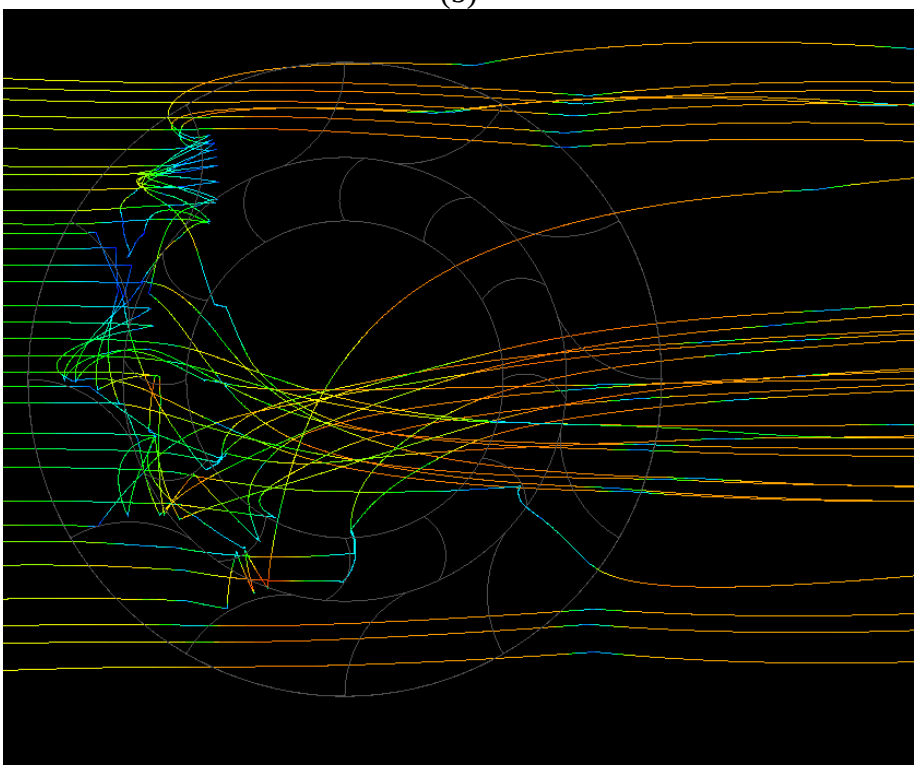

(c)

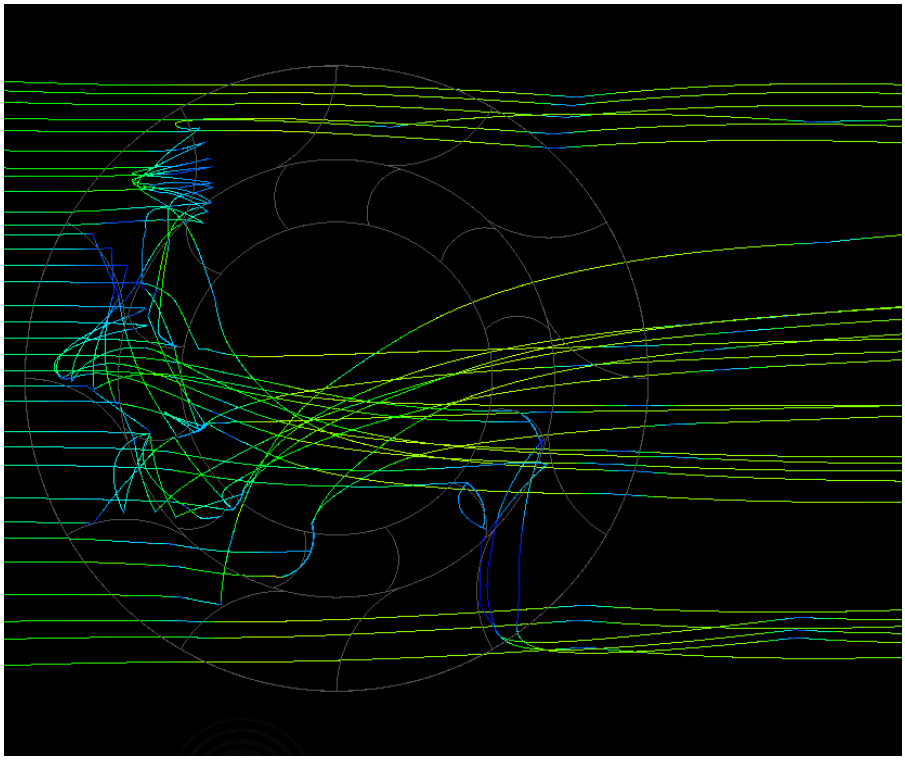

(d)

Figure 5.11 Sand particles' tracks, coloured by velocity, in the vicinity of the VAWT at (a) 0º (b) 3º (c) 15º (d) 27º for sand particles' diameter of 500microns at 1kg/sec mass flow rate

Figure 5.12 depicts the comparison of the instantaneous torque output from the VAWTs for sand particles' diameters of 125microns and 500microns. It can be seen that the presence of bigger sand particles in the flow domain degrades the performance output of the VAWT by reducing its average torque. This is because although the higher torque values for the two are nearly the same, the lower torque values for 500microns are considerable lower than for 125microns. The average torque generated by the VAWT for 500microns is 1.66% less than for 125microns.

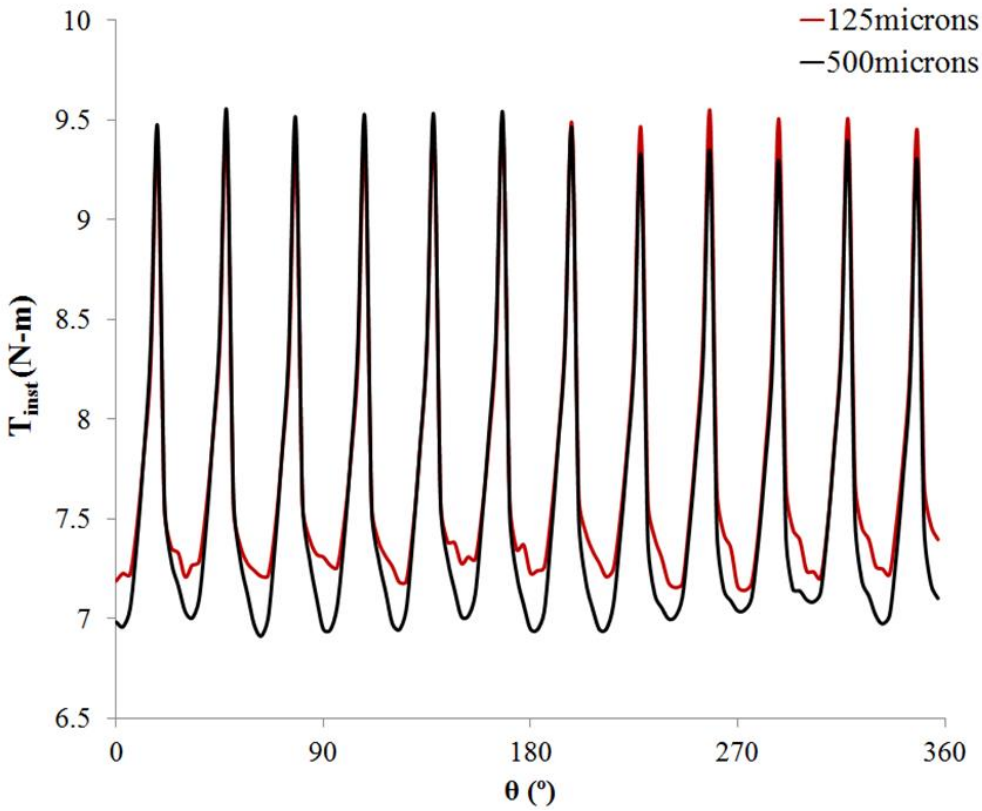

Figure 5.12 Instantaneous torque output comparison of the VAWTs operating in dusty environment with sand particle diameters of 125microns and 500microns

Figure 5.13 depicts the contribution of individual rotor blades towards the total torque generated by the VAWT for sand particles' diameter of 500microns. In comparison with figure 5.6, it can be noticed that RB9, RB10 and RB12 rotor blades are generating lesser torque. This is because of more erosion on these rotor blades, because of:

- Higher flow velocity on the lower sections of the VAWT (discussed above)
- More number of sand particles exiting the VAWT (discussed above)

Table 5.2 summarises the difference in the torque outputs from VAWTs for 125microns and 500microns sand particles. It can be noticed that although the peak-to-peak amplitude of the torque signals from the VAWT for 500microns sand particles is 2.63N-m, which is 9.69% higher than for 125microns (as observed and discussed in figure 5.12), however, the average torque generation from the VAWT is 1.66% less. An increase of 10.58% in the standard deviation of the torque output for 500microns, as compared to 125microns, further indicates that the structural integrity of the VAWT is seriously compromised.

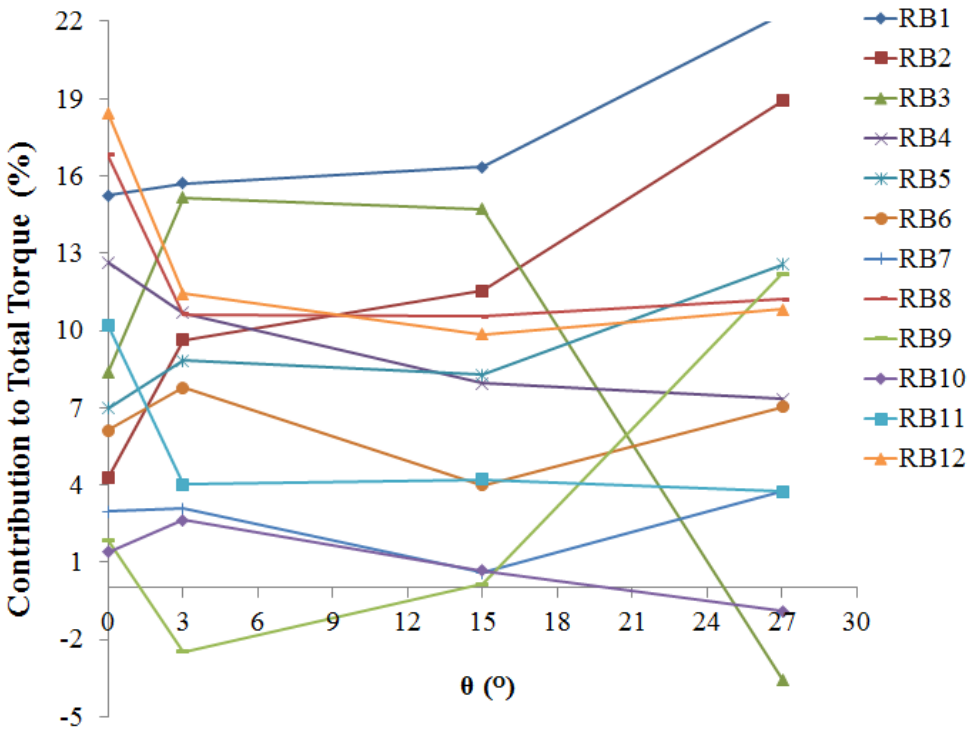

Figure 5.13 Contribution of each rotor blade to the overall torque generated by the VAWT operating in dusty environment with sand particle diameter of 500microns and mass flow rate of 1kg

Table 5.2 Performance analysis of the VAWT operating in dusty environment with sand particle diameter of 500microns and mass flow rate of 1kg

Torque Output (N-m)		Difference w.r.t. sand particles of 125microns diameter (%)
Max	9.54	0.04
Min	6.91	-3.20
Max-Min	2.63	9.69
Average	7.59	-1.66
Standard Deviation	0.74	10.58

Figure 5.14 depicts the instantaneous erosion rate on RB1 for one complete revolution of the VAWT, where the sand particles' diameters are 125microns and 500microns. It can be clearly seen that the erosion rate for bigger sand particles is significantly higher, with the maximum erosion rate of 1.25mm/yr. The general trend of the erosion rate, however, remains that same i.e.

higher erosion rate when the rotor blades are either on the windward or the leeward sides of the VAWT. Furthermore, as the accretion capability of the sand particles has reduced for bigger sand particles, there are fewer geometrical positions of the rotor blades where there is negligible erosion rate.

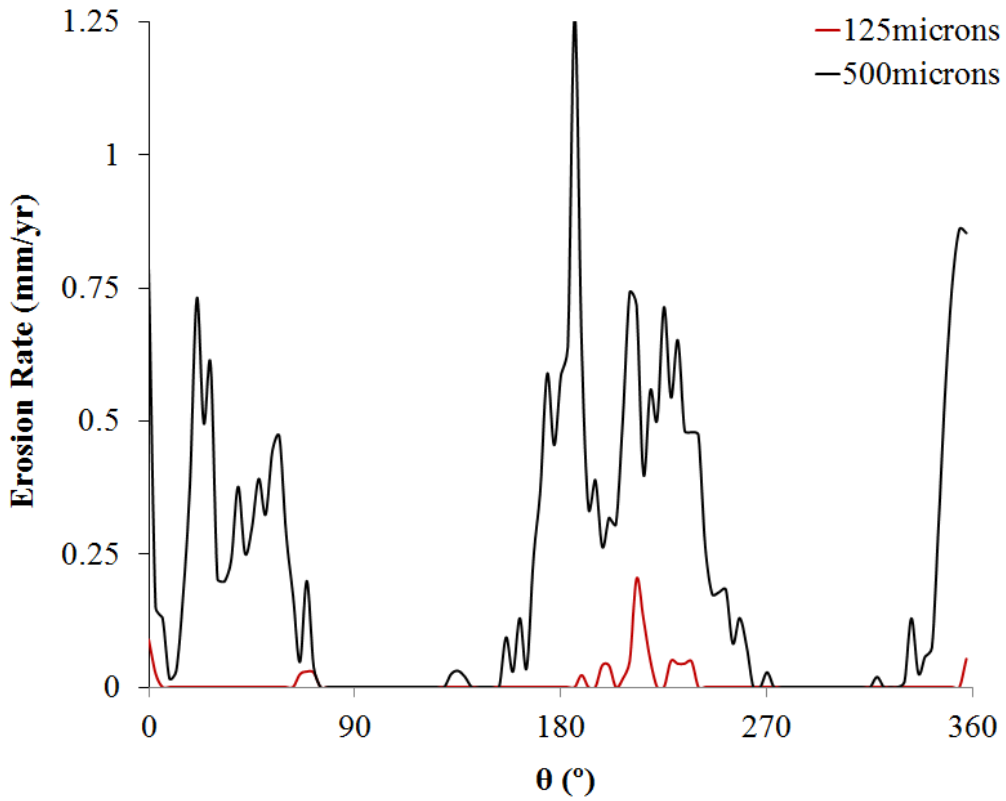

Figure 5.14 Instantaneous variations in the erosion rate (mm/yr) of a rotor blade for sand particles' diameters of 125microns and 500microns at 1kg/sec mass flow rate

5.4 Effect of Sand Particles' Mass Flow Rate on the Performance Output of a VAWT

Figure 5.15 depicts the variations in the static gauge pressure in the vicinity of the VAWT for the four different geometrical configurations when the mass flow rate of the sand particles is 2kg/sec. It can be seen in figure 5.15(a) that the high pressure regions are on the windward and leeward sides of the VAWT, whereas the low pressure regions occur primarily on the upper and lower sections of the VAWT. The general trend remains the same for all the different geometrical configurations of the VAWT considered here. However, there are significant local variations in the static gauge pressure distribution for different geometrical configurations.

When a rotor blade crosses a stator blade (figure 5.15(b)), the windward section of the VAWT depicts lower pressure. The high pressure regions in the vicinity of the rotor blades also shrink.

Furthermore, when a rotor blade comes exactly in-between two stator blades, it has been noticed (in figure 5.15(c)) that more number of blades exhibit higher pressure zones. It can be further observed in figure 5.15(d) that the higher pressure regions grow considerably when a rotor blade approaches a stator blade, but there still exist a small degree of misalignment between the two. The trends shown here are inline with the one observed in case of VAWT with sand particles' mass flow rate of 1kg/sec.

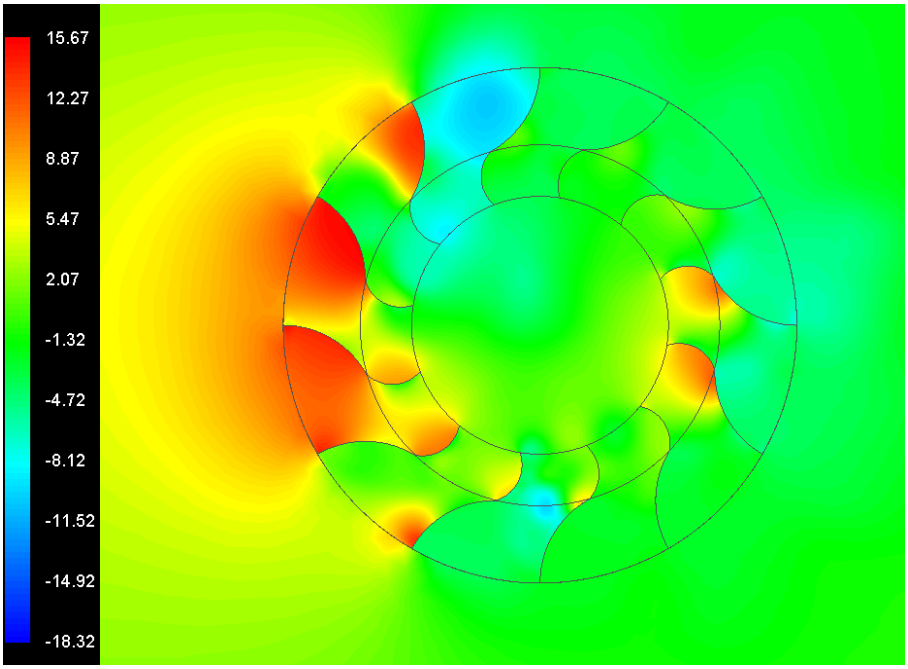

(a)

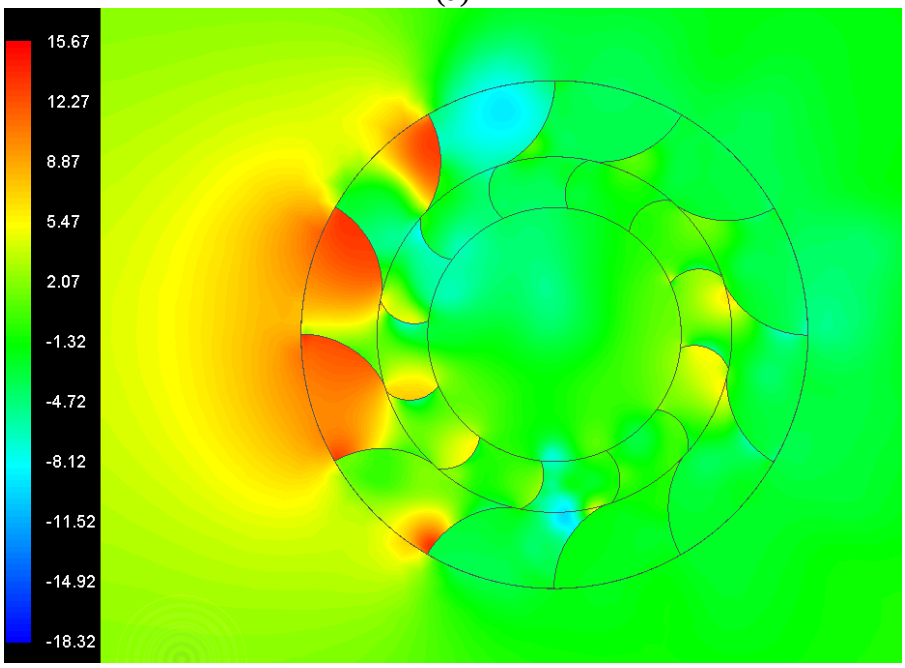

(b)

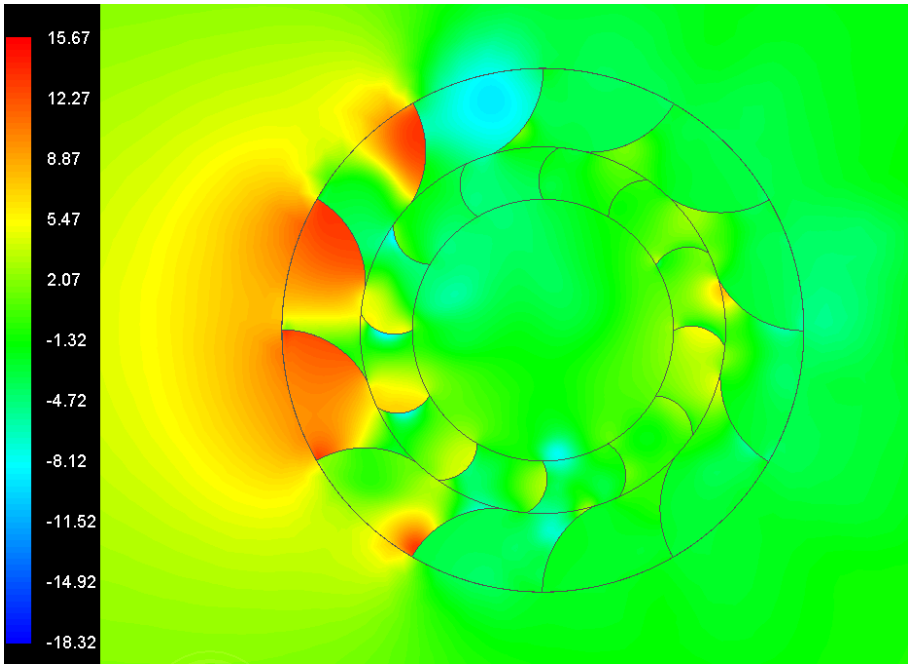

(c)

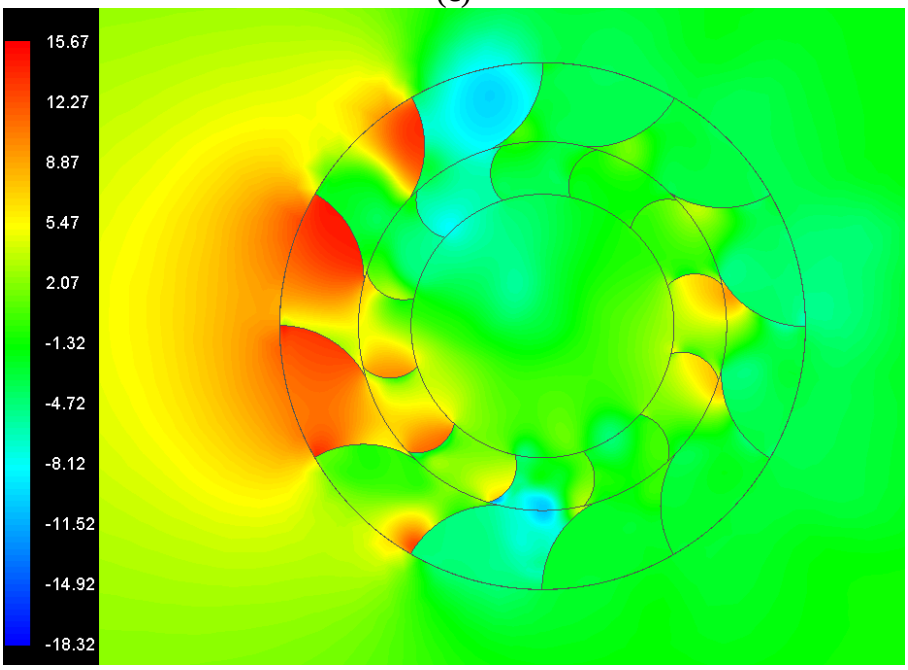

(d)

Figure 5.15 Static gauge pressure (Pa) variations in the vicinity of the VAWT at (a) 0º (b) 3º (c) 15º (d) 27º for sand particles' mass flow rate of 2kg/sec and diameter of 125microns

Figure 5.16 depicts the variations in the flow velocity for the different geometrical configurations of the VAWT when the mass flow rate of the sand particles is 2kg/sec. It can be seen in figure 5.16(a) that the flow velocity is high in the passages formed between stator and rotor blades, whereas it is considerable lower in the zones where there is more resistance to the flow path

(such as the upper and lower sections of the VAWT). Moreover, due to the concave profile of the stator blades, the lower section of the VAWT depicts higher flow velocities as compared to the upper section of the VAWT. An important point to note over here is that, as compared to sand particles' mass flow rate of 1kg/sec (figure 5.2), the flow velocity is lower throughout the flow domain.

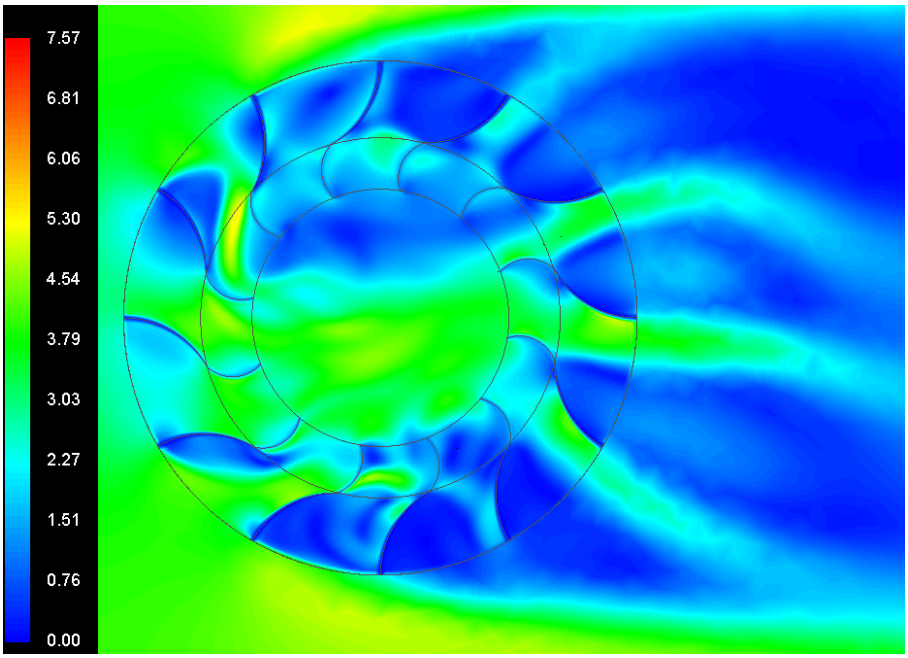

(a)

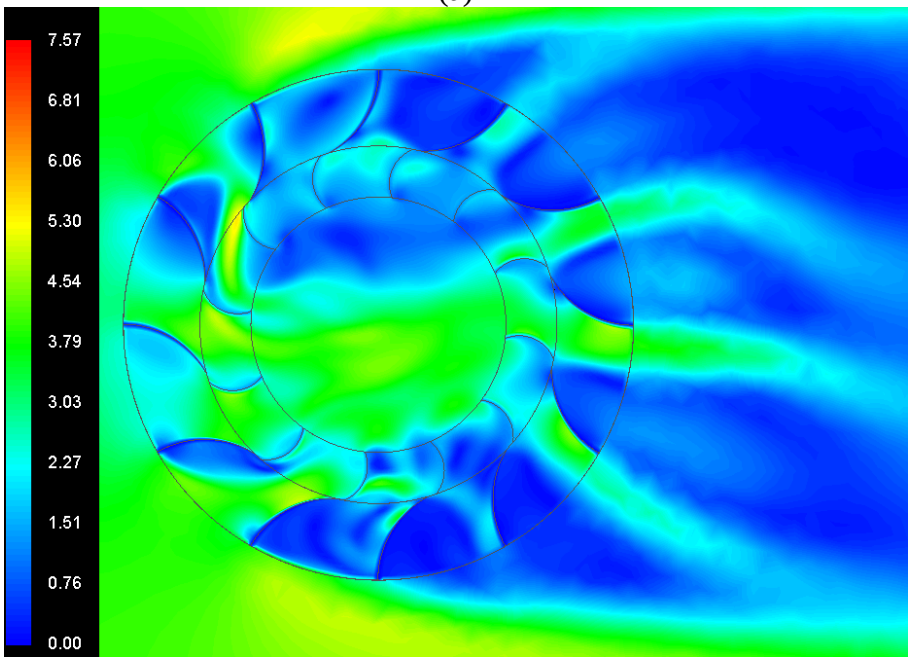

(b)

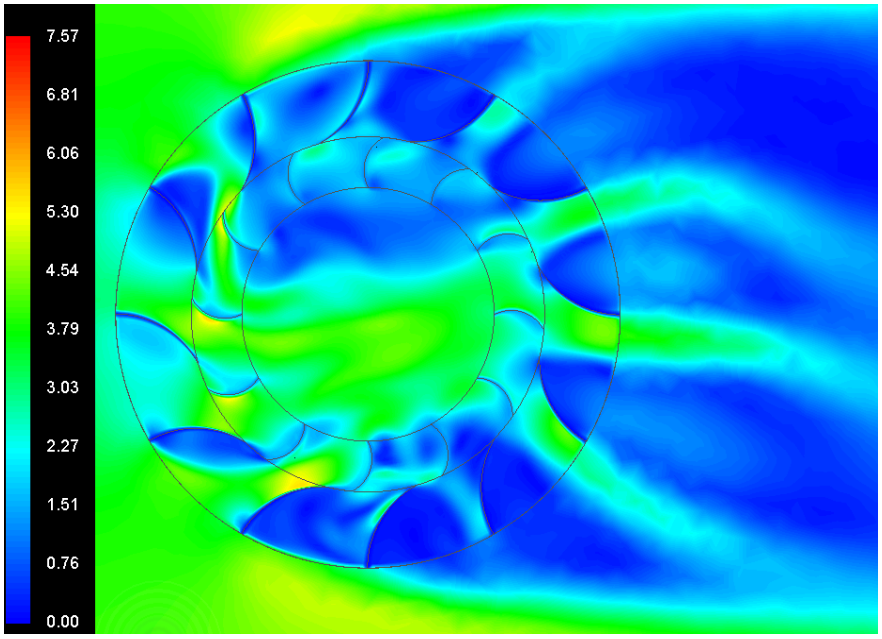

(c)

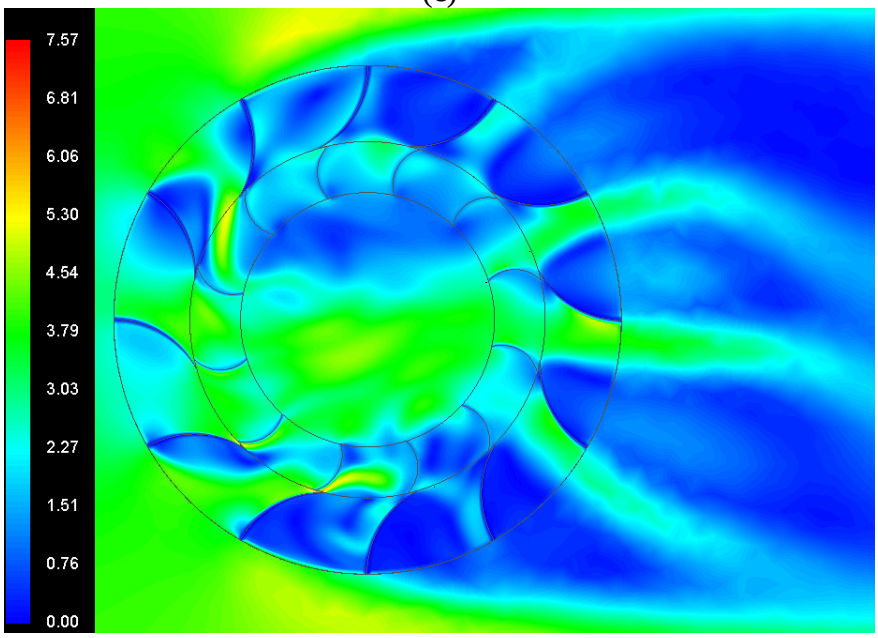

(d)

Figure 5.16 Velocity magnitude (m/sec) variations in the vicinity of the VAWT at (a) 0º (b) 3º (c) 15º (d) 27º for sand particles' mass flow rate of 2kg/sec and diameter of 125microns

Figure 5.17 depicts the flow pathlines in the vicinity of the VAWT for sand particles' mass flow rate of 2kg/sec. Comparing figure 5.17 with figure 5.3 (1kg/sec) it can be seen that the disturbance in the flow domain is considerably higher for more sand particles. This is especially true at the leeward section of the VAWT. This is due to fact that when the mass flow arte of the sand particles increases, there is more resistance to the flow of air and hence more disturbance in the flow domain.

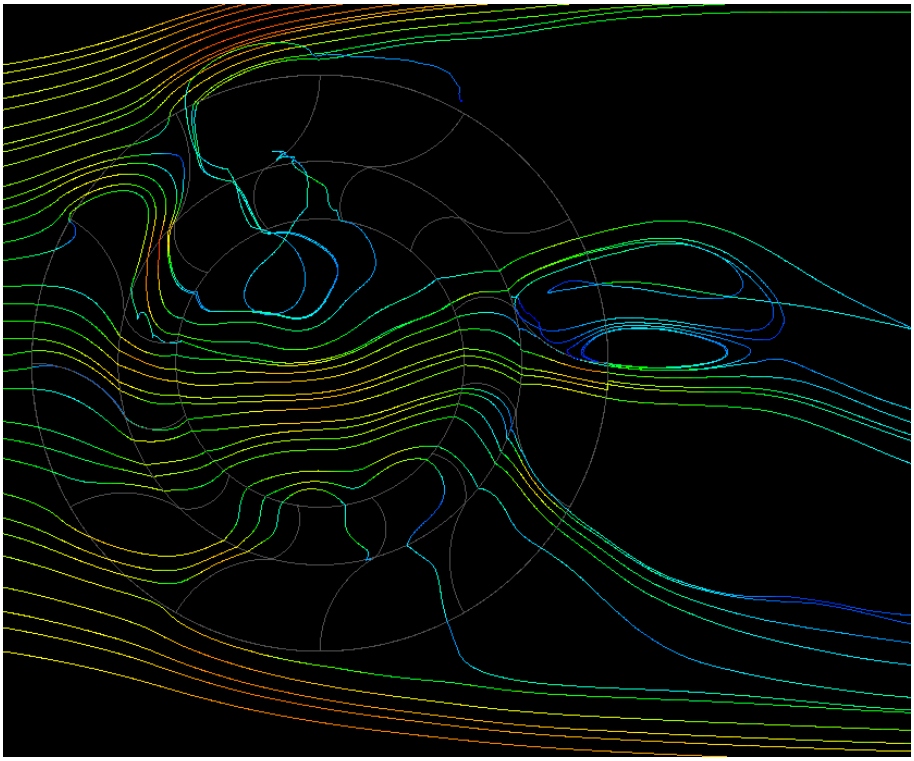

(a)

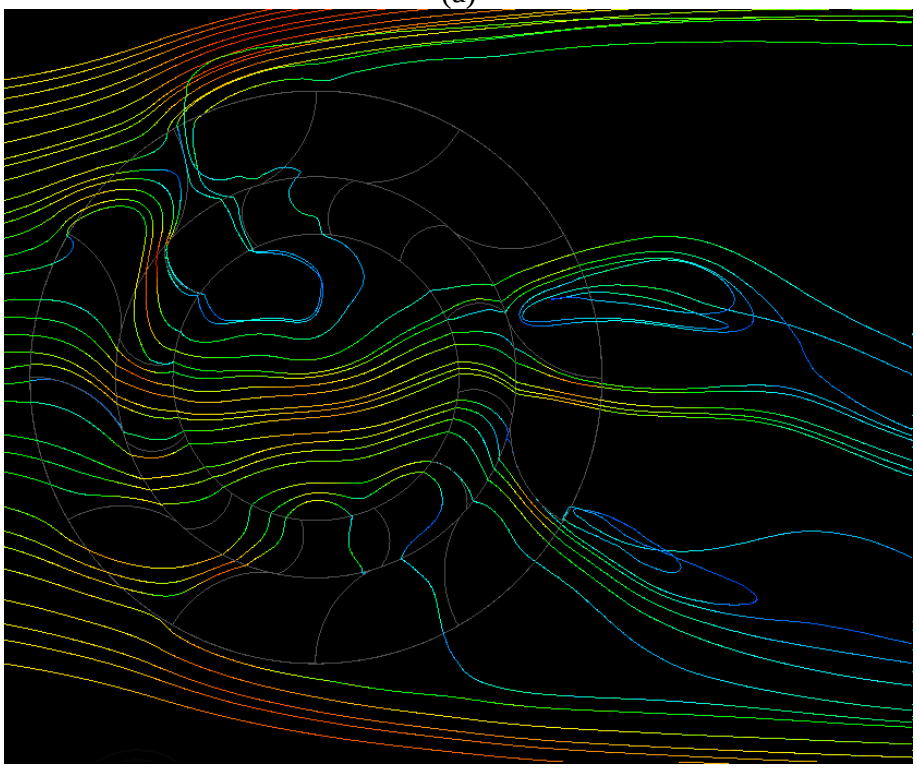

(b)

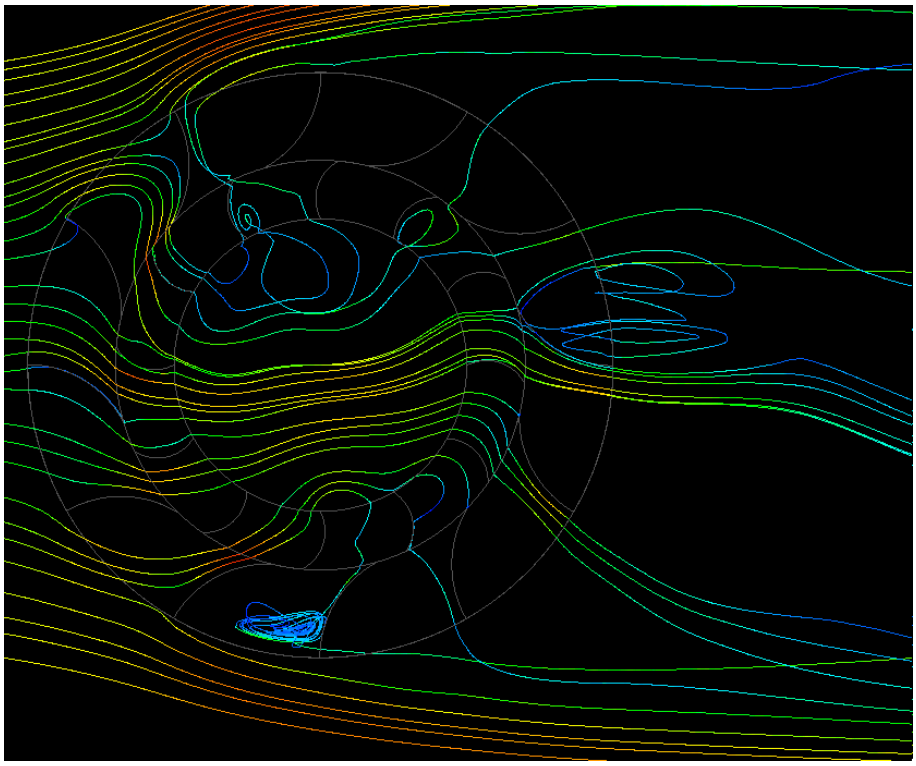

(c)

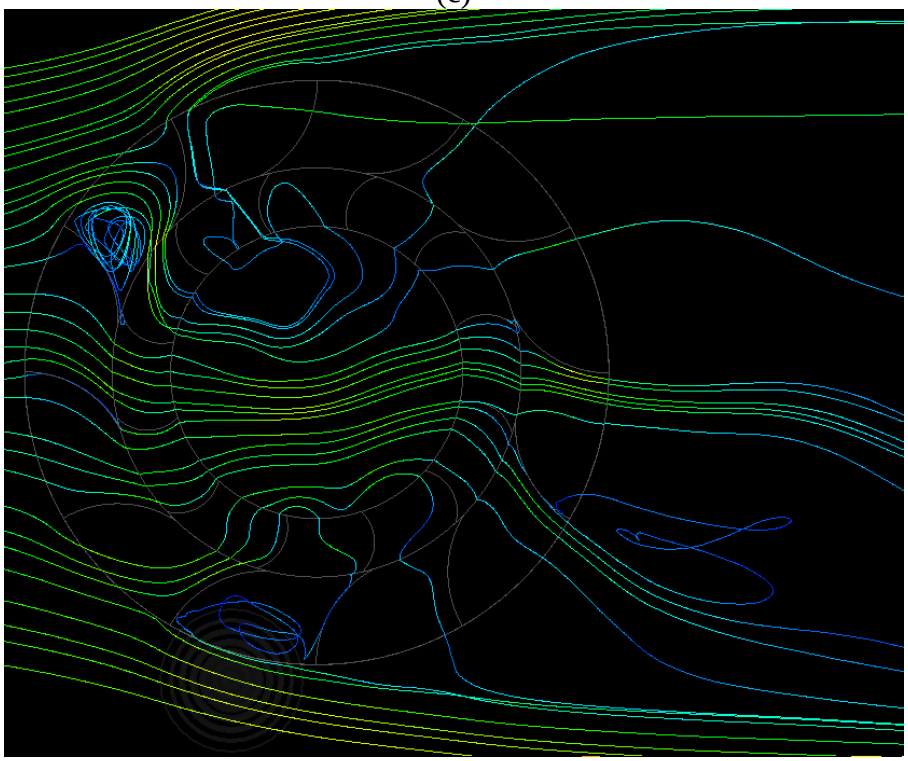

(d)

Figure 5.17 Flow pathlines', coloured by velocity, in the vicinity of the VAWT at (a) 0º (b) 3º (c) 15º (d) 27º for sand particles' mass flow rate of 2kg/sec and diameter of 125microns

Figure 5.18 depicts the flow pathlines in the vicinity of the VAWT for sand particles' mass flow rate of 2kg/sec. In comparison with figure 5.4 (1kg/sec), it can be seen that there is no appreciable difference in the particle tracks. One possible reason for this trend could be that the because of more sand particles being introduced in the flow domain, the path they follow will not change, and the only difference would be that more sand particles will follow that path.

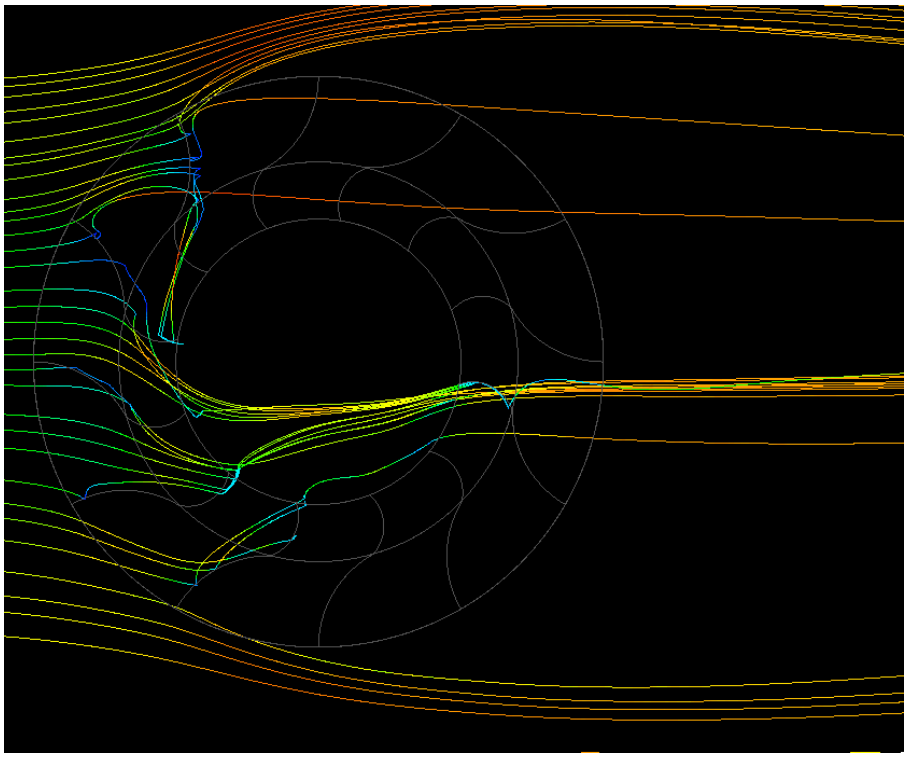

(a)

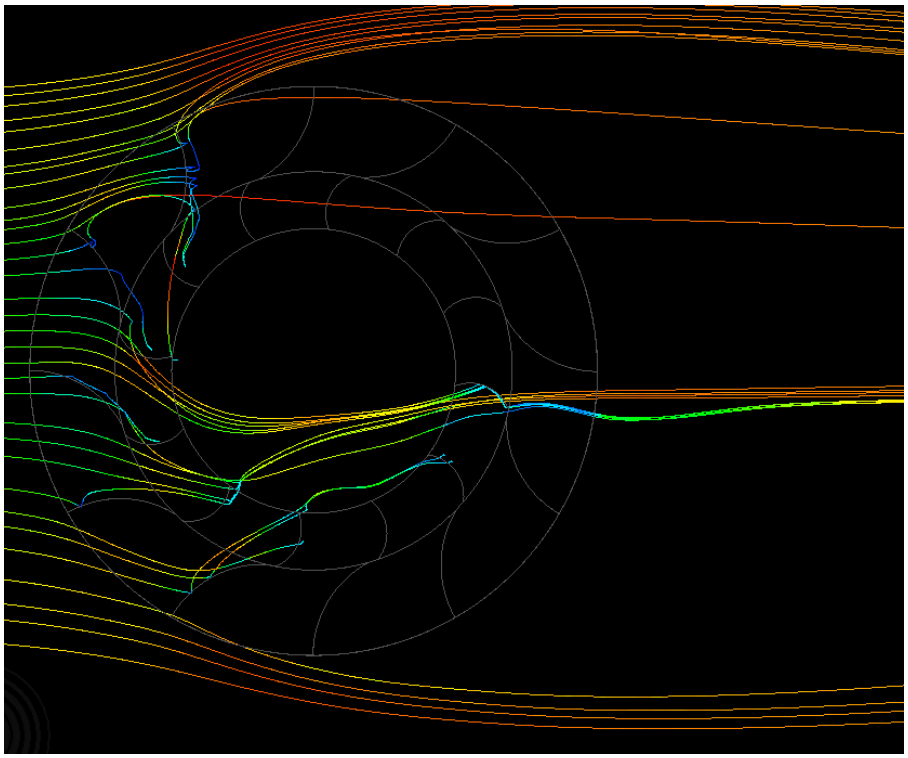

(b)

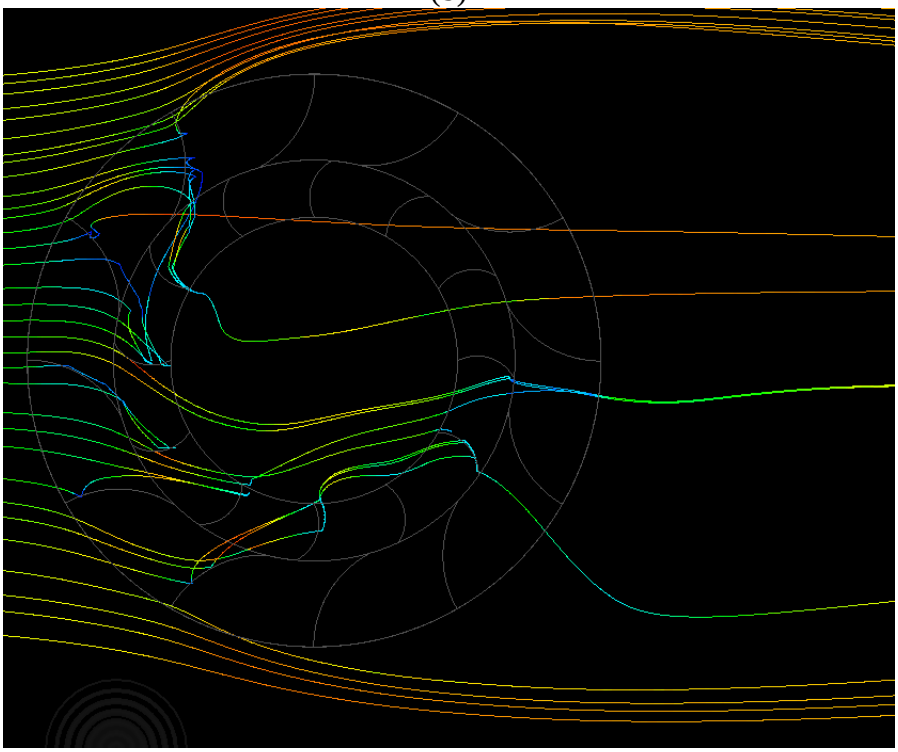

(c)

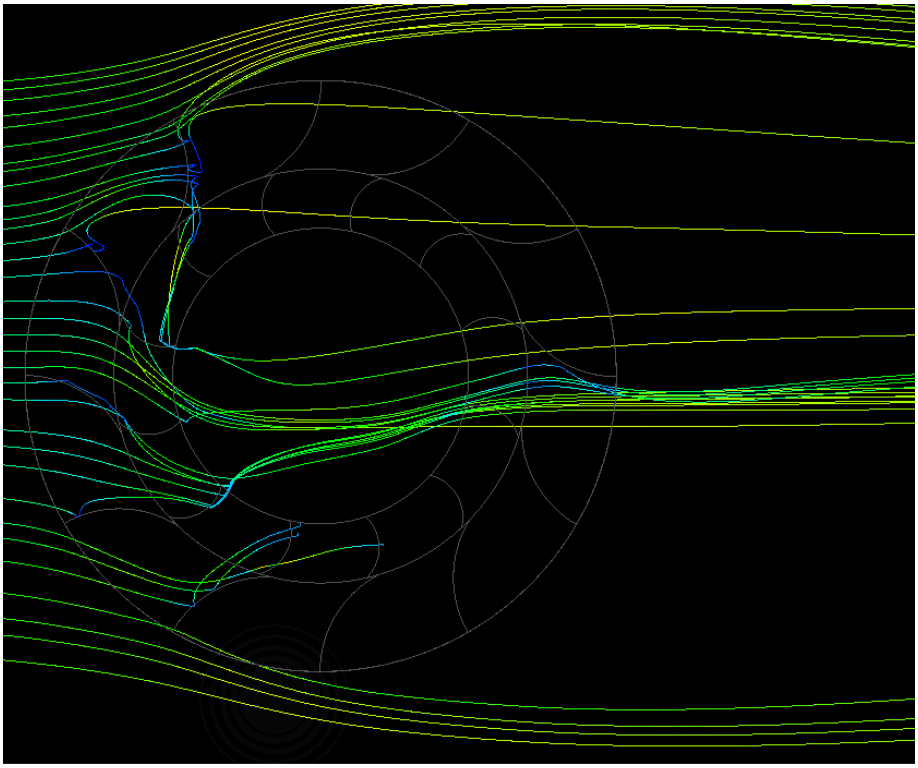

(d)

Figure 5.18 Sand particles' tracks, coloured by velocity, in the vicinity of the VAWT at (a) 0º (b) 3º (c) 15º (d) 27º for sand particles' mass flow rate of 2kg/sec and diameter of 125microns

Figure 5.19 depicts the comparison of the instantaneous torque output from the VAWTs for sand particles' mass flow rates of 1kg/sec and 2kg/sec. It can be seen that the presence of more sand particles in the flow domain slightly degrades the performance output of the VAWT by reducing its average torque. This is because although the lower torque values for the two are nearly the same, the upper torque values for 2kg/sec are lower than for 1kg/sec. The average torque generated by the VAWT for 2kg/sec is 0.52% less than for 1kg/sec.

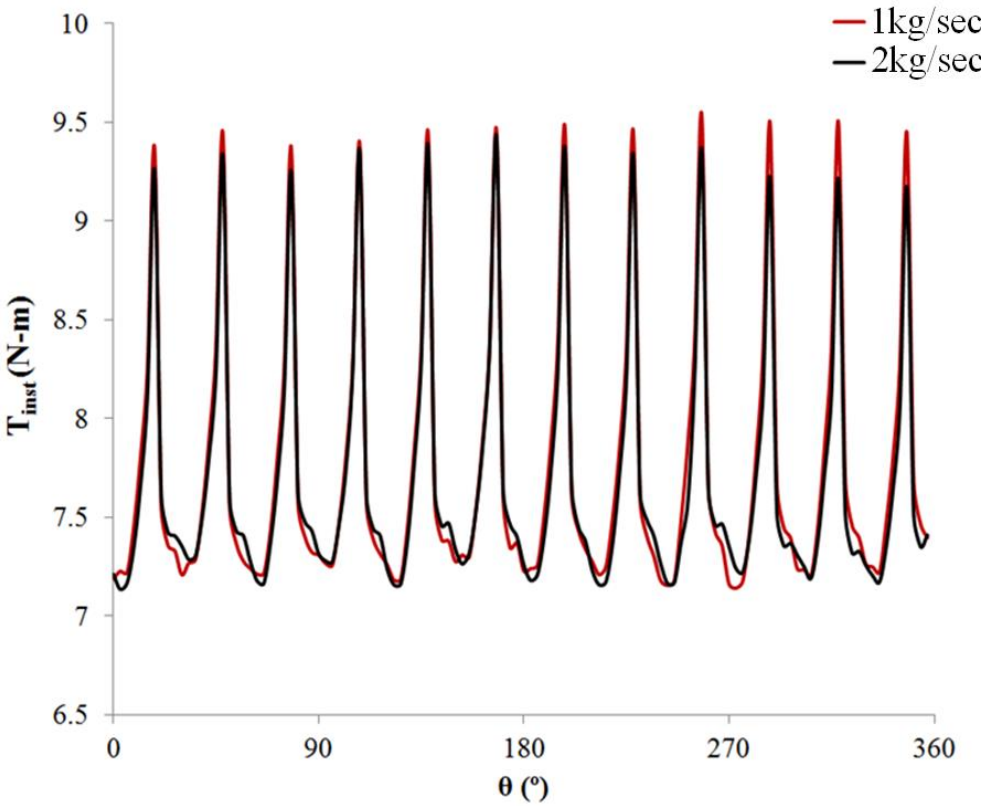

Figure 5.19 Instantaneous torque output comparison of the VAWTs operating in dusty environment with sand particles' mass flow rates of 1kg/sec and 2kg/sec and diameter of 125microns

Figure 5.20 depicts the contribution of individual rotor blades towards the total torque generated by the VAWT for sand particles' mass flow rate of 2kg/sec. It can be clearly seen that some rotor blades are in churning condition i.e. extracting energy from the flow rather than generating it.

Table 5.3 summarises the difference in the torque outputs from VAWTs for 2kg/sec and 1kg/sec sand particles. It can be noticed that the peak-to-peak amplitude of the torque signals from the VAWT for 2kg/sec sand particles is 2.29N-m, which is 4.43% lower than for 1kg/sec. Furthermore, there is a decrease of 0.52% in the average torque output of the VAWT.

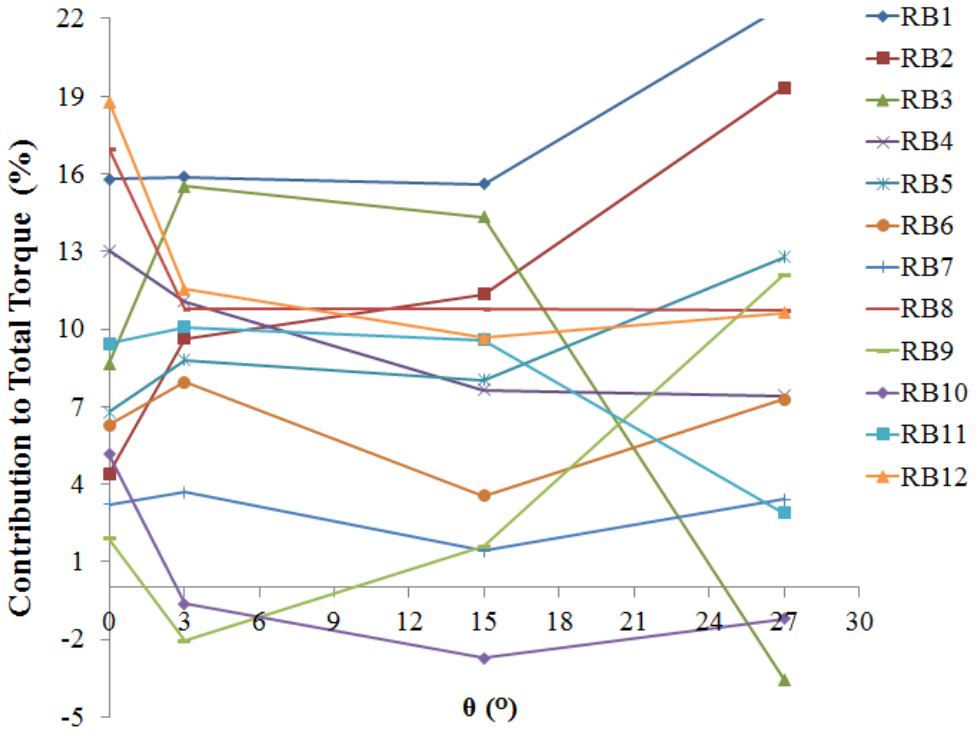

Figure 5.20 Contribution of each rotor blade to the overall torque generated by the VAWT operating in dusty environment with sand particles' mass flow rate of 2kg/sec and diameter of 125microns

Table 5.3 Performance analysis of the VAWT operating in dusty environment with sand particles' mass flow rate of 2kg/sec and diameter of 125microns

Torque Output (N-m)		Difference w.r.t. sand particles mass flow rate of 1kg (%)
Max	9.43	-1.18
Min	7.13	-0.09
Max-Min	2.29	-4.43
Average	7.68	-0.52
Standard Deviation	0.62	-7.81

Figure 5.21 depicts the instantaneous erosion rate on RB1 for one complete revolution of the VAWT, where the sand particles' mass flow rates are 2kg/sec and 1kg/sec. It can be clearly seen that the erosion rate for 2kg/sec sand particles is higher, with the maximum erosion rate of

0.33mm/yr. The general trend of the erosion rate, however, remains that same i.e. higher erosion rate when the rotor blades are either on the windward or the leeward sides of the VAWT.

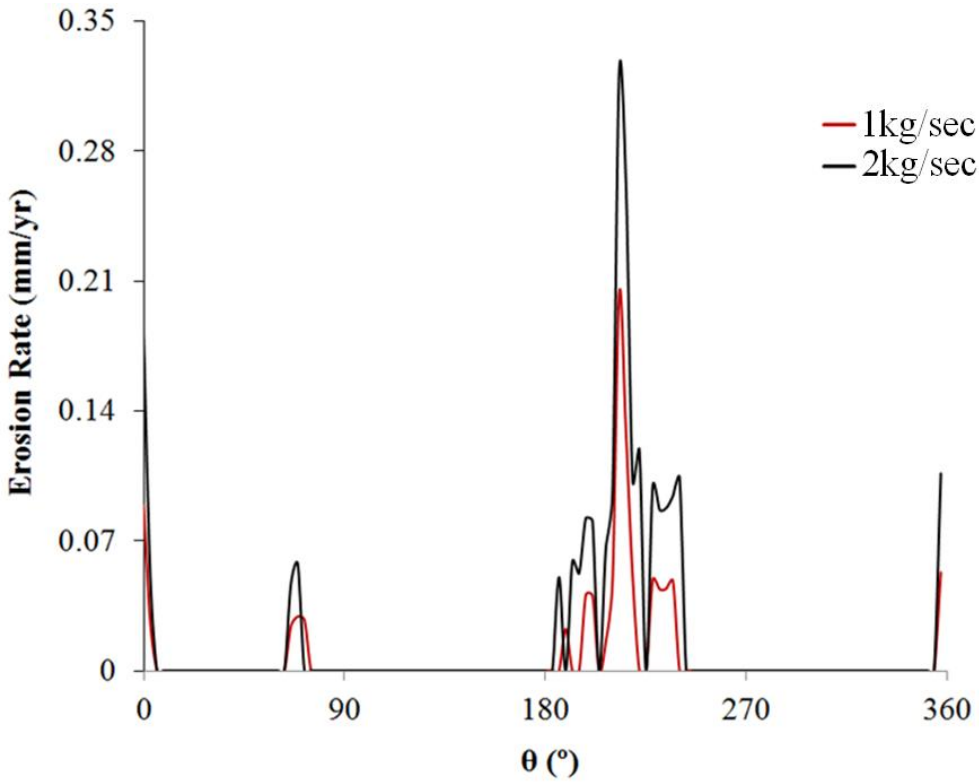

Figure 5.21 Instantaneous variations in the erosion rate (mm/yr) of a rotor blade for sand particles' mass flow rates of 1kg/sec and 2kg/sec, with particle diameter of 125microns

Using advanced statistical tools, such as multiple variable regression analysis, a novel semi-empirical expression for predicting the torque coefficient of the VAWT operating in dusty environments has been developed and presented as follows:

$$C_T = 0.767\ \frac{\theta^{\,0.0042}\left(\frac{\dot{m}_p}{\rho_p\, A\, V}\right)^{0.0056}}{\left(\frac{d}{R}\right)^{0.063}} - \left(1.385\,\theta^{\,0.0012} - 1\right) \qquad (5.1)$$

where m_p is the mass flow arte of the sand particles, ρ_p is the density of the sand particles (1550kg/m^3 in this study) and d is the diameter of the sand particles (m). It is noteworthy that the first term in equation (5.1) is the torque generating term when the VAWT is operating is dusty environments and the second term corresponds to the torque generation in clean environments (same as equation (4.3)).

In order to valid equation (5.1) with the CFD predictions presented in this chapter regarding the torque generated by the VAWT, torque generated using this equation needs to be compared against the CFD results. It has been found that the average difference in the torque predicted by

equation (5.1), and the torque obtained through the use of CFD, is 6% for 100% of the data. Hence, equation (5.1) can be sued to predict the instantaneous torque generated by a VAWT, operating in any environment, with reasonable accuracy.

CHAPTER 6
CONCLUSIONS

From the results obtained in the previous chapters, where the performance characteristics of a Vertical Axis Wind Turbine has been evaluated under clean and duty environmental conditions, detailed conclusions are drawn in this chapter. The major achievements and contributions to the existing knowledge base are summarised, and wherever possible, referred back to the initial aims of this study. Finally, the work carried out in this study is evaluated, and requirements for future work, in the area of VAWT performance evaluation, are discussed.

6.1 Research Problem Synopsis

The need for performance evaluation of Vertical Axis Wind Turbines forces the VAWT designers to explore the effects of environmental conditions on VAWT's performance. Although some experimental studies are available I the published literature, limitations were found regarding the detailed transient flow field analysis and linking it to the performance characteristics of the VAWT. Furthermore, the performance evaluation of VAWTs operating in dessert conditions is an area where the published literature lacks the most. In order to explore these limitations, especially in the dusty environments, numerical investigations were carried out.

In order to accurately predict the performance output of a VAWT, a set of aims and objectives were formulated, which define the scope of this research study. A summary of the primary aims of the thesis is provided in the following sections, along with the major achievements and contributions. For reference, the detailed objectives within each of these aims were provided in chapter 2. With the advent of powerful computing machines, and sophisticated software to analyse the flow fields, it has now become possible to computationally model a Vertical Axis Wind Turbine, and study the flow behaviour within and in the vicinity of these machines under various operating and environmental conditions.

6.2 Research Aims and Major Achievements

The major achievements of this study, against the aims laid out in chapter 1, have been discussed here.

Research Aim # 1: Analyse the performance characteristics of a Vertical Axis Wind Turbine operating in a clean environment

Achievement # 1: This study provides detailed CFD based analysis on the performance characteristics of a Vertical Axis Wind Turbine operating in a clean environment. Detailed flow field analysis of important flow parameters revealed interesting patterns/trends, and indicated the complex pressure and velocity fields in the vicinity of the VAWT. These analyses are very crucial for the VAWT manufacturers as it provides an in-depth understanding of the VAWT's transient behaviour under various operating conditions. Furthermore, VAWT designers can immensely benefit from the transient analysis carried out at various geometrical configurations of the rotor blades with respect to the stator blades, which are very difficult to carry out in real world (experimental) studies. This study has established that CFD can be used as an effective tool for the analysis of a VAWT operating in a clean environment with reasonable accuracy.

Research Aim # 2: Analyse the performance characteristics of a Vertical Axis Wind Turbine operating in dusty environments

Achievement # 2: The most important achievement of this study is the detailed transient analysis of a VAWT operating in various dusty environments, and predicting the instantaneous erosion rates on the rotor blades. The analysis approach adopted in this study clearly highlights the differences in VAWT's performance between clean and dusty environments, and helps the VAWT designers to understand which parameters are most important in the VAWT's performance evaluation studies. Furthermore, the development of a novel semi-empirical predictor expression for the torque coefficient of the VAWT, taking into account both the clean and the dusty environments, is the highlight of this study.

6.3 Thesis Conclusions

A comprehensive study has been carried out to support the existing literature regarding the optimisation and performance characteristics of automotive diffusers. The major conclusions from each facet of this research are summarised here.

Research objective # 1: Flow diagnostics and Performance Characteristics evaluation of the VAWT operating in a clean environment

Detailed flow analysis within and in the vicinity of the VAWT operating in a clean environment has been carried out in the present study. Both qualitative and quantitative analyses show that the static gauge pressure is considerable higher on the windward and leeward sections of the VAWT, whereas it is relatively lower on the upper and lower sections. For some degree of misalignment between the rotor and the stator blades, the high pressure zones shrink in size, leading to decrease in the torque generating capabilities of the VAWT. Furthermore, the VAWT behaves differently when a rotor blade leaves a stator blade and when a rotor blade approaches a stator blade, where the degree of misalignment between the two is the same, because of the curvature of the blades in the VAWT.

It has been observed that the flow velocity is high in the passages formed between stator and rotor blades, whereas it is considerable lower in the zones where there is more resistance to the flow path. The effects of flow jets formed in the passages between the rotor and the stator blades can be noticed even within the core region of the VAWT. As the rotor blades cross the stator blades, and there is some degree of misalignment between them, it has been observed that further jets appear in the core region. Moreover, it has been noticed that the flow smoothly propagates through the passages formed in between the blades, following the line of the blade's curvature for those pathlines that are very close to them. However, as rotor blades cross the stator blades, opening up a small passage, the pathlines escape through this passage.

A cyclic variation in the instantaneous torque output of the VAWT has been noticed in the present study, where the torque generated by rotor blades on the windward side of the VAWT is

generally higher as compared to the rotor blades present on the leeward side of the VAWT at a particular instance. A semi-empirical predictor expression has been developed for the torque coefficient of the VAWT operating in a clean environment.

Research objective # 2: Flow diagnostics and Performance Characteristics evaluation of the VAWT operating in various dusty environments

Detailed flow analysis within and in the vicinity of the VAWT operating in various dusty environments has been carried out in the present study. Both qualitative and quantitative analyses show that the static gauge pressure is considerable higher on the windward and leeward sections of the VAWT, whereas it is relatively lower on the upper and lower sections, which is inline with the observations in clean environment. Sand particles' tracks show that most of the sand particles enter the VAWT through the passages formed between the rotor and stator blades on the windward side of the VAWT. However, due to a number of blades in their path, most of the sand particles get settled on these blades, whereas some particles escape the VAWT through the passages on the leeward side of the VAWT.

It has been further noticed that in case of sand particles with larger diameters, deflection from the blades of the VAWT on the windward side is significantly higher. More sand particles escape through the VAWT because of their higher inertia. Furthermore, the accretion of sand particles and the torque generated by the VAWT reduces, whereas, the instantaneous erosion rate on the rotor blades increases significantly. Moreover, increasing the mass flow rate of the sand particles increases the instantaneous erosion rate, and hence decreases the torque generating capabilities of the VAWT.

Research objective # 3: Development of a novel semi-empirical torque prediction tool accounting a range of different operating environments for the VAWT

A cyclic variation in the instantaneous torque output of the VAWT has been noticed in the present study for the different operating environments, where the torque generated by rotor blades on the windward side of the VAWT is generally higher as compared to the rotor blades present on the leeward side of the VAWT at a particular instance. A semi-empirical predictor expression has been developed for the torque coefficient of the VAWT operating in various environments. This predictor expression takes into account the transient motion of the rotor blades within the VAWT, and the parameters describing the sand particles considered in the present study. The validation of the predictor tool has shown that it can be used for predicting the torque output of the VAWT with reasonable accuracy.

6.4 Recommendations for Future Work

Performance characteristics of a VAWT operating under various environmental conditions have been analysed in the present study, such that the gaps identified in the literature could be bridged. In light of the concluding remarks provided in the previous section, a vast potential for further research in this potential area has been unlocked. The main areas identified for further work are described below, which are associated with further performance evaluation of the VAWT.

Recommendation # 1

More advanced modelling techniques have now become available such as two degree of freedom model, six degree of freedom model etc. Using such models, the impact of flow on rotating bodies can be analysed with much better accuracy. In these techniques, the VAWT is treated as free a body, partially or completely, and the rotor blades revolve under the action of aerodynamic forces being generated on the blades. These advanced models do not require any inputs in terms of the rotor blade angular velocity. The aerodynamic forces acting on the blades are enumerated on-the-fly and necessary modifications are carried out for the orientation of the rotor blades. These advanced modelling techniques are indeed computationally very expensive and requires massive computational power. Furthermore, these tools require extra computational skills in terms of writing complex scripts to define the changing mesh structure and extraction of the data.

Recommendation # 2

Condition based health monitoring of vertical axis wind turbines is essential for its widespread commercial acceptability. A structured condition based health monitoring and fault detection system is required that can predict the faults in a VAWT. This leads toward predictive maintenance and hence a catastrophic structural damage can be avoided. The condition monitoring strategy includes the development of prediction models that links the severity and number of blade faults to the performance outputs of the VAWT. Such type of research can be carried out using advanced CFD tools but in order to do so high performance computing facilities are required that can handle the massive computational power required.

Recommendation # 3

It has been shown in the present study that errors arise in the prediction model due to certain elements like not considering the effect of the blade thickness in the computational model etc. These errors can be minimised by using an accurate blade profile rather than a simplified one. This can be achieved by using advanced CAD software and then integrating those designs with the computational fluid dynamics tools. However, the translation from CAD to CFD compromises some of the intricate details in the CAD model. Nowadays, advanced translators

are available in the market that takes care of this issue. Hence, a real model of the blades will enable to remove some of the errors in the torque prediction model presented in this study.

REFERENCES

[1] Tabassum-Abbasi, M. Prenalatha, M. and Abbasi, S. A. (2014) Wind Energy: Increasing Deployment, rising environmental concerns, Renewable and Sustainable Energy Reviews, 31, 270-28

[2] Keegan, M. H. Nash, D. and Stack, M. (2013) Issues associated with the leading edge of wind turbine blades, Journal of Physics D: Applied Physics, 46 (38), 1-9

[3] Salem, H and Diab, A. (2014) A preliminary study on the performance degradation of a wind turbine blade in dusty environments, Available at www.di-eunean.com

[4] Freedenthal, C. (2010) New book gives good arguments on using fossil fuels for power, Pipeline and Gas Journal, 134

[5] Chow, J. Copp, R. J and Portney, P. R. (2003) Energy resources and global development, Science, 302, 1528-1531

[6] Kennesaw State University (2011) Fossil fuels: Coal, Environmental Science Activities for the 21st Century, Available at http://esa21.kennesaw.edu/activities/coal/coalactivity.pdf

[7] Natural Gas (2011) Natural gas and the environment, Available at www.naturalgas.org/environment/naturalgas.asp

[8] Eriksson, S.H. Bernhoff, and Leijon, M. (2006) Evaluation of different turbine concepts for wind power, Renewable and Sustainable Energy Reviews, McGraw-Hill, New York

[9] Argonne National Institute (2014) Wind energy basics, Available at http://windeis.anl.gov/guide/basics/index.cfm

[10] Asim, T. Mishra, R and Ubbi, K. (2013) Effect of the shape of stator blades on the Performance output of a vertical axis marine current turbine, 26th International Congress of Condition Monitoring and Diagnostic Engineering Management, Helsinki, Finland

[11] JMT (2007) Horizontal Axis Wind Turbine, Retrieved from Wikipedia on March 1, 2009

[12] Mittal, N. (2001) Investigation of Performance Characteristics of a Novel VAWT, Thesis submitted for the M.Sc. degree, Department of Mechanical Engineering, University of Strathclyde, Glasgow, UK

[13] Akhmatov, V. (2007) Influence of Wind Direction on Intense Power Fluctuations in Large Offshore Windfarms in the North Sea, Wind Engineering, 31, 59-64

[14] Darrieus, G. (1931) Turbine Having It's Rotating Shaft Transverse to the Flow of the Current, United States Patent No.1

[15] Savonius, S. (1931) The S-Rotor and its applications, Mechanical Engineering, 53, 333-338

[16] Sutherland, H. J. and Berg, D. E. Ashwill, T. D. (2012) A retrospective of VAWT technology, Available at www.ntis.gov/help/ordermethods.asp?loc=7-4-0

[17] Energy Bible (2012) Wind Turbines, Retrieved from http://energybible.com/wind_energy/wind_turbines.html

[18] Hameed, M. S. and Afaq, S. K. (2013) Design and analysis of a straight bladed vertical axis wind turbine blade using analytical and numerical techniques, Ocean Engineering, 57, 248-255

[19] Castelli, M. R. Englaro, A. and Benini, E. (2011) The Darrieus wind turbine, Energy, 36, 4919-4934

[20] D'Ambrosio, M. and Medaglia, M. (2010) Vertical Axis Wind Turbines, Master Thesis in Energy Engineering, Hogskolan, Halmstad

[21] Modi, V. and Fernando, M. (1989) On the Performance of the Savonius Wind Turbine, Journal of Solar Energy Engineering, 111/71

[22] Sheldahl, R. (1978) Wind Tunnel performance data for two and three bucket savonius rotors, Energy, 2, 160-164

[23] Sivasegaram, S. (1978) Secondary parameters affecting the performance of resistance-type vertical-axis wind rotors, available at http://adsabs.harvard.edu/abs/1978WiEng...2...49S

[24] Clayton, B. (1978) Observations of the flow in and around Savonius and Darrieus rotors, Proceedings of the First British Wind Energy Association Conference, Cranfield, 24-31

[25] Fujisawa, N. Shirai, H. and Mizuno, Y. (1987) Hot wire anemometer measurements of flow fields around savonius rotors in open circuit wind tunnel, Laser and hot wire/film velocimetries and their applications, 109-122

[26] Walker, S. L. (2011) Building mounted wind turbines and their suitability for the urban scale: A review of methods of estimating urban wind resource, Energy and Buildings, 43, 1852-1862

[27] Bhutta, M. M. Hayat, N. Farooq, A. U. Ali, Z. Jamil, S. R. and Hussain, Z. (2012) Vertical axis wind turbine – a review of various configurations and design techniques, Renewable and Sustainable Energy Reviews, 16, 1926-1939

[28] Colley, G. (2012) Design, Operation, and Diagnostics of a Vertical Axis Wind Turbine, Ph.D. Thesis, School of Computing & Engineering, University of Huddersfield, UK

[29] Mohammed, G. K. and Aboelyazied, M.K. (2007) Effect of dust on the performance of wind turbines, Desalination, 209 (1-3), 209-220

[30] Blackwell, B. (1974) The Vertical Axis Wind Turbine: How It Works, Sandia Laboratories No. SLA-74-0160

[31] Khalfallah, M. G.and Kollub, A. M. (2007) Effect of dust on the performance of wind turbines, Desalination, 209 (1-3), 209-220

[32] Park, K. (2013) Optimal Design of a Micro Vertical Axis Wind Turbine For Sustainable Urban Environment, Ph.D. Thesis, University of Huddersfield, U.K

[33] Park, K. Asim, T. and Mishra, R. (2013) Effect of Blade Faults on the Performance Characteristics of a Vertical Axis Wind Turbine, 26th International Congress of Condition Monitoring and Diagnostic Engineering Management, Helsinki, Finland

[34] Park, K. Asim, T. Mishra, R. (2012) Computational Fluid Dynamics based Fault Simulations of a Vertical Axis Wind Turbines, Journal of Physics: Conference Series, 364, 012138

[35] Asim, T. Mishra, R. Kaysthagir, S. and Aboufares, G. (2015) Performance Comparison of a Vertical Axis Wind Turbine using Commercial and Open Source Computational Fluid Dynamics based Codes, The International Conference on Jets, Wakes and Separated Flows, Stockholm, Sweden, 311-3116

[36] Shahzad, A. Asim, T. Mishra, R. Paris, A. (2013) Performance of a vertical axis wind turbine under accelerating and decelerating flows, Procedia CIRP, 11, 311-316

[37] Shahzad, A. Asim, T. Park, K. Pardhan, S. Mishra, R. (2012) Numerical simulations of effects of faults in a vertical axis wind turbine performance, 2nd International Workshop and Congress on eMaintenance, Lulea, Sweden

[38] Colley, G. Mishra, R. Rao, V. and Woolhead, R. (2009) Performance evaluation of three cross flow vertical wind axis turbine configurations, Computing and Engineering Annual Researchers' Conference, Huddersfield, UK

[39] Colley, G. Mishra, R. Rao, V. and Woolhead, R. (2010) Effect of rotor blade position on Vertical Axis Wind Turbine performance, Proceedings of the International Conference on Renewable Energies and Power Quality (ICREPQ'10), Granada, Spain

[40] Colley, G. and Mishra, R. (2011) Computational flow field analysis of a vertical Axis Wind Turbine. In international conference on Renewable Energies and Power Quality, Las Palmas, Gran Canaria

[41] Colley, G. Mishra, R. Rao, V. (2011) Performance characteristics of a vertical axis wind turbine under transient conditions, 24th International Congress on Condition Monitoring and Diagnostics Engineering Management, Stavnger, Norway

[42] Gharali, K. Johnson, D. A. (2011) Numerical modeling of a S809 airfoil under dynamic stall, erosion, and high reduced frequencies, Applied Energy, 93, 45-52

[43] Erpul, G. Gabriels, D. Norton, L. D. (2003) The combined effect of wind and rain on interrill erosion processes, Lecture given on Soil Physics, Trieste

[44] Ren, N. Ou, J. (2009) Dust effect on the performance of wind turbine airfoils, Journal of Electromagnetic Analysis and Applications, 1, 102-107

[45] Khakpour, Y. (2007) Aerodynamic performance of wind turbine blades in dusty environments,Master's thesis, Illinois Institute of Technology, Available at http://vufind-devl.carli.illinoi.edu/all/vf-hrt-record/10000373

[46] El-Batsh, M. S. (2001) Modelling Particle Deposition on Compressor and Turbine Blade Surfaces, Institute of Thermal Turbo Machines and Power Plants, Vienna

[47] Versteeg, H. K. and Malalasekera, W. (1995) An Introduction to Computational Fluid Dynamics, Longman Scientific and Technical, UK, ISBN: 0131274988

[48] Pozrikidis, C. (2001) Fluid Dynamics Theory, Computation and Numerical Simulation, Kluwer Academic Publishers, U.S.A., ISBN: 038795869X

[49] Tuncer, C. Jian, P. S. Fassi, K. and Eric, L. (2005) Computational fluid dynamics for engineers

[50] Blazek, J. (2001) Computational Fluid Dynamics Principles and Applications, Elsevier, ISBN: 0080430090

[51] Lomax, H. Pulliam, T. H. and Zingg, D. W. (2001) Fundamentals of Computational Fluid Dynamics. Springer, ISBN: 3540416072

[52] Hoffmann, K. A. and Chiang, S. T. (2000) Computational Fluid Dynamics, Engineering Education System, U.S.A., ISBN: 0962373133

[53] Ansys 13.0.0 User Guide accessible at http://www1.ansys.com/customer/content/documentation/130/wb2_help.pdf

[54] Morsi, S. A. and Alexander, A. J. (1972) An Investigation of Particle Trajectories in Two-Phase Flow Systems, Journal of Fluid Mechanics, 55, 193-208

[55] Edwards,J.K. McLaury,B.S. and Shirazi,S.A.(2000) Evaluation of Alternative Pipe Bend Fittings in Erosive ServiceIn Proceedings of ASME FEDSM'00: ASME 2000 Fluids Engineering Division Summer Meeting, Boston.